Co-delivery of Two Growth Factors From Combined PLGA and PLLA/PCL Microsphere Scaffolds for Spinal Cord Injury Repairs

by

Zhongxuan. Li

Thesis submitted to the

Faculty of Graduate and Postdoctoral Studies

in partial fulfillment of the requirements for the degree of

Master of Applied Science

Chemical Engineering

University of Ottawa

Ottawa, Ontario, Canada

Abstract

The purpose of this study is to demonstrate the effectiveness of spheres-in-tube structured scaffolds to sequentially deliver two biomolecules during two phases of tissue regeneration following spinal cord injury (SCI). Scaffolds were synthesized of a poly (lactic-co-glycolic acid) (PLGA) base combined with Poly (L-lactic acid) / Poly (ε-caprolactone) (PLLA/PCL) microspheres.

The scaffolds are constructed by leveraging the different solubilities of PLGA, PLLA and PCL in super critical carbon dioxide and ethyl acetate during fabrication processes. Microspheres can reduce the pore size and porosity of PLGA scaffolds; this enhances their mechanical strength and enables them to provide long-term treatment without collapse.

The release of the epidermal growth factor (EGF) and basic fibroblast growth factor (FGF-b) are being used to study the release profiles of the designed scaffolds. The analysis shows that FGF-b is released from high porosity PLGA base as the first delivery vehicle and completes the release in the first week. PLLA or PCL microspheres, having the property of sustainably delivering encapsulated EGF in 36 days, are used as the second drug delivery vehicle.

FGF-b released within the first week can mimic biomolecules used to protect the surviving neurons and promote the development of sprout axons. The sustained

release of EGF from microspheres is used for long-term therapy to differentiate multipotent cells into determined types at the injury site.

The results demonstrate that these enhanced parameters along with the ability of sequential co-delivery of growth factors, make these designed scaffolds a promising candidate in SCI studies.

Résumé

L’objectif de cette étude est de démontrer l’efficacité des hyper-structures de type sphère dans un canal cylindrique pour émettre deux biomolécules de façon séquentielle pendant deux phases de régénération des tissues suite à un traumatisme médullaire. Les hyper-structures en question sont fabriquées à base de poly lactique-co-glycolique d'acide (PLGA) avec des microsphères d’acide polylactique/polycaprolactone (PLLA/PCL).

La fabrication des hyper-structures se fie sur les différentes solubilités du PLGA, PLLA, et PCL dans le CO2 supercritique et l’acétate d'éthyle. Les microsphères peuvent réduire les diamètres des pores et la porosité des hyper-structures de PLGA, améliorant ainsi leur résistance mécanique pour les traitements à long terme.

Les profils d’émissions des facteurs de croissance épidermique (EGF) ainsi que des facteurs de croissance des fibroblastes (FGF-b) sont ensuite déterminés dans ces hyper-structures. L’analyse démontre que, dans un premier temps, le FGF-b est livré à l’aide du PLGA à haute porosité pendant une période d’une semaine. Par la suite, les microsphères PLLA ou PCL servent de véhicules de livraison. Ces microsphères ont la propriété d’émettre les EGF encapsulés de façon continue sur une période de 36 jours.

Les FGF-b émis dans la première semaine peuvent imiter les biomolécules qui protègent les neurones survivants ainsi que stimuler la croissance de nouveaux

bourgeons axonaux. Pour le traitement à long terme, l'émission continue d'EGF à l'aide des microsphères sert à différentier les cellules multipotentes.

Les résultats démontrent que les améliorations dans la fabrication des hyper-structures couplée avec la livraison séquentielle des facteurs de croissance offrent un mécanisme prometteur dans le traitement des traumatismes médullaires.

Acknowledgements

I take great pleasure in thanking the many people who have helped me in my studies at the University of Ottawa. First and foremost, I would like to express my sincere appreciation and deep thanks to my supervisor, Dr. Xudong Cao, for giving me the opportunity to complete a master's degree in chemical engineering under his guidance. His encouragement and advice greatly helped me in both my research and in writing this thesis.

I also would like to thank Donald McLachlan, Patrick Assouad, and Dr. Thibault for their assistance with my thesis writing. I would like also to thank the help form my research group throughout my research project.

Last but not the lease, I would like to extend my thanks to my parents Min Li, Ru Zhang, and my grandfather Bifa Zhang, whose encouragement have always sustained me.

Contents

List of Figures

List of Tables

Abbreviation

ANG-1	Angiopoietin-1
AP	Alkaline phosphatase
BDNF	Brain-delivered neurotrophic factor
BMP	Bone morphogenetic protein
BMSC	Bone marrow stromal stem cell
BSA	Bovine serum albumin
CAD	Computer-aided design
CAM	Computer-aided manufacturing
ChABC	Chondroitinase ABC
CNS	Central nervous system
CpG	C phosphate G
CS	Chitosan
CSPG	Chondroitin sulfate proteoglycan
CyA	Cyclosporin A
DCM	Dichloromethane

Dox	Doxorubicin
Dtxl	Decetaxel
ECMS	Extracellular matrices
ECT	Encapsulation cell technology
EDK	Elisa development kit
EGF	Epidermal growth factor
ELISA	Enzyme-linked immunosorbent assay
EPO	Erythropoietin
ES	Embryonic stem cells
FGF	Fibroblast growth factor
FGF-2	Fibroblast growth factor-2
FGF-b	Fibroblast growth factor-basic
FGF-b	Fibroblast growth factor-basic
GDNF	Glial cell line-derived neurotrophic factor
GF	Growth factor
HAEC	Human aortic endothelial cell
HGF	Hepatocyte growth factor

IGF-1	Insulin-like growth factor-1
IL-10	Interleukin-10
K-wires	Kirschner wires
MAG	Myelin-associated glycoprotein
MS	Microsphere
NGF	Nerve growth factor
NP	Neural progenitor cell
NSPC	Neural stem cell/ Progenitor cell
NT-3	Neurotrophin-3
OEC	Olfactory ensheathing cell
PCL	Poly (ε-caprolactone)
PDGF	Platelet-derived growth factor
PDLA	Poly (D-lactide)
PDLLA	Poly (DL-lactide)
PGA	Poly (glycolic acid)
PHEMA	Poly (2-hydroxyethyl methacrylate)
PLGA	Poly (lactic acid-co-glycolic acid)

PLLA	Poly (L-lactic acid)
PNS	Peripheral nervous system
POE	Poly (orthoester)
PPF	Precision particle fabrication
PVA	Poly vinyl alcohol
PVC	Poly vinyl chloride
RA	Retinoic acid
RNAi	Ribonucleic acid
SC	Schwann cell
SCI	Spinal cord injury
SEM	Scanning electron microscopy
Shh	Sonic hedgehog
TGF-β	Transforming growth factor-β
TMC	Trimethylene carbonate
TNT	Titania nanotube

Chapter 1 Introduction

1.1 Spinal cord injury

The human nervous system consists of two regions, the central nervous system (CNS) and the peripheral nervous system (PNS). The CNS, which consists of the brain and the spinal cord, integrates information from the PNS, processes and then guides the activity. In the spinal cord the CNS is made up of two parts, grey matter in a butterfly-shaped core consisting of neuronal cell bodies, surrounded by white matter containing the long axons. The spinal cord is encased in the bony vertebral column and is attached to the brain stem conveying information from the skin, joints, and muscles of the body to the brain via spinal nerves.

Spinal cord injury (SCI) is caused instantly by physical impact trauma or gradually by illness such as tumors or infection. Function loss on the motor and sensory pathways, are typically associated with two types of spinal cord injuries, complete spinal cord injury (of both the motor and the sensory pathways) and incomplete spinal cord injury (partial random preservation of the motor or the sensory pathway).

According to a worldwide literature survey, 223-755 per million people spent their life in wheelchairs due to medical comorbidity [1]. The latest data provided on Spinal Cord Injury Awareness estimates 275000 people in the US and 86000 people in Canada

are living with spinal cord injury. In Canada approximately 4300 people are paralyzed every year due to SCI, resulting in an overall estimated cost to the health care system of $3.6 billion [2]. Road traffic accidents, domestic and work-related accidents, sports injuries and acts of violence are the top reasons for traumatic injury. Bacterial and viral infections to spinal nerve cells and pressure from the growth of cysts or tumors blocking blood supply are the main reasons that cause SCI without trauma. In SCI, over 50% of the cases happened to people under 30 years old, with over a 4:1 male to female ratio [2]. SCIs often require lifelong high cost treatment and therefor are a big concern to society. The green ribbons (shown in Figure 1), symbols for SCI, are customized to various gifts in Zazzle Canada's unique collection, expressing people's expectations for research to find a cure for patients [3].

Figure 1 Green ribbon for Spinal Cord Injury

Pathophysiology of injury has been studied for decades; however, full understanding of spinal cord injuries is still a long way off. It is believed that the CNS

has the potential of self-reparation after injury due to spontaneous regenerative events. Axons could sprout and persist after the injury, but with limited cellular, molecular mechanisms and other reasons, the capacity for regeneration is still limited [4].

After initial trauma displaced fragments of bone, lost tissue, damaged vessels, axons and neurons at the injured site can disrupt long tract neural connections [5]. Then the damage site on the injured spinal cord may rapidly swell within minutes (caused by immune responses) thereby affecting the nerve pathways. During the post-traumatic stage, built up amino acids from ruptured vessels and damaged cells result in toxicity to the surrounding environment. During this process, secondary cell loss occurs to resident cells and scar tissue is formed by inflammation cells [6, 7]. The secreted and transmembrane molecules from scar tissue, in turn, inhibit axon growth [8]. All these regeneration inhibitors have cross affects on each other at the injury site as shown in figure 2 [9]. Up to now, though various cellular and molecular strategies have been used, no single strategy or efficient medical treatment method has been reported to successfully get full functionality back after injury. SCI is still a complicated regeneration hurdle that requires further research.

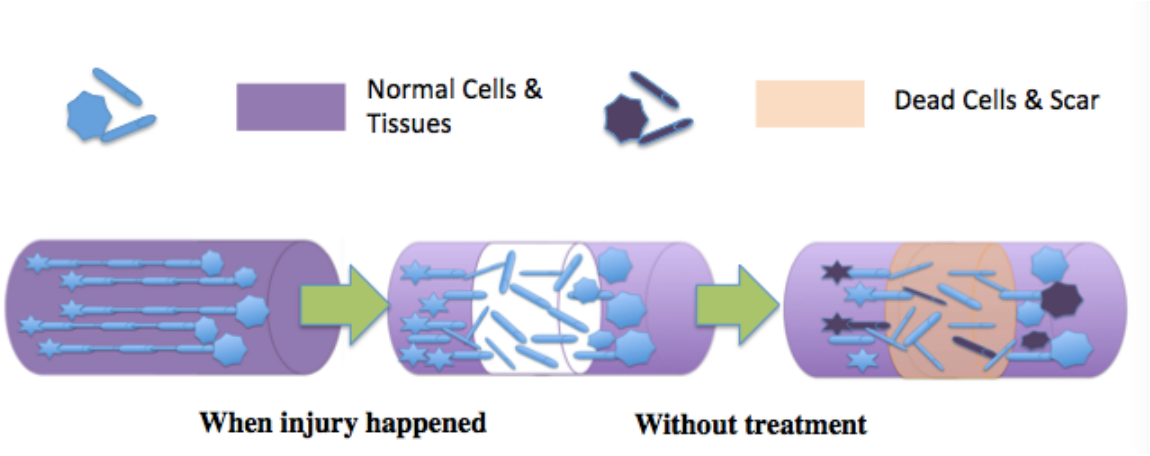

Figure 2 Spinal cord injury degeneration process

In recent studies, it is commonly believed that four major principal strategies must be involved in a "cure" to regenerate the injured spinal cord: (1) Prevent tissue loss and replace the damaged neurons and glia caused by trauma. (2) Delivery of molecules, including growth factors or neurotrophins, to stimulate the proliferation and differentiation of local cells or implanted cell grafts. (3) Prevent secondary injury and bridge axons to grow out of the lesion site to proper targets. (4) Correct the synaptic connections [9, 10].

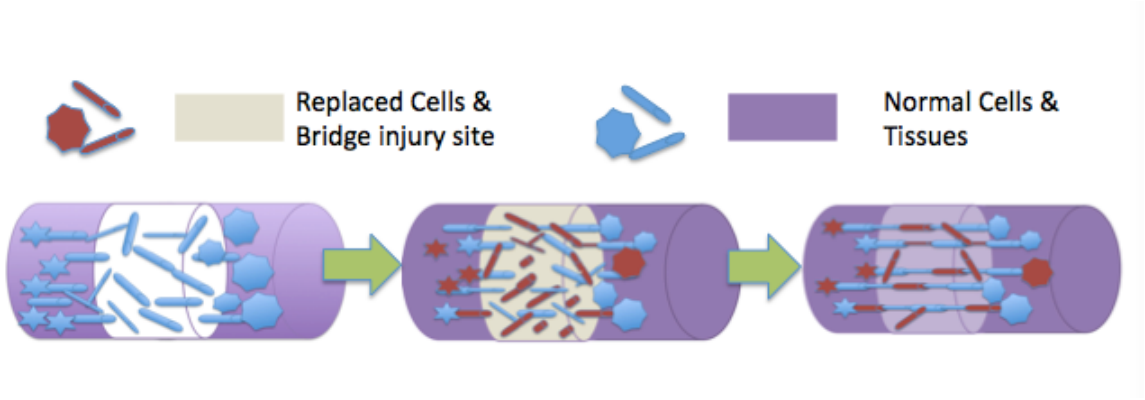

Figure 3 Approaching regeneration process

With the aim of achieving better functional recovery, the goal is to create a special microenvironment that will support these four major principal strategies. In a SCI study, as depicted in Figure 3, a combination of cellular treatment, delivery of molecules and other bio-strategies have been reported to approach such principals.

1.2 Time-line for SCI treatment

Previous research also found that, the damage would last for years after the injury initially happened. Within this time line, it is common to separate the whole time into three phases, the acute, the secondary tissue loss and the chronic phases [11]. The acute phase happens right after the injury and lasts for days, during which mechanical injury to the spinal cord causes local neurons, astrocytes, oligodendrocytes and endothelial cells to die immediately [12, 13]. The second damage phase, starts within minutes to weeks after the injury with more complicated reactions. These affects consist of

biochemical alterations and cellular reactions. The biochemical alterations include the release of excitatory biochemical alternations like amino acids, lipid peroxidation and cytokines [14], and the cellular reactions are caused by inflammation by the over reaction of immune cells like macrophages, neutrophils and T cells [15, 16]. Results from the previous two phases continue into the chronic phase. Lost tissue and inflammation cause the build up of fluid-filled cysts, demyelination, and wallerian degeneration [13, 15, 16].

According to the injury time line, the first step to repair the damaged spinal cord is to protect further cell loss and to propagate endogenous cells. Guaranteeing a sufficient quantity of potential therapeutic cells at the injury site provides a positive environment to both inhibit scar formation and recruit sufficient number of cells for the next step. The second period is a long process focusing on guiding the rebuilding of connections. This is achieved by stimulating the differentiation potential ability of therapeutic multifunctional cells with specific biomolecules and cell-to-cell contact interactions. Guided by the surrounding environment, determined types of cells at the injured site then reconnect together and fix the connection.

1.3 Scaffold design

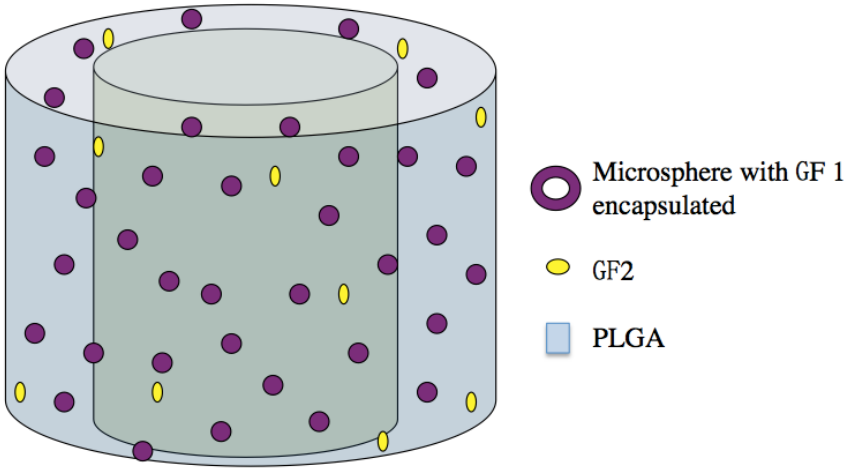

Figure 4 Structure of designed scaffold and distribution of drug location.

1.3.1 Introduction of Designed Scaffold

The scaffolds designed in this project consist of two growth factors encapsulated in biodegradable co-polymers (either PLGA and PLLA or PLGA and PCL). The two growth factors are used to mimic the release behavior of biomolecules that stimulate proliferation and differentiation at different periods of the regeneration process. The growth factors are located in different places (microspheres or base) of the scaffold. As Figure 4 shows, the whole device is designed in the shape of a tube. The walls of the tube are constructed of PLGA as the based material. Microspheres containing GF1, and GF2 are encapsulated in the PLGA base.

The scaffold in Figure 4 has a 4mm outer diameter and a 3mm inner diameter to match the spinal diameter of rats. The height of the scaffold is in a range of 24.50-25.50 mm (limited by the height of the mold). Each scaffold can be cut to the desired length with a surgical blade as needed.

1.3.2 Solubility of Material

The scaffold contains different materials of different solubility in aqueous phase or solvent phase. Biomolecules, like growth factors used in spinal cord injury repairs, are hydrophilic, and polymers PLGA, PLLA, PCL are hydrophobic. Ethyl acetate is used in this research because while it dissolves PLGA it does not dissolve PLLA and only partially dissolves PCL [17, 18]. The benefit derived from this characteristic is microspheres made of PLLA/PCL can be integrated into PLGA base scaffolds.

1.3.3 Super Critical CO_2 Foaming Process

Fabrication of the determined scaffold is based on super critical CO_2 foaming technology. Different solubility and diffusivity of CO_2 in polymers make it possible for two types of polymer-structured drug delivery systems to exist in one scaffold. In morphology, it is not easy for CO_2 to diffuse into crystalline polymers like PCL and PLLA, therefore the structure of the microspheres are not affected by the CO_2 [19]. Amorphous polymer PLGA provides more free volume for CO_2 diffusion constructing the porous structure [20]. When scaffolds, made of PCL/PLLA microspheres with

PLGA matrix, are foamed under super critical CO_2, PLGA is expanded into the determined shape based on molds being used, while PCL/PLA maintains its spherical shape.

1.3.4 Release of Biomolecules

By combining microspheres and PLGA foamed scaffolds together as shown in Figure 4, the release behavior of GF2 (loaded in the PLGA base) follows that of a supercritical carbon dioxide foamed PLGA scaffold. The PLGA base, working in a similar manner as a barrier, slows down the release of GF1 encapsulated in microspheres, achieving release behavior similar to that of double-walled microspheres. By integrating different types of deliver systems and co-delivered growth factors in one scaffold, the initial goal for using this scaffold for spinal cord injury repairs can be met, with one growth factor released at the beginning and the other gradually released over time.

1.4 Research Approach

Hypothetically, spinal cord injury can be better repaired when the cell behaviors are controlled at specific regeneration stages. In particular, a scaffold synthesized with co-polymer is designed to enhance cell growth, to direct cell differentiation and then in return to rebuild the connection and to prevent the scar formation at injured site. The

first released growth factor is used to recruit and sustain cell growth and the second released growth factor is used to obtain various desired cell types that are used to reconstruct the connections at the injury site.

The goal in this project is to design an implant drug delivery scaffold to regenerate the damaged spinal cord. Working as a delivery system, the determined scaffold is designed with a benefit of time controllable delivery. Two growth factors are localized at different places in the same scaffold to obtain different release profiles. The first biomolecule is to be released instantly after the scaffold is implanted, enhancing the quantity of cells. A second different biomolecule is ideally to be released later to obtain various cell types. Co-polymers as fundamental materials, with a sphere in tube architecture made using a green synthesization process are used in this research. Enhanced mechanical properties and slowed degradation provide a positive clue for long-term regeneration studies. Used as a biomolecules delivery vehicle, this scaffold is specially designed for SCI repairs, however it also has a potential to be used in other research to deliver two different biomolecules at different times.

1.5 Research Goals

The goals of this project have been listed as follows:

a) To design and to fabricate co-delivery growth factors microsphere-in-tube structured scaffolds for SCI studies.

b) To study release behavior of each growth factor released from the designed scaffold.

c) To characterize the synthesized scaffolds by morphology, degradation, and mechanical properties in vitro over time.

Chapter2 Literature review

2.1 Cellular Therapy

After SCI, cells are lost at both initial stage and during the following periods. Cellular therapy used in SCI is to reduce cell death and cyst formation, promote remyelination of intact axons, overcome the physical impediments preventing the replacement of lost neural tissue, and optimize the surrounding circulation [21]. All these functions create a positive environment for regeneration. For these reasons, certain quantities and various types of cells are required at the injury site. Stem cells are well known to have the potential of indefinite self-renew and have the ability to differentiate into all cell types [21, 22]. This differentiation can be guided such that they will become the type of cell required. Progenitor cells can also differentiate into various cell types but compared with stem cell they are more restricted in they types of cells they can become. For example, glial progenitors and neuronal progenitors can be differentiated into neurons [23, 24]. These multicomponent cells used in cellulose therapy, have the potential either to self-renew, to replace the lost tissue or to differentiate into demanded cell types to rebuild the neural connection. This differentiation can be controlled by the local environment or with stimulation factors. To repopulate the various cells in the CNS, both the transplantation of exogenous cells and the stimulation of endogenous multifunctional therapeutic cells have been studied

[8].

2.1.1 Different Cell Types Used in Cellular Treatment

Neural Stem Cell/Progenitor Cell (NSPCs), consisting of majorly progenitor cells and a small amount of stem cells, are located in the ependymal zone and throughout the peripheral white matter of the adult spinal cord [25]. NSPCs are subculture cell types from pluripotent cells and can be divided from embryonic neural tissues, induced pluripotent stem cells, and non-neural adult tissue stem cells [26]. Having the capacity of self-renew and cellular totipotency, NSPCs can differentiate into neuronal restrict precursors and glial restrict precursors [27]. Glial precursor cells can differentiate into glial-based cells and neuronal precursor cells that can differentiate into specific mature neurons [26]. In in vitro studies, using exogenous cells, NSPCs have been successfully cultured into neurons, oligodendrocytes and astrocytes [28]. Experiments using human NSPCs in primate studies indicate NSPCs have the ability to differentiate into neurons, astrocytes and oligodendrocytes in vivo, indicating this technique is promising for cell therapy in humans. The various differentiated cells could improve motor functional recovery without tumors formation [29]. However, one study also indicates the implanted NPSCs are mostly differentiated into astrocytes [30]. Astrocytes as a type of glial cells in CNS are activated after injury. The astrocyte proliferation results in glial scars, which are known to act as physical and chemical barriers for regeneration [31]. To overcome the glial scar, further work has been done to restrict differentiation of

NPSCs by using growth factors. Growth factors can provide specific signals; for example, by delivering bone morphogenetic protein, NPSCs differentiate toward neurons and oligodendrocytes rather than astrocytes [32]. Similar improvements can be found by using other growth factors, for example, ciliary neurotrophic factor [33].

Embryonic Stem Cells (ES cells) are subculture pluripotent stem cells, which are derived from the inner cell mass of the blastocyst. With the ability of self-renew and the potential to differentiate into a various types of progenitors ES cells are widely used to enhance neuronal cells including stem cells, neuron, and glial proliferation [34]. Preclinical studies have focused on the advantages of easy to culture and long-term differentiation potential after several generations by culturing ES cells [35]. Transplanting ES cells into mouse CNS as a preclinical model results in a formation of oligodendrocytes and astrocytes and indicates a potential ability to restore myelination [36]. Another clinical study on mice shows ES cells can survive over 50 days after transplantation and are capable to be used in long-term treatments [37]. ES cells have the positive characteristics of highly proliferative, unrestricted development, and sensitivity to the environment; unfortunately these characteristics also mean they have a high risk of tumor formation [38]. To reduce the over expression of undesired differentiation, ES cells are not usually directly transplanted in animals but pre-differentiated into restricted progenitors cells or subculture stem cells, like oligodendrocytes progenitor cells, neural progenitors first. Then transplant the pre-differentiated cells are transplanted to treat neurological disorders and traumas,

including SCI [39]. For example, oligodendrocytes progenitor cells differentiated from human ES can generate mature oligodendrocytes and restore myelination [40].

Bone marrow stromal stem cells (BMSCs) containing a subfraction of mesenchymal stem cells are multipotent stem cells derived from bone marrow [41]. In SCI studies it has been shown that implanting BMSCs can improve post-injury recover. Working similarly like stem cells, rat and human BMSCs can differentiate into specific neurons and glia both in vivo and in vitro [42]. Functional BMSCs can aid the neuronal differentiation and at the same time the secreted neurotrophic factors from BMSCs including, BDNF and NT-3 can support extensive axon growth [43, 44]. Harvested from bone marrow, transplanting BMSCs in treatment has fewer ethical problems that need to be taken into consideration.

Schwann Cells (SCs) working to produce the myelin sheaths that surround the neurons in PNS can promote the axons regeneration. Although SCs cannot be differentiated into other cell types, the benefit of plastic characteristic SCs also made it involved in SCI studies. SCs have been investigated to aid regeneration of injured spinal cords by creating a permissive environment. They aid regeneration both by limiting the formation of scar tissue, and by accumulating neurite growth promoting factors, including NT-3, NGF, and FGF at injury site [45]. Evidence suggests that Schwann or Schwann-like cells are capable to be generated endogenous after SCI [46]. Schwann cell-like cells naturally present at the lesion site are generated by endogenous

CNS precursors. The PNSs-derived SCs can also migrate into lesion sites. The SCs regenerated in the CNS and those that migrated from the PNS together rebuilt the connection after injury. Transplantation of Schawann cells has also been done on rats and primates for SCI treatment. However, efficacy and safety issues of using transplanted SCs in human clinical trials haven't been reported yet [8].

Olfactory Ensheathing Cells (OECs) are glial cells generated from embryonic, adult olfactory bulb, or mucosa. OECs play an important role in the lifelong neural regeneration capacity of olfactory neurons in SCI studies [47]. OECs can create a permissive microenvironment at the injury site and enhance the migration of sprouted axons in damaged CNS tissue. The migration of sprouted axons within the spinal cord can reduce the cavity formation and lesion size [48]. There are a few clinical experimental studies using OECs for CNS neuronal regeneration. Implanting human OECs into rodent spinal cord injuries improves the remyelination [49]. SCI studies show OECs can improve long-distance growth of axons, which can be used as a therapeutic application in CNS [50].

2.1.2 Exogenous-based Therapies for SCI

To harvest a high quantity of therapeutic cells, some recent studies focus on culturing various types of exogenous precursors, including both stem cells and progenitor cells [51, 52]. These stem cells or multi-differentiated precursor cells can be cultured in vitro into a three-dimensional structure named 'neurospheres'. These

spherical shaped cells are diverse collections of glial and neuronal precursors with a potential to differentiate into multi-desired cells at an injury site [23, 53].

Though the benefit of this technique results in simple cell replacement, there are still some concerns on the overall ability of using implanted multifunctional cells at the injured spinal cord. There are several preclinical safety studies on transplanted cell-based therapies for SCI. Although there are benefits of using pluripotent cells to get various therapeutic cells, it also causes the undesired phenotypes resulting in a major safety concern to SCI treatment. Although transplanted stem cells have the ability to be differentiated into neurons and oligodendrocytes, stem cells can also promote the sprout of undesired sensory fiber within the spinal cord [38]. Other safety concerns related to the use of transplanted cells are immune rejection and apoptosis. Cell-death associated inflammatory response and toxicity to local tissue bring a high risk of side effects for SCI regeneration [54]. Teratomas, caused by the rapid generation of undifferentiated stem cells, form large tumors, which is safety, concern, therefor limiting the usefulness of exogenous stem cells for SCI treatment [55]. Studies on SCI by using NSPCs found the implanted cells have the ability to migrate to a number of the other CNS structures, which could potentially lead to undesired side effects [24, 56]. Considering all the listed risks, using cell transplanted-based therapy for SCI need to overcome regulatory and manufacturing hurdles for commercial and clinical use.

2.1.3. Endogenous-based Therapies for SCI

Progenitor cells exist in adult human body, which have capacity of producing new neurons and glial cells and can be used as a potential source of cells to replace the degenerated ones [57, 58]. Specifically in the spinal cord, the population of the endogenous cells is significantly reduced after trauma [59]. This dramatic neurogenesis loss is one of the common findings of all proliferation studies in adult spinal cord studies [60]. Around the trauma site, the progenitor cells from near by tissue could be stimulated to proliferate and to migrate toward the injury site. Progenitor cells are born every day in the spinal cord. After injury, cell birth gets a trend to be enhanced [4]. Although the newborn cells likely replace part of the lost cells, functional recovery is still restricted by their sensitivity to the surrounding environment [61]. Another study indicates that endogenous progenitors are differentiated into glial cells, rather than neurons that, depending on their type, can also inhibit the regeneration [62].

The properties and function of endogenous NPCs are governed by both cell-to-cell contact interactions and through a multitude of molecular signals including growth factors [63], cytokines [64] and bone morphogenetic proteins [24, 56]. Deliver of a combination of molecules can promote the survival of endogenous NPCs and direct their cell fate, such as maximum proliferation or differentiation [21]. For instance, in previous studies EGF and FGF delivered to injured spinal cord promoted endogenous NPC survival and directed their cell fate [65].

Using transplanted cells for SCI treatments have been limited by scar formation due to immune response, and inhibited cellular expression. A benefit of using endogenous cells genetically matched to the injured tissue, is that they may reduce the immune response and eliminate an ethical hurdle. There are several approaches trying to enhance the functional recover after SCI. Using enzymes to break down the scars or to deliver growth factors to awaken the regeneration capacity of progenitor cells around the injury site both of which have the potential ability to achieve functional recovery after SCI [4].

2.1.4 Conclusion

Besides the individual problems mentioned above, use of cellulose treatment has also been generally limited by undesired differentiation and limited mechanism in local tissue. Research proved that even the restricted neural stem cells would differentiate primarily towards glial cells rather than neuron cells without specific molecular guidance [29, 66]. Therefor, molecular modification or the use of pharmacologic agents as guidance is important to cellular therapy to achieve the desired tissue regeneration [67]. Mechanism of cells or newly generated tissues is not supportive enough to the surrounding environment. In general, practical research should provide a material that can enhance the cellulose therapy by creating a certain surface to localize implanted cells or to use as a delivery media to prevent damage caused by pressure from surrounding tissue [68]. As a result, cellulose therapy can hardly be approached

individually. Discovery of a proper delivery system will enhance the result of cellulose treatment.

2.2 Molecular Therapy

Delivery of therapeutic molecules has been used by tissue engineering in different regeneration procedures. Along with a proper delivery procedure, various biomolecules can effectively encourage regeneration of endogenous cells or exogenous cells at the demanded site.

For SCI, molecules are mainly used for four purposes. 1. Protecting the surviving axons. 2. Overcoming the inhibitory factors for regeneration. 3. Stimulating proliferation of newly grow neurons. 4. Differentiating stem cells into the required cell types in surrounded environment [69]. To date, many studies have shown the positive effects by delivering one molecule or combined molecules with therapeutic cells in combination therapy.

2.2.1 Protecting the Spinal Cord

The pathophysiology of SCI is a complicated process in regeneration. One of the barriers in current research is the inflammation caused by the immune response around the injury site. In clinical research, delivery of the anti-inflammatory drug methylprednisolone provides several potential benefits to avoid deleterious effects [47].

Erythropoietin (EPO) is a glycoprotein hormone. Cooperating with various other growth factors in erythropoietin, EPO has various functions including promoting angiogenesis, proliferating smooth muscle fibers, and protecting neurons [70]. It can also control inflammation by decreasing lipid peroxidation at the injury site [71]. Using EPO for treatment can functionally increase the level of hematocrit, which may decrease the lesion size [72]. For such reasons, EPO has been involved in further investigation as a neuronal protective molecule for SCI.

Minocycline is a broad-spectrum tetracycline antibiotic with a potential function of anti-traumatic inflammation [73]. Minocycline treatment is mainly used for the purposes of encouraging axonal sparing, reducing lesion size and cavitation [74]. Minocycline can reduce apoptosis of oligodendrocytes and can inhibit the production of microglia. Both of these functions may improve the recovery after SCI [75].

Interleukin-10 (IL-10) is a homodimer protein and it works as anti-inflammatory cytokine with pleiotropic effects in immunoregulation and inflammation [76]. Presenting IL-10 can reduce the lesion size and can protect the SCI site from secondary damage [77]. It has been demonstrated that IL-10 can activate neuronal IL-10 receptors. Activated neuronal IL-10 receptors then provide trophic support and survival cues to overcome the toxic effects on neurons [78].

2.2.2 Overcoming Inhibitions

After SCI, cell loss encourages the cellular reactions by increasing the inhibitors

around the injury site. Inhibitors directly stimulate the glial scar formation and encourage the build up of a physical barrier for axonal outgrowth of the injury [47]. For such reasons, overcoming effects given by the inhibitions after injury is a main subject in SCI studies.

Chondroitinase ABC (ChABC) is an enzyme catalyst and it is involved in various chemical reactions including the degradation of chondroitin sulfate proteoglycan (CSPG). CSPGs are the principal inhibitory component of glial scars, which are highly enriched at an injury site [79]. It works by activating the behavior of astrocytes, which inhibits the neurite outgrowth both in vitro and in vivo [80]. ChABC has been used to degrade CSPGs in some pre-clinical experiments to provide a permissive environment for axon regeneration [81].

Myelin-associated Glycoprotein (MAG) is a trans-membrane glycoprotein localized in periaxonal Schwann cells and oligodendroglial membranes of myelin sheaths. It works as an axonal receptor needed for the maintenance of myelinated axons, and it also works as an axonal signal to promote the differentiation and survival of oligodendrocytes [82]. Briefly, it has a significant positive effect in glia-interactions and myelination.

2.2.3 Stimulating the Axonal Growth

Molecules are strongly related to cell growth, guidance, and existing through out the treatment. Growth factors are either proteins, steroidal hormones, or are a naturally

occurring substance, all of which are capable of stimulating cell proliferation, differentiation, migration, adhesion, and gene expression [83]. They are widely used to stimulate axonal growth. Neurotrophic factors, including nerve growth factor (NGF), brain-delivered neurotrophic factor (BDNF) and neurotrophin-3 (NT-3) have been used to promote axonal growth individually or together. To achieve similar functional recovery other growth factors, for example fibroblast growth factors (FGF), epidermal growth factor (EGF), and Glial cell line-derived neurotrophic factor (GDNF), have also been used to enhance axonal growth.

Nerve Growth Factor (NGF) is a secreted protein used as a signaling molecule to enhance growth, and to maintain the survival of nerve cells [84]. The effect of NGF is strongly related to the population of the where TrkA receptors located [85]. In neuroprotection and neural reparation, NGF plays an important role in the response to injury or disease [86]. Recently there is also a conflict in using NGF for treatment. NGF can lead nociception in SCI models and may induce autonomic dysreflexia [87].

2.2.3.2 Neurotrophin-3 (NT-3)

NT-3 is the third neurotrophic factor in the NGF family. NT-3 has been proven to support the surviving neurons and to stimulate the newly generated neurons [88]. Similar to BDNF, NT-3 works by improving the descended neurons caused by injury, sprouting of spared fibers, and enhancing myelination [89]. The presence of NT-3 also increases the amount of pligodendroglial tissue by reducing the astrogliotic and

microglial responses [90].

Brain-delivered Neurotrophic Factor (BDNF) is a series of secreted growth factors that can promote and support the survival of existing neurons and encourage the proliferation and differentiation of new neurons in both CNS and PNS [91]. Using BDNF can also improve the environment for axonal growth at the injury site by degrading growth inhibitors. Delivery of BDNF can prevent retrograde atrophy of neuronal cells as well as the over express of immune response which inhibits regeneration [92]. All these functions may enhance the axons beyond the lesion site and remeylination in SCI treatment [93]. In clinical trails, there are also evidences indicate that, BDNF therapies have yielded good results in animal models, as well as in underway human subject studies [94].

Besides using individual neurotrophic factors for SCI treatments, deliver of combined neurotrophic factors are also showing positive results to enhance regeneration. Deliver of BDNF and NT-3 have been reported to have the ability to enhance spinal axonal regeneration of a specific population of brain stem neurons [95]. NGF and BDNF together can develop and protect surviving neurons at specific peripheral and brain locations [96]

Fibroblast Growth Factors (FGFs) are belonging to a family including over twenty members working as structurally related signaling molecules [97]. FGF_2, known as FGF-b is widely involved in neuronal protection, neurite outgrowth enhancement, and axonal survival regeneration [98]. The use of FGF in another study promoted both

survival of existing neurons and neurite outgrowth of identified neuronal subtypes [99]. There is no positive clue to promote substantial regeneration by using EGF individually [100]. Delivery of both FGF-2 and EGF together, based on synergic effect of the two growth factors, has been reported to have the function of stimulating the proliferation of neural precursors [52, 101].

Glial Cell Line-derived Neurotrophic Factor (GDNF) is a protein used to promote the survival and differentiation of neurons from progenitors, as well as to prevent apoptosis of motor neurons [102]. Therefore GDNF has been involved in current research as a potential therapeutic agent for the treatment of neurodegenerative related SCI [103]. Using GDNF can also promote survival of other neurons, for example, central spinal motor neurons, sensory neurons, and non-adrenergic neurons [104]. However, due to the inadequate diffusion of GDNF in clinical treatment, up to now, using GDNF individually has been confirmed not to improve the functional recover [105].

2.2.4 Cell Differentiation

To date, most recent research focuses on delivery of molecules to stimulate multifunctional stem cells or progenitor cells for cellulose therapy. A signal to guide the behavior of cell growth into a desired connection is required. To promote differentiation, different types of molecules have been used in previous studies.

Vascular Endothelial Growth Factors (VEGFs) is a signal protein with functions

to stimulate the vasculogeneses and angiogenesis. It works by creating new blood vessels during embryonic development and after physical injury to bypass blocked vessels [106, 107]. The expression of VEGF receptors in the endothelium of both developing and mature blood vessels suggests that VEGF might regulate endothelial differentiation, blood vessel growth, and vascular repair [108].

Platelet-derived Growth Factor (PDGF) is one of the protein-based growth factors regulating cell growth and division. PDGF has five individual forms including PDGF-A to PDGF-D, and homo- or hetero- of PDGF-AB (PDGF-AA, PDGF-BB, and PDGFAB) [109]. Responding through specific binding of PDGFs to PDGF receptor-α or PDGFR receptor -β, delivery of PDGFs play distinct roles in differentiation and development of the progenitor cells [110]. Using PDNF to direct meshenchymal proliferation successfully guides the migration and differentiation during development and in adult animals [111]. There is also evidence to indicate infusing PDGFs to adult CNS functionally supports neuronal differentiation [112]. All these positive results make PDGF popular in SCI research.

Transforming Growth Factor-β (TGF-β) is a superfamily of secreted proteins, including inhibins, activin, anti-müllerian hormone, bone morphogenetic protein, growth/differentiation factors, decapentaplegic, and Vg-1 [113]. This family of molecules have been involved in various biological actions including cell-cycle control differentiation and immune responses [114, 115]. In CNS, three isoforms of TGF-β (TGF-β1, TGF-β2, TGF-β3) are produced by glial and neuronal cells. They have been

found to regulate essential tissue functions in early development and differentiation, neuron survival and astrocyte differentiation [116]. TGF-βs are not neurotrophic in general, but when working with other molecules like FGF-8 or Sonic hedgehog (Shh) together, they exhibit a great promotion for neuronal survival [117]. BMP, a member of the TGF-β family, also promotes neuronal differentiation of cortical ventricular zone precursors [118].

Int/Wingless (Wnt) proteins are belonging to a family of secreted lipid-modified signaling glycoproteins. This family consists of over 17 members and works on the development of CNS [119]. Wnt signaling appears to regulate cell proliferation, apoptosis, migration, and differentiation, which greatly enhance the CNS regeneration [120]. As an essential component of the canonical Wnt signaling system, catenin has been used with different concentrations to guide neuronal progenitors to proliferate or to differentiate [121]. In another study, Wnt has been shown to have the function of leading multifunctional cells to be be less likely to differentiate into oligodendrocytes and astrocytes, which may enhance neuron regeneration [122].

Sonic hedgehog (Shh) is a multifunctional growth factor working in several functions to repair an injured spinal cord including cellular differentiation and proliferation [123]. Shh, providing guidance for neuronal cell differentiation, aids to create a permissive environment. With the delivery of Shh, ventral cord progenitor cells are guided to differentiate into motor neurons and oligodendrocytes. Shh is also found to have the function of leading the axon guidance [124]. Therefor, Shh inhibits the

differentiation of progenitor cells into astrocytes thus reducing scar formation. All these effects in return stimulate myelination and promote neurons survival after SCI [125].

Retinoic Acid (RA) is a metabolite of vitamin A. It has been investigated in serving as a trigger for pre-existing coordinated pathways of neural gene expression, and for inducing neural differentiation [126]. Treatment with high RA concentration has the ability to promote the differentiation of neuronal progenitors into olfactory neuronal cells [127]. RA has been also used to induce posteriorization of ES cells derived neural precursors and to promote differentiation of neural crest derivatives [128]. For these reasons, RA has been considered as an important extrinsic inductive signal that can be used for neural differentiation [127].

2.2.5 Conclusion

In previous research, delivery of individual molecule treatments have been done in SCI, however, with the problems associate with the simple molecule treatment achieved only limited functional recovery. Since the SCI cannot be solved by delivery of any one molecule, the combination therapies came into research field by increasing permissive cues together with reducing non-permissive ones at the same time. As all the different purposes of using molecules in treatments, there are many possible ways to operate the combination procedures. However, how many therapies can be combined and how much invasiveness can be limited are the main concerns in practical research [85].

Protecting survived cell growth, slowing down inflammation and stimulating axonal regeneration need to be done in SCI [10]. According to injury time line, all these requirements are distributed in different periods of the regeneration stages. For such reasons in combination therapy, an on-demand delivery of molecules is required. A delivery system with the ability to sequentially co-deliver molecules in different demanded periods is an essential requirement in combination therapy.

2.3 Delivery of Growth Factors

Growth factors are a group of critical molecules that provide instructions that guide cell development. In tissue engineering including SCI repairs, they have been used to direct cell behaviors, for instance, stimulating cell migration, growth and differentiation [129]. To date, many studies have shown the positive effects by delivering one biomolecule or combined biomolecules in different therapies.

In the previously spinal cord injury studies, one of the limitations of regeneration is observed due to insufficient growth factors support and unregulated level of axonal growth inhibitors [129]. The growth factors, having the characteristic of short biological half-life, require a different mode of delivery than other polypeptide [130]. Therefore, delivering growth factors at the target location at an appropriate time, at a specific concentration and at a specific rate of delivery affects the final regeneration results. For these reasons, extracellular matrices (ECMS) are involved in most of the

growth factor delivery system design.

The release rate of growth factors are based on the diffusion rate of the growth factor from the ECMS material and by rate of degradation of the ECMS material.. In tissue engineering, the specific types of growth factors to be delivered, the time-dependent delivery schedule and the sequential release of growth factors strongly affect cell migration, differentiation and proliferation [130, 131]. The control-released growth factors need to meet the demands of local environments to optimize the efficiency of reparation.

2.3.1 Co-deliver Growth Factors at Same Time

Individual growth factors have their individual functions based on target tissue. Combining appropriate growth factors together has several potential advantages, for example, synergistic effects on growth factors, suppression of drug resistance, and balances the dosage of drugs [132]. Co-delivery of multiple growth factors has been widely used in tissue engineering. It has a more promising future to handle complex process treatments than single growth factor treatments [133].

Co-delivering two factors has been used in a wide range of research fields. To attain the desired co-deliver results, different delivery vehicles also have been designed and tested. In general, most studies first mix the growth factors together and then integrate them into various deliver systems. The mixed growth factors are mostly chosen with the same characteristics. To achieve simple access to the injury site, the

mixed growth factors can be easily delivered by injection, infusion, or (if they are mixed into the scaffold material during the manufacturing process) by diffusion.

Specifically in the studies on SCI, delivering two growth factors can provide better results than delivering a single growth factor. In many studies NT-3 or BDNF have both been shown to provide similar positive effects on the extent of axonal growth from multiple channel scaffolds [129, 134]. It has been demonstrated that simultaneous delivery of NT-3 and BDNF together results in increased neuron survival rates compared with individual delivery [95, 135]. Positive results were also found when delivering combined NGF and BDNF together. Results indicate co-delivering two growth factors can develop surviving neurons at specific peripheral and brain locations [96]. Fibroblast growth factor-2 (FGF-2) used with epidermal growth factor (EGF) has been reported to stimulate the proliferation of neural precursors [52, 101]. All these positive clues light up the regeneration process by co-delivering two growth factors to injured spinal cord.

Delivering three or more growth factors can be integrated into scaffolds by soaking the dry scaffold into a mixed growth factors solution. For example a scaffold consisting of alginate-sulfate/alginate, vascular endothelial growth factor (VEGF), platelet-derived growth factor-BB (PDGF-BB) and transforming growth factor-b1 (TGF-b1) has been proved functionally superior to delivery of FGF-b only [136]. Although the scaffold has more growth factors inside, in many studies, the poor release control from the scaffold limited the potential benefits. A follow-up study needs be

done to compare the benefit of three growth factor delivery scaffolds versus with two growth factor delivery scaffolds.

Delivery of specific combined growth factors in recent studies indicates improved functional recovery versus delivery of individual growth factors. Additionally, most multi-treatment injury studies require sequential delivery of different growth factors at different times in order to achieve optimal regeneration.

2.3.2 Sequential Delivery of Growth Factors

In several medical fields, regeneration studies indicated that sequential release of growth factors or small molecules achieve better regeneration than delivery them at the same time. In bone regeneration, sequential release of BMP-2 with BMP-7, BMP-2 with VEGF, IGF-1 with TGF-β1 has been studied by encapsulating these growth factors into different delivery systems [131, 137, 138]. Positive results indicate delivery of multiple growth factors sequentially can affect different cell behaviors. Enhanced proliferation and stimulated differentiation on an injury site both affect bone formation. Similar sequential release has also been done in angiogenesis studies. Release of VEGF-A_{165} [139] followed by PDGF-BB, angiopoietin-1 (ANG-1), or TAT-HSP27 (transcriptional activator) [140-142] has shown functional improvements after myocardial infarction. Individual delivery of VEGF growth factor can stimulate the blood vessel formation, but forms immature or shot-lived blood vessels. Subsequent release of growth factors like HGF, PDGF-BB, or ANG-1 can recruit mural cells

around the new vessels to strengthen them [140]. Thus, sequential delivery of two growth factors can produce more mature blood vessels and improved functionality of the networks. Multifunctional sequential drug delivery systems have also been designed to deliver combinations of drug and drug, drug and peptide, and RNA and RNA in anticancer studies [143]. In anti-cancer studies, the surface modified agent can recognize the target site first, and then the attached particles can deliver the encapsulated drug at the target site. This delivery system has a potential to reduce the toxicity of encapsulated drug working on non-target cells in the environment and it has greatly improved the efficiency of target site drug delivery [143].

In SCI studies, following the time line after injury, it has been shown that the sequential delivery of growth factors can be used to prevent degeneration of cells. This was achieved by first delivering one specific growth factor to promote cell proliferation, and then delivering another specific growth factor to differentiate the expression of a desired phenotype [138]. Specific to spinal cord studies, the extra requirement of specific required mechanical properties makes it more difficult to design a desired scaffold in an appropriate structure [130].

Several structures have been studied to achieve sequential release of different growth factors. One of the sequential release models that has been tested used multifunctional particles having one drug encapsulated inside the particles and another drug attached to its surface.

2.3.2.1 Sequential Release from Particles

The multifunctional drug delivery particle shown in Figure 5 is composed of a central core with small hydrophobic drugs encapsulated inside and branches of hydrophilic agents attach to the surface. The release behavior from these particles is determined by the order in which they are assembled. The first drug located on the surface of particles having ability to target the cells or tissues is released first, and the other drug encapsulated in particles will gradually release due to diffusion and degradation of the polymer shells. The slight difference in time (5-20 hours) with 20% dosage to release the surface attached drug and encapsulated drug has been teasted by delivering decetaxel (Dtxl) and doxorubicin (Dox) [132]. The purpose of using multifunctional particles in most of the similar research is to achieve simultaneous synergistic effect, in order to enhance tumor vasculature targeting [144-146]. Particle sizes in multifunctional systems are usually designed to be 1-200 nm in diameter. Considering biodistribution and toxicological profiles of any nanoparticles may arise, which could limit using nano size particles in treatments in other fields [147]. Thus, localized co-delivery of factors has potential to increase the safety and efficacy of growth factor-mediated techniques [148]. Sequential release particles are generally used in anti-cancer studies for the purpose of short-duration on target delivery. As a result, few research studies have focused on long-duration controlled release of molecules, including SCI studies.

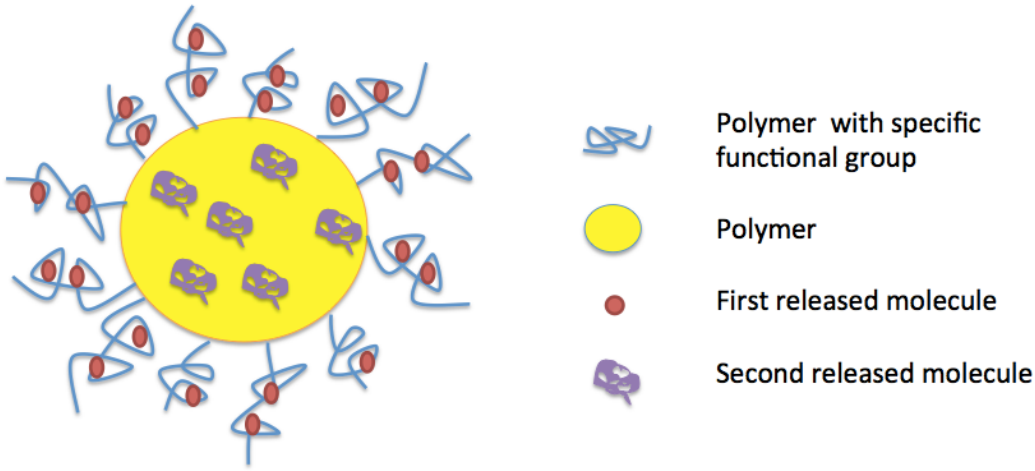

Figure 5 Scheme of two molecules sequentially release from multifunctional particles as drug carrier

2.3.2.2 Sequential Release from Extracellular Matrices

There are several research approaches to release drugs sequentially from extracellular matrices. The design of the structure, controls the directions drugs can be sequentially released from the matrices. The next three sections describe structures that can sequentially release molecules in one, two, and three dimensions.

1）One-dimensional release is achieved by encapsulating different drug layers in a well structure as shown in Figure 6. This well-capped system provides release of drugs just from the top. Ideally the drug placed closest to the surface drug released first, followed by the drug placed at the bottom of the well. The combined titania nanotube (TNT) arrays and the polymer micelles implant has been used in nano-engineered drug delivery systems. Working as a multi-drug carrier, it has ability to sequentially release

different drugs. The different orders drugs in polymer micelles arranged in the device affect the time drugs been eluted [149]. Another similar design to release growth factors sequentially is to load different growth factors in different surface-eroding polymer layers. These layers of polymers are placed in a polystyrene well. Doxycycline loaded in bottom layer is released after simvastatin loaded in the top layer, which makes a small difference in their release times [150]. The use of this type of structured device is limited in tissue engineering because:

- drug delivery is not uniform in all directions,
- the nano size device is difficult to place drugs in by layers
- the well must be removed after drug delivery is complete.

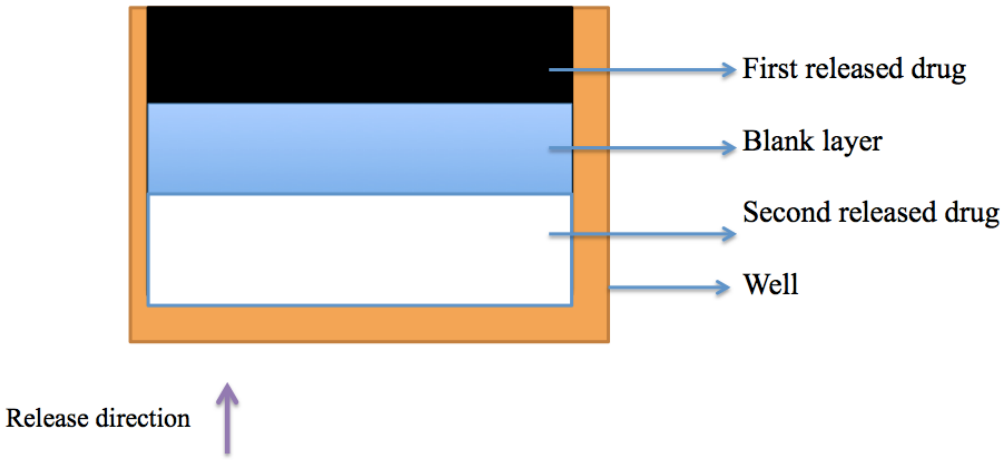

Figure 6 Scheme of two molecules sequentially release from polymer well as a drug carrier

2）Two-dimensional release is achieved by layer coating lengths of scaffold material, as shown in Figure 7. The synthesized sandwich structure system allows multiple layers to be used to deliver different drugs at different times. The sequence of different drugs released is determined by the layer they are encapsulated in. Basically, drug in the outer layers has short diffusion distance to the aqueous environment and releases first. The release of the other drug located in the inner layer is delayed by the degradation of the polymer and sandwich structure, resulting in sustains the release fashion. This two-dimensional deliver system has been tested by various studies.

Using trimethylene carbonate (TMC) based elastomers with an osmotic mechanism release, two growth factors have been used to proliferate of human aortic endothelial (HAEC) and CCL 208 monkey lung epithelial cell lines [141]. Using this system, although VEGF released slightly faster than hepatocyte growth factor (HGF) in the first two days, after the first two days similar release rates were observed for both growth factors.

A different study used a gelatin coating technique to make two similar structures, one to deliver BMP-2 followed by IGF-I, and one to deliver BMP-2 IGF-1at the same time [151]. This test indicated sequential release has positive results in cell culture studies, compared with simultaneous release. Unfortunately no release profile was published.

Coating different concentrations of poly (D, L-Lactide) (PDLLA) layers with BMP-2, IGF-I and gentamicin loaded has been used in other studies to synthesize

implants for soft tissue regeneration. The drug loading implants are designed to release sequentially depending on the order they coated on titanium Kirschner wires (K-wires) [152]. This design has a potential to sequentially release more than two growth factors, but current results indicate the system has poor release control. The time difference among growth factors happened in the first two days and the all of the release finished in three days.

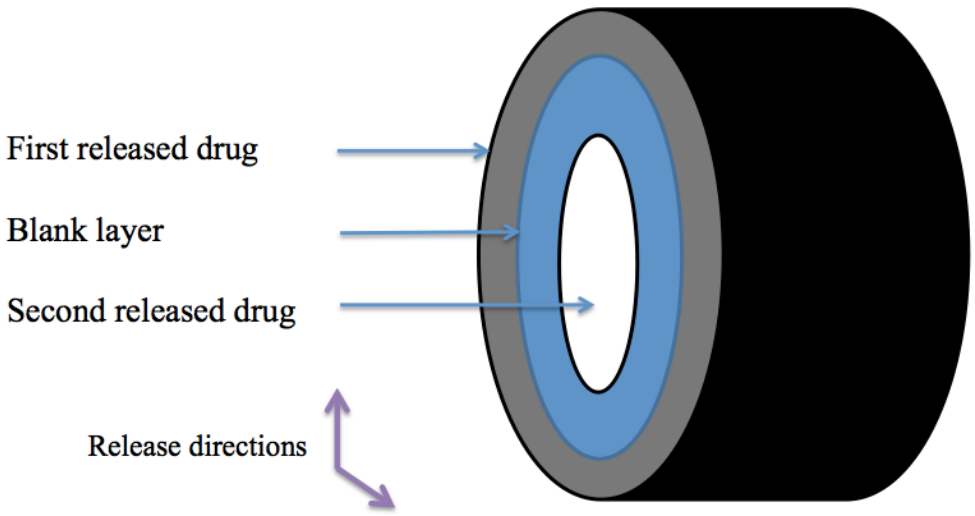

Figure 7 Scheme of two molecules sequentially release from coating based two-dimensional drug carrier

3）For the three–dimensional sequential release case, more types of structures have been designed. These studies take advantage of the fact that different drugs have different release rates from the same or different types of materials. Different

techniques are used to synthesize these drug delivery systems and the release of different drugs at different times is achieved by combining the different drugs in different gels or particles. The most commonly used three-dimensional release structure consists of multiple drugs or drug loaded particles suspended in gels, as shown in Figure 8.

In Figure 8 A, the gel can first release encapsulated drug from system, followed by the drug from small particles. In a bone regeneration study, IGF-1 (drug 2) has been first loaded in gelatin microspheres then integrated in a chitosan gel together with BMP-2 (drug 1)[153]. Release of BMP-2 from chitosan gel has an initial release, and it is followed by a sustainable release of IGF-1 from the microspheres. In soft tissue regeneration, interleukin-2 (IL-2) is incorporated into alginate microspheres. These microspheres are then coated with CpG oligonucleotides to form a sequential release system. These microspheres are then suspended in alginate gel solutions [154]. The CpG located closer to the surrounding environment releases sooner than the IL-2.

In Figure 8 B, two types of drug encapsulated particles are localized in the same gel. This system has been done in two different cases: using different drugs separately encapsulated in the same type of material, and using different materials to encapsulate different drugs. In a brain tissue regeneration study EGF encapsulated in PLGA nanoparticles and erythropoietin (EPO) encapsulated in PLGA nanoparticles coated with poly (sebacic acid). Then the mixed particles are dispersed in a hyaluronan methylcellulose (HAMC) hydrogel [155]. With the coting of poly (sebacic acid) EPO

receives better physical release control and it releases slower than EGF from not coated PLGA nanoparticles.

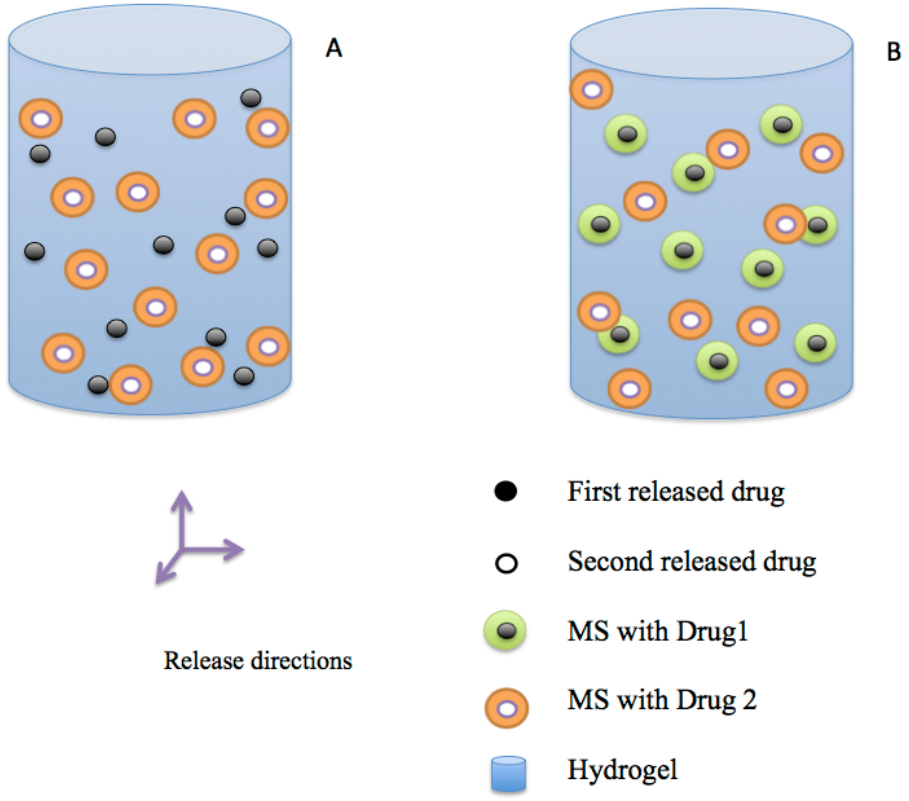

Figure 8 Scheme of two molecules sequentially release from particles in gel structured three-dimensional drug carrier

A model of combine alginate hydrogels in different molecular rate together has been used to deliver VEGF-A and PDGF-BB. Using a high molecular weight alginate hydrogel with PDGF-BB; and a low molecular rate alginate hydrogel with VEGF-A are combined together [156]. PDGF-BB was found to be released more slowly than VEGF-A in first three days, but afterwards this delivery system has similar growth

factor release rates for both drugs due to the use of same gel as the based material.

Microspheres can be combined together through a certain technique to synthesize a scaffold. In a study of PLGA microspheres, IGF-I and TGF-β1 are separately encapsulated using a spontaneous emulsion method. Each type of microsphere is individually used to fabricate a scaffold with dichloromethane vapor method [138]. During release study, IGF-I is released faster than TGF-β1 first fifteen days, and then both growth factors will keep releasing until releases complete in 60 days.

In general, three-dimensional release systems provide longer controlled release of sequentially co-delivered growth factors than other systems. For use in treatment, by changing the base material of the microspheres, the release rate for different drugs can be separately controlled. This has positive implications for multi-step therapies. Never the less there are some technical limitations by using current three-dimensional delivery models. As we mentioned in Figure 8, the gel-structured base has low mechanical properties and poor drug release control. There are few studies that report using other materials or fabrication processes to create three-dimensional sequential release scaffolds

2.3.3 Controlled Release

In sequentially co-deliver growth factors system, most devices or scaffolds are made from natural polymer gels, such as collagen, chitosan, and hyaluronic acid starch. These natural materials are mostly soluble in water and can be fabricated in relatively

mild conditions [157]. In tissue engineering design, these materials also have some common problems limiting use as delivery vehicles. These gels degrade quickly which leads to rapid and burst release of growth factors as well as fast decrease of their structural properties [158]. On natural polymers, increasing the molecular weight distribution, modifying gels with chemicals, and blending polymers together have been done to control the undesired release profile [130].

Synthetic polymers including a member of the α-hydroxy acid class of compounds, poly (glycolic acid)(PGA), poly (L-lactic acid)(PLLA), poly (lactic acid-co-glycolic acid)(PLGA), poly (lactide-co-caprolactone)(PLCL), and poly (ε-caprolactone)(PCL), have been made into nano/microparticles by using the emulsion-solvent evaporation technique [159]. Simply by encapsulating particles into another polymer to form core-shell structures one can efficiently control the release profile. As shown by the results listed in Table 1, sustainable release has been achieved and initial burst has been reduced.

Material	**Encapsulated durg**	**Results**
PLLA/PLGA	Hydrophilic abtibiotics	40% cumulative drug release for 30 days[18]
PLGA/CS	Protein	Reduce initial burst and extend

		release[160]
PLA/PLGA	Hydrophobic drugs	Extend to week-to-month controlled release[161]
PLGA/PLA	GDNF	Sustain delivery of bioactive GDNF over 50 days[162, 163]
POE/PLGA	BSA and CyA	CyA released faster due to double walled structure[164]

Table 1 Sustainable release from double-wall microsphere

Based on the core-shell control release theory, regular microspheres could be integrated into scaffolds, if made of the same material as the shell in core-shell structured microspheres. The acaffold base can now work as the shell providing long-term sustainable release.

2.4 Scaffold Delivery Systems

Different strategies have been used to repair damaged spinal cords. The introduction chapter promising treatments are listed in recent research. When doing practical treatment, a delivery system is required to integrate cellulose therapy, delivery of biomolecules, or both into the injured site. A well-designed delivery system, having the ability to control the release in the treatment site, can achieve maximum results

when combined with positive elements found in current studies.

2.4.1 Co-delivery Systems

2.4.1.1 Mini-pump

An osmotic mini-pump is implanted in vivo, by taking advantage of the osmotic gradient between the tissue and the pump, to infuse determined delivery agents. With a catheter, the pump can deliver liquid molecules directly into the venous or the arterial systems. These pumps have been used to deliver growth factors to aid in promoting neurons to regenerate at a specific time and place. Brain-derived neurotrophic factor (BDNF) [4] and neurotrophin-3 (NT-3) [135] have been delivered using mini-pumps. The benefits of using mini pumps are their small size and ease of access. However, inflammation caused by using mini-pumps has been reported to block the catheter [165, 166]. After therapy, another surgery is required to remove the mini device. This extra surgery causes additional damage to the local tissues. To date, no research has been done to transplant cells by using a mini-pump at the injured site. The required extra surgery and a risk of inflammation limit the use of osmotic mini-pumps in SCI repairs in current research.

2.4.1.2 Oral

Oral delivery of growth factors is the most straightforward way for treatment. Benefits of oral deliver include easy access and time control [167] therefor oral delivery

has been used in early research. Positive results have been reported by taking growth factor orally. Taken orally, a sufficient quantity of derived growth factors can reach the injury site to effect treatment [168]. When taken orally, due to their poor absorption rate, an increased consumption dosage of biomolecules is required. This large general concentration of biomolecules in the blood, may result in potential side effects, and may affect non-target tissues in long time therapy [161].

2.4.1.3 Injection

Injection can deliver biomolecules and cells directly into the injury site, strongly enhancing local regeneration. Injection has proved to provide positive results in delivery of both liquid biomolecules and cell loaded injectable gels. According to the limit by using a catheter through injection, a solution or non-concentrated gel is required as foundation material [101, 169]. Release of biomolecules from low density solutions cannot be well controlled, with release finish right after injection, thus greatly limiting their use in long-term treatment [4]. Multiple injections have been used to overcome this disadvantage, but having the added risk of causing extra damage to the local tissue.

2.4.1.4 Scaffold

Specifically in SCI, historical research proved that without tension between the tissues, surgical treatment could reconstruct the nerves, transfer tendon, and muscle to

help recovery [170]. However, after injury, a nerve gap (less than 5mm) caused by sutured back ends of tissue creates a hurdle for using surgical treatment without a bridge [171]. For such reason, scaffolds are involved in the design of recent research.

Nerve guidance scaffolds have been widely used in combination therapy. Working as a bridge in between damaged tissue, scaffolds have the advantages of preventing scar formation, supporting attached cells, and delivering molecules. In cellulose therapy, work has been focused on portfolio strategies including direct cell implants, pre-cultured tissues implants, and direct in situ tissue regeneration [172], in which scaffolds were used as a foundation. Biomolecule-encapsulated scaffolds can be used as carriers, thus enabling biomolecules to be sustainably released at the specific site with the benefit of minimizing systemic blood-drug concentration related side effects [173]. Scaffolds can provide a substrate to fill cystic cavities [174] and to slow down the formation of scar tissue and lesion build up [175].

Previous studies also obtained positive results from integrating different elements together in one delivery system. The combination of using encapsulation cell technology (ECT) of immobilized therapeutically active cells [176] and bidirectional diffusion of molecules [173] within a three-dimensional microenvironment matrix between the damaged tissues has been studied in recent research [177, 178]. Better functional recovery has been achieved by using such multi-therapy integrated biomaterial scaffolds in treatment [179].

To avoid problems with using scaffolds as an implant device, some additional

critical elements need to be taken into consideration during the design. Biocompatibility, adequate biodegradability, mechanical properties, low toxicity, malleability, and ease of manufacture [180] are commonly used to qualify a scaffold in tissue engineering [181].

2.4.2 Materials

Scaffolds synthesized of proper materials can efficiently bridge the nerve gap by creating a microenvironment similar to local tissue thus promoting cell growth and differentiating the multifunctional cells with permissive surroundings [178]. To rebuild the microenvironment, both natural and synthetic materials have been tested in research. There are several critical properties in choosing materials for research that need to be taken into consideration at the beginning of the design. Firstly, the scaffold must be constructed of a biocompatible material. Using such a device implanted in vivo, minimizes the chances of inflammation or allergic reactions caused by the immune system. Secondly, materials with the ability to deliver biomolecules and encourage cell attachment provide better modification possibility. Thirdly, the material should be strong enough through out the reparation period to avoid secondary damage that could be caused by premature scaffold collapse.

2.4.2.1 Non-degradable Materials

Non-degradable materials benefit from being simple to synthesize, having fewer batch differences [159] and remaining stable in vivo. After the fabrication process, all

the parameters can be well maintained, particularly the mechanical properties will not change over time. Additionally non-degradable materials are superior to degradable materials, because they produce no toxicity degradation products, therefor allowing them to be used in implant device design. In current research, commonly used nondegradable materials are poly (2-hydroxyethyl methacrylate) (PHEMA [182] and Polyvinylchloride (PVC)[159].

The problem in using PVC for further study is from the initial fabrication process, specifically with the organic solvent used during the fabrication process. A chance of residual solvent causing unacceptable toxicities and a risk of side effect on target animals limited the use of this material in clinical applications [183].

There are some common limitations of using non-degradable material to synthesize a delivery system. Firstly, there is a high risk of inflammation during the regeneration process, which may block the reconnection of neurons to proper targets. Then the well maintained-structured scaffolds are more difficult for further modification used for either cell attachment or biomolecule delivery. Implants constructed of such non-degradable material also have a problem in that, for in vivo studies, they need to be removed after treatment is complete. As a result it is more suitable for a lifetime replacement in bone tissues than the spinal cord.

2.4.2.2 Degradable Materials

Degradable materials have played an important role in a number of tissue

engineering attempts. Synthesized degradable devices do not have to be removed with a second surgery after the regeneration process is finished, and therefor perfectly meet the demand of temporary presence of a scaffold in reparation. Mostly these materials came from natural resources with porous rich structures providing potential space for molecules or specific cell adhesion [184]. Most research also proved that degradation products from biocompatible degradable materials that naturally exist in the human body and can be flushed out by normal metabolic processes. As a result, there is less chance for inflammation will occur [185]. In the study of SCI most of the biodegradable materials used are either cross-linked polymers or co-polymers. Newly regenerated tissue takes the space of the degraded polymer and rebuilds the connection to achieve functional recovery after injury.

Using biodegradable material to fabricate scaffolds has some elements affecting the selection of materials. From Table 2, we can see the advantages and disadvantages for most biodegradable materials. Natural materials are easily harvested from resources but come with complicated purification processes. Some highly cross-linked materials have been integrated into other strategies. To enhance the mechanical strength, some materials are modified with toxic agents. High water solubility also results in low concentration in final material products, leading a fast degradation. For long-term repair processes, a synthesized material with sufficiently long lasting mechanical properties, desired degradation speed, and with the ability to accept therapeutic agents is an ideal choice for device design.

The poly (glycolic acid)/poly (lactic acid)(PGA/PLA) family of compounds is a member of the α-hydroxy acid class of compounds. This family includes poly (glycolic acid)(PGA), poly (L-lactic acid)(PLLA), poly (lactic acid-co-glycolic acid)(PLGA), poly (lactide-co-caprolactone)(PLCL), and poly (ε-caprolactone)(PCL). This family of compounds has been found to have various degradation times, mechanical properties based on different ratios of monomer units, stereochemistry of monomer units and molecular weight distribution [159].

Material	Advantages	Disadvantages
Collagen	Naturally exist in animal tissue. Easy process integrate cell and bimolecular treatment.[159]	Complicated purification process.[186] Poor mechanical property.[187]
Chitosan	Excellent biocompatibility and easy harvest. Degradation compressive strength and cell attachment can be controlled. [188]	Poor mechanical property. [189]
Alginate/Agarose	Easily fill the cavity and low immune response.[190]	Mitogenic and cytotoxic impurity.[191]

Hyaluronic Acid	Biocompatible，completely degradable[192], and non-toxic. [193]	High water solubility and fast dispersesion.[194, 195]
Polyethylene glycol	Reduces the volume of cavity at injury site.[196]	Low protein and cell adhesion properties.[183]

Table 2 Advantages and disadvantages of using different biodegradable materials

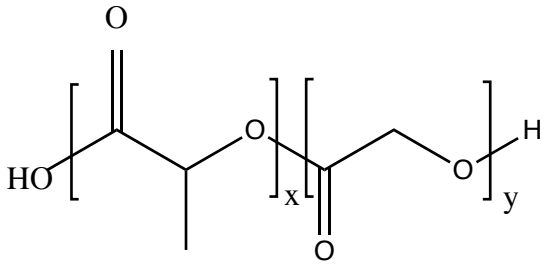

poly(lactic-co-glycolic acid) (PLGA)

Figure 9 Structure of Poly (lactic acid-co-glycolic acid)(PLGA)

PLGA, shown in Figure 9, is a commonly used material in drug delivery studies and in the tissue engineering field. It has the properties of being biocompatible, biodegradable, and (depending on the ratio of lactice to glcolide and molecular weight) it has a wide range of degradation speed and mechanical properties. These properties make it flexible for drug delivery device design [197]. Its decomposition products of lactic acid and glycolic acid can easily metabolized by the human body, thereby it minimizing systemic toxicity. PLGA has been used to make scaffolds seeded with

murine neural stem cells. Such scaffolds have been shown to provide an improvement in functional recovery [198]. The ratio of lactic acid and glycolic acid affects the degradation rate of the materials. Previous research has studied the physical properties of materials created using the super critical carbon dioxide foaming method with lactic acid to glycolic acid ratios of 85:15, 75:25, 65:35 and 50:50., It was found that co-polymers with lower ratios of lactic acid to glycolic acid have smaller pores and less porosity [199]. The PLGA degradation rate is directly related to the ratio of lactic acid to glycolic acid. Lower ratios of lactic acid to glycolic acid enhance the degradation rate of PLGA. Based on the same theory, PLGA degrade faster than PLLA [200, 201].

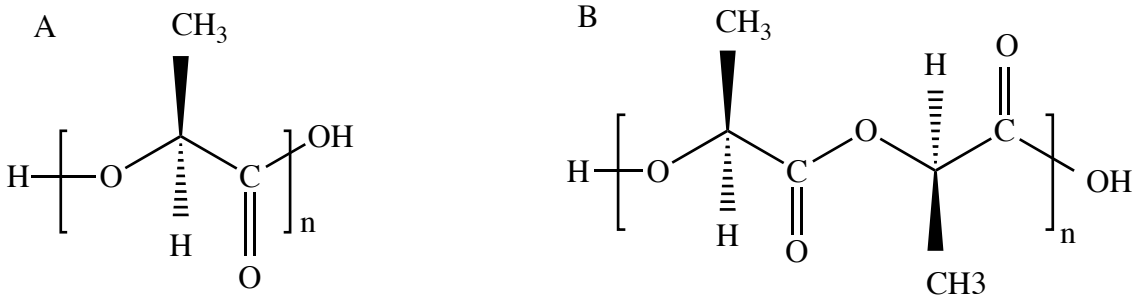

Figure 10 Structures of Poly (L-lactic acid)(PLLA) and Poly (DL-lactic acid)(PLLA)

Poly (lactic acid) (PLA) based products are biocompatible materials and can be degraded by hydrolysis. Based on the combination of the naturally occurring monomers L-lactic and D-lactic can form three types of poly lactide: poly (L-lactide)(PLLA), poly (D-lactide) (PDLA), and poly (DL-lactide) (PDLLA) [202]. In the human body, only

L-lactic is produced. For this reason, partially crystalline poly (L-lactic acid)(PLLA) and amorphous poly (DL-lactic acid)(PDLLA) that degrade into L-lactic acid that subsequently metabolizes into water and carbon dioxide are widely used in medical fields. The structure of PPLA and PDLLA are shown in Figures 10A and 10B. PDLLA and PLLA have different mechanical properties due to their different crystallization. PLLA has better mechanical properties than PDLLA, which makes it more commonly used in research fields [203]

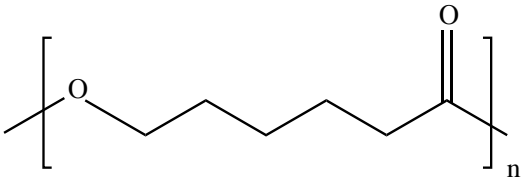

Poly Caprolactone (PCL)

Figure 11 structure of Poly (ε-caprolactone)(PCL)

PCL, shown in Figure 11 has been studied and exhibits outstanding mechanical properties, flexibility, and biocompatibility [204]. Compared with PLGA and PLLA, it degraded more slowly than PLLA, and has been more used for long-term scaffold design [203]. PCL has a semi-crystalline structure with a lower glass transition temperature (T_g) of -60 ^oC. At room temperature PCL exists in the rubbery state and has better mechanical properties than other α-hydroxy acid compounds [205]. The slow degradation speed of PCL makes it suitable for a long-term sustainable delivery [17].

Each member of the α-hydroxy acid class of compounds has its unique degradation

speed and mechanical properties. They have been used individually to fabricate scaffolds for different reparation purposes but the potential of blending different compounds together [206] or reorganizing the structures of integrated materials in determined devices, means more varieties of different mechanical properties and different degradation speeds.

2.4.3 Fabrication Techniques

Co-polymers used to deliver biomolecules can be synthesized through different techniques into various forms and sizes. Stability and delivery speed of the same biomolecule from the same material can be different based on various fabrication techniques. To meet the requirements of specific device design, fabrication techniques need to be involved during the initial design.

In scaffold design, pore size, porosity, and inter-connectivity strongly influence cell growth and factors release profile [84]. Thus, a proper fabrication process is required in scaffold design.

In Table 3 the advantages and disadvantages of different processes to synthesize scaffolds are listed. Synthesized scaffolds working as implanted devices delivering biomolecules need to maintain the bioactivity of the delivered molecules throughout the whole treatment period. For this reason high temperature and solvent involved processes, which may denature or reduce bioactivity of the biomolecules, cannot be used.

Carbon dioxide, an important commercial and industrial solvent with advantages of low toxicity, low cost, low processing temperature, high environmental impact, high stability, and high solubility of most compounds, has been involved in different polymer synthesized drug delivery systems in tissue engineering studies. After reaching its critical temperature (304.25K) and critical pressure (72.9 atm), carbon dioxide turns into a supercritical fluid with gaseous filling and liquid density. This supercritical fluid can easily plasticize a wide range of polymers according to research studies [207]. Under this condition, polymers are plasticized, lowering their viscosity, and allowing them to suspend insoluble particles [208].

Synthesize process	**Advantages**	**Disadvantages**
Electro Spinning	Highly interconnected scaffold	Organic solvent is required[209]
Solvent Casting Particulate Leaching	Simple handling process and high porosity	Poor morphologies and organic solvent required [31]
Emulsification freeze-drying	Control over porosity and pore size	Organic solvent is required[210]
Liquid-Liquid phase separation	Control over porosity and pore size	Difficulty in morphology control[211]

CAD/CAM Technology	Over control architecture	High process temperature, solvent required[212]
Polymer melt process	No organic solvent process and control over porosity	High Temperature required [213]

Table 3 Advantages and disadvantages for various scaffold syntheses methods

Polymer and biomolecules are dissolved evenly in supercritical CO_2 when synthesizing a delivery device. Then the mixture expands, the polymer declines in solubility and crystallization in that supercritical environment. Porous structured scaffolds foamed by this process provide a template and guidance for cell growth. Pore sizes can be controlled during the fabrication process. By adjusting the temperature, the pressure, the molecular weight, and the chemical composition of polymers, scaffolds with different porosities can be made[208]. This solvent free process elevates protein activity for long-term release study [207].

In this research this solvent free process is used to create scaffolds that can release two biomolecules according to the desired long-term release profile.

Chapter 3. Experimental

3.1 Materials

Polymers: Poly （DL-lactide-co-glycolide） with 50:50 monomer ratio (PLGA 50 : 50) easter terminated at an inherent viscosity range (I.V.) of 1.0-1.3 dL/g in $CHCl_3$, Poly (ε-caprolactone) easter terminated at an (I.V.) range of 1.0-1.3 dL/g in $CHCl_3$, Poly (L-lactide) easter terminated at an (I.V.) range of 0.9-1.2 dL/g in $CHCl_3$, Poly (DL-Lactide-co-ε-caprolactone) (80:20) initiated with 1-Dodecanol at an (I.V.)=0.85 dL/g in $CHCl_3$ were purchased from Lactel Absorbable Polymers (Birmingham, AL, USA).

Bioassays and biomolecules: Human FGF-basic Elisa Development Kit (EDK) and Human EGF (EDK) were purchased from PeproTech, (Rocky Hill, NJ, USA). BCA Protein Assay (linear working range of 5-250μg/mL) and Micro BCA Protein Assay Kit (linear working range of 0.5-20μg/mL) were purchased from Pierce, (Rockford, IL, USA). Albumin from bovine serum was purchased from Sigma, (St Louis, MO, USA). Human FGF-basic growth factor and Human EGF growth factor were purchased from PeproTech, (Rocky Hill, NJ, USA).

Chemicals: Sodium Azide was purchased from BDH Inc., (Toronto, ON, Canada). Phosphate buffered saline tablet (pH 7.4) and Tween-20 were purchased from Sigma,

(St Louis, MO, USA). 2,2'-azino-bis(3-ethylbenzothiazoline-6-sulphonic acid), ABTS substrate liquid was purchased from aMRESCO, (West Chester, PA, USA). Ethyl Acetate was purchased from VWR International LLC, (West Chester, PA, USA). Dichloromethane (DCM) was purchased from ACROS ORGANICS, (NJ, USA).

3.2 Scaffold Preparation

Scaffolds in this research were synthesized in two different steps. Microspheres were synthesized first, and then integrated into tube shaped scaffolds based on the different dissolvability of PLGA and PLLA/PCL in ethyl acetate.

3.2.1 Microsphere

Based on different requirements of tests, microspheres with different types of molecules encapsulated were used to create different types of scaffolds.

3.2.1.1 Blank Microsphere

The fabrication of microspheres follows the oil-in-water (o/w) single emulsion evaporation process. Dissolve 1000.00 mg of PLLA in 7.50 ml DCM at room temperature. Add the mixed solution into 30.00 ml 1% (W/V) PVA (the internal aqueous phase) with homogenizer (Brinkmann, NJ, USA) to get the emulsion mixture. Add the emulsion mixture into 300.0 ml 0.1%(W/V) PVA (the internal aqueous phase) and mechanically stir for 3 hours at 300 rmp until the DCM is evaporated. Centrifuge

the emulsion at 1000 rmp for 10 min and wash the microspheres collected at the bottom 5 times with dd-water. Freeze-dry and store the microspheres at -20 °C until they are used in further experiments. The same process is used to prepare the PCL microspheres.

3.2.1.2 BSA Loaded Microsphere

Finely grind BSA powder with a mortar and pestle to obtain 100.00 mg of refined BSA (lyophilized powder, ≥96%). Dissolve 1000.00 mg of PLLA in 7.50 ml DCM at room temperature. Add the 100.00 mg of refined BSA into the mixture of PLLA and DCM. (BSA: polymer / 1:10 in wt%). According to solubility table, BSA is suspended in DCM solvent mixture. The s/o mixture needs to be kept stirring adding it into 30.00ml 1%(W/V) PVA (the internal aqueous phase). Follow the same procedure in 4.2.1.1 to prepare BSA loaded microspheres.

3.2.1.3 Growth Factor Loaded Microsphere

Before opening the bottle of growth factor, centrifuge it at 3000 rpm for 5 minutes. Dilute 1 mg of EGF in 1.00 ml dd-water. Transfer the growth factor solution into a 50.0 ml volumetric flask with together with 1000.00 mg BSA and add dd-water to obtain 50.0 ml of solution. Freeze-dry the solution to get EGF-BSA mixed powder.

Finely grind EGF-BSA powder with a mortar and pestle to obtain 100.00 mg of refined EGF-BSA. Dissolve 1000.00 mg of PLLA in 7.50 ml DCM at room temperature. Add the 100.00 mg of refined EGF-BSA into the mixture of PLLA and

DCM. (EGF-BSA: polymer / 1:10 in wt%). According to solubility table, EGF-BSA is suspended in DCM solvent mixture. Follow the same procedure in 4.2.1.1 to prepare growth factor loaded microspheres.

3.2.2 Scaffold Tube

Dissolve 1000.00 mg PLGA in 10.00 ml ethyl acetate. Then add 1000.00 mg prepared microspheres (the specific type of microspheres depends on the requirements of specific tests). Using a mechanical stirrer mix the ethyl acetate PLGA and microsphere mixture in a 40 ml beaker until a uniformly mixed. Pour the mixed solution into a cylinder-shaped glass vial. As shown in Figure 12, dip a 3.00 mm (diameter) glass rod into this mixed solution for 30 seconds, then pull out the glass and using a drill rotate the rod at 300 rpm. Keep the glass rod in parallel position to the ground and kept rotating for 30 minutes until the ethyl acetate completely evaporated. While the glass rod is rotating, return the mixed solution to the 40 ml beaker and continue stirring it. Repeatedly continue to transfer the mixed solution into the cylinder-shaped glass vial to the same height, dip and rotate the glass rod, return the mixed solution to the stirring beaker, until the desired diameter is achieved. (4.00 mm for PLLA (MS)-PLGA scaffolds, 4.20 mm for PCL (MS)-PLGA scaffolds.) The quantity of materials prepared is sufficient for six scaffolds of 30.00 mm in height. After the dip-coating process, keep the glass rods under a 20 bar vacuum, for another 7 days ensure all the solvent is evaporated.

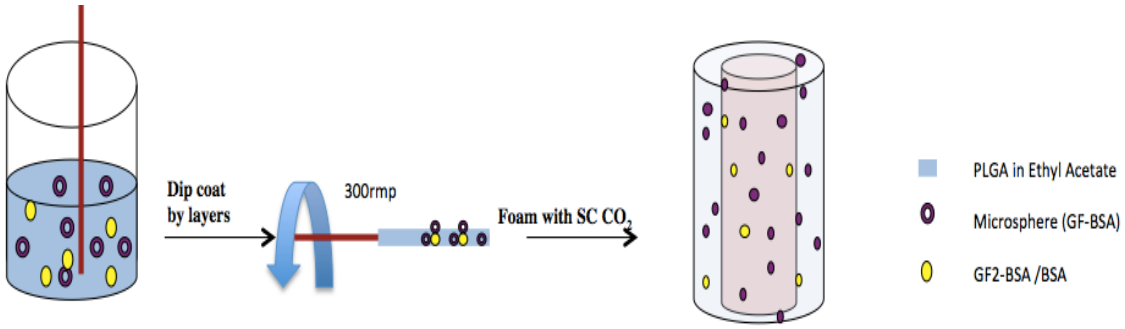

Figure 12 Dip-coating synthesized process

Place each dried sample into a Teflon mold and seal the top and bottom with screws. Place all loaded mold into high-pressure chambers and foam with carbon dioxide at 5.38 MPa (780psi). After 7 hours 30 seconds (saturation time 1-4 hours according to reports [214]), release the pressure and keep the samples at room temperature overnight (around 16 hours). Unload scaffolds from the molds, and then remove the glass rods from the center of the scaffold. Keep all samples at -20 °C in the freezer (according to polymers and growth factors storage condition) within a zip bag. Before using for any test, allow the samples reach room temperature before open the zip bag.

To prepare BSA or FGF-b loaded PLGA base tubes, add 100.00 mg BSA or FGF-b and BSA mixture, depending on experiments requires, in the mixed solution before the dip-coating process. For making growth factor FGF-b encapsulated tubes, mix 40.00 mg of freeze-dried FGF-b-BSA mixed powder (prepared using the same

process as was used for the EGF growth factors in 4. 2. 1. 3) with 60.00 mg BSA together (add up to 100 mg), then add it into the polymer solution.

3.3 In Vitro Release

Release studies of EGF growth factor, FGF-b growth factor, and BSA were done. BSA is widely used in drug release studies to mimic the release behavior from delivery systems, which has similar molecular weight and solubility as EGF and FGF-b. The easy detection, long lasting stability, and less sensitivity to harsh environments (specifically pH) together make it commonly used as a model for protein-based drugs in release studies. The problem with using only BSA in this research is in order to measure the release profile from two different parts of one scaffold, release behaviors must perform by at least two tests. The differences in amount of BSA loaded on different scaffolds through the fabrication process can affect the release profiles. In the first test the BSA is impregnated into location one a scaffold, and the second test the BSA in impregnated into a second location of a second scaffold, and the two release profiles would have to be combined. To achieve release profiles from one scaffold using different growth factors, on the other hand, can be detected separately by using specific ELISA-kits in a complicated mixed solution. For this reason a single test can be used to determine their separate release profiles, and which part of the scaffold they came from. In this project, to confirm the final result, both growth factor release and

BSA release studies were done.

3.3.1 BSA Release

To validate the BSA release profiles from the different types of scaffolds, samples are prepared following Table 4. The scaffolds must first be synthesized using the previously described processes. To create the sample, in an individual microtube (blocked with BSA) immerse 50.00±5.00 mg of each component shown in Table 4 is immersed in 1000.0 µl PBS solution (with 0.1wt% sodium azide as a bacteriostatic agent). All the samples were then incubated (Junior purchased from Isotemp, MA, USA) at 37 °C. Then 500.0 µl sample of each solution were extracted at day 1, 2, 4, 6, 8, 10, 12, 14, 18, 22, 26, 30, 34, 38, 42 and all the samples were kept in a freezer at -20 °C before being tested by BCA protein assay together with micro BCA protein assay. After extracting a sample, each solution was topped up with 500.0 µl fresh PBS (with 0.1% W/V sodium azide). All the required samples were collected in 42 days. Before performing the BCA test, incubate all collected samples to 37 °C.

Using a 96-well plate: for each sample, place 25.0 µl of the sample into 3 separate wells. Then for each concentration of standard solution, place 25.0 µl of standard solution into 3 separate wells. Then add 200.0 µl of mixed BCA-kit (reagent A: B / 50: 1) in each well. Incubate at 37 °C on a shaker at 100 rpm for 30 min. The concentration of BSA in each well can be determined by color conversion and can be measured by UV absorbance at 562 nm. The measurement is performed by using an Epoch plate

reader (BioTek, VT, USA).

When the concentration is below the detection limit of the BCA-kit (20 μg/ml) a BCA-micro protein assay kit is used to measure the concentration. Using a 96-well plate: for each sample, place 150.0 μl of the sample into 3 separate wells. Then for each concentration of standard solution, place 150.0 μl of the concentration of standard solution into 3 separate wells. Then add 150.0 μl of mixed BCA-micro protein assay kit (Reagent A: Reagent B: Reagent C/ 25: 24: 1) in each well. Incubate at 37 °C on a shaker at 100 rpm for 30 min. The concentration of BSA in each well can be determined by color conversion and can be measured by UV absorbance at 562 nm. The measurement is performed by using Epoch plate reader (BioTek, VT, USA).

Group / BSA location	1	2	3
PLLA Microsphere	BSA	/	BSA
PLGA base	/	BSA	BSA
Group / BSA location	①	②	③

PCL Microsphere	BSA	/	BSA
PLGA base	/	BSA	BSA

Table 4 Components in each group of scaffold in BSA release test

The concentrations of BSA, tested by either BCA-kit or BCA-micro kit, fit linear Eq1.

$$C_{t_n} = a \times Abs_{t_n} + b$$

Eq 1

Where

Abs_{t_n} stands for absorbance read at t_n test point

C_{t_n} stands for concentration of BSA C_{t_n} at the point

a and b are equation parameters related to standard curve on each plate.

Quantity of protein can be calculated following Eq2

$$m_{t_n} = C_{t_n} \times V$$

Eq 2

Where

m_{t_n} stands for amount of protein

V stands for volume of solution sample in each microtube in release study

Released protein samples at each pick up point can be detected by BCA-Kit or BCA-micro protein assay kit. The absolute amount of protein released during the period needs to be calculated. As per the procedure mentioned above, after extracting 500.0 µl of each sample solution, top up each solution with 500.0 µl fresh PBS (with 0.1% W/V sodium azide). Each time 500.0 µl of each sample solution is replaced with 500.0 µl of fresh PBS, only half the mass (concentration) of the BSA remains in the sample solution. The absolute amount of released BSA is calculated using Eq 3 when (n>1).

$$m_{p_n} + \frac{1}{2} m_{P_{n-1}} = m_{t_n}$$

Eq 3

Where

m_{p_n} stands for absolute amount of BSA released at point n

$m_{p_{n-1}}$ stands for absolute amount of BSA released at point $n-1$

m_{t_n} stands for detect amount of BSA released at test point n

When (n=1), use Eq 4.

$$m_{P_n} = m_{t_n}$$

Eq 4

By using the results of Equitation 3, (when n>1) Eq 5 is used to calculate the BSA release profile over time from each scaffold.

$$m_{A_n} = m_{P_n} + m_{A_{n-1}}$$

Eq 5

Where

m_{A_n} stands for the accumulation of BSA released up to point n

$m_{A_{n-1}}$ stands for the accumulation of BSA released up to point $n-1$

At the first pick up time point (when n=1), accumulation of BSA released is the same as detected amount of BSA, shown in Eq 6.

$$m_{A_n} = m_{t_n}$$

Eq 6

3.3.2 Growth Factor Release

For growth factors the release profiles were measured by using an enzyme-linked immunosorbent assay (ELISA) test. ELISA test is a known technique used in quantifying specific concentrations of determined target biomolecules in complex solutions. The concentration of target biomolecule present is determined by color conversion and can be measured by UV absorbance at 450nm with a correction at 650nm. To make sure the kit is designed to measure the growth factor used, the Human FGF-basic (EDK) Elisa Development Kit and the Human EGF (EDK) Elisa Development Kit should be purchased from the same company that supplied the EGF and FGF-b growth factors. Each kit can quantifies only the amount of the respective growth factor released from the synthesized scaffolds.

To create the sample, in an individual microtube (blocked with BSA) immerse 100.00±5.00 mg of each component shown in Table 5 into 1000.0 µl PBS solution (with 0.1% W/V sodium azide as a bacteriostatic agent). All the samples are then incubated at 37 °C. Extract 500.0 µl sample of each solution at day 1, 2, 4, 6, 8, 10, 12, 14, 18, 20, 24, 30, 36 and keep all the samples in a freezer at -20 °C until tested with the appropriate ELISA-kit. After extracting a sample from each solution top up each solution with 500.0 µl fresh PBS (with 0.1wt% sodium azide). It takes 36 days to collect all the required samples. Before performing the ELISA-kit test, incubate all collected samples to 37 °C.

Group / Materials	(1)	(2)
Microsphere	PLLA (EGF-BSA) 50% Wt	PCL (EGF-BSA) 50% Wt
PLGA base	FGF-b (BSA) 50% Wt	FGF-b (BSA) 50% Wt

Table 5 Components of each scaffold in growth factors release test

Dilute the concentration of the samples to the working range required by each ELISA kit (EGF Elisa Development Kit with specific working range of 10-1000 pg/mL and FGF-basic Elisa Development Kit with working range of 40-4000 pg/ml). By following ELISA protocol (in attachment), the colored product can be found 5 minutes after the ABTS substrate is added. The measurement is performed by using Epoch plate reader (BioTek, VT, USA). Based on the standard samples on each plate, the accumulation releases of the growth factors are calculated with equations 1-6.

3.4 Characterization of Scaffold

3.4.1 Scanning Electron Microscopy

Scanning Electron Microscopy (SEM) in this project was used to present morphologies of all scaffolds. Structures and changing of morphology regarding to the polymer degradation are shown in visualized pictures. All of the samples used in this SEM characterization were synthesized following the process in 4.2 with components of microspheres and PLGA base listed in Table 6.

Groups / Material	A	B	C
Microsphere	PLLA (BSA) 50% Wt	PCL (BSA) 50% Wt	/
Base	PLGA (BSA) 50% Wt	PLGA (BSA) 50% Wt	PLGA (BSA) 100% Wt

Table 6 Components of each group of samples used by SEM and compressive test

Perpendicularly cut synthesized scaffolds into ring sections. Stick each ring shaped sample onto a stub and test with Phenom Pro desktop SEM under 5kV

(PHENOMWORLD, Eindhoven, Netherlands)

3.4.2 Degradation Study

Degradation study on synthesized scaffolds is characterized by two parameters: the changed structures (SEM) in 4.4.2.1 and the mass loss 4.4.2.2 of scaffolds over time.

3.4.2.1 Structure

Create 45 rings following the procedure in section 4.4.1, 15 (5 sets of 3) from each of the groups/materials in Table 6. For each of the 45 rings, place them into an individual microtube and add 1000.0 µl PBS solution to each microtube. Incubate all the samples at 37 °C. After (1, 2, 4, 6, 8, 10, 12, 14, 18, 20, 24, 30, 35, days) extract 500.0 µl of each solution from each microtube, and throw it away, and then top up each microtube with 500.0 µl fresh PBS. In addition, each week remove 1 set of 3 microtubes from each of the groups/materials and wash the rings with dd-water, freeze dry the microtubes with the rings, and keep them in a freezer at -20 °C. It takes 5 weeks to collect all the required samples. After the 5 weeks: before performing the SEM test let the microtubes warm up to room temperature before opening the microtubes (to avoid up take of moisture from the surrounding environment).

Stick each ring shaped sample onto a stub and test with Phenom Pro desktop SEM under 5kV (PHENOMWORLD, Eindhoven, Netherlands) to obtain pictures of the degradation of the ring material over time.

3.4.2.2 Mass Loss

Degradation is a critical parameter for biodegradable materials, which affects the drug release profile and the mechanical strength of the material over time. The in vitro degradation of scaffolds is presented by mass loss based on Eq 7.

$$\%degradation = \frac{m_{st_0} - m_{st_n}}{m_{st_0} - m_t}$$

Eq 7

Where

m_{st_0} stands for the initial weight of scaffold and the tube

m_{st_n} stands for weight of scaffold and tube at week n

m_t stands for weight of tube

Groups / Material	a	b	c
Microsphere	PLLA (50% Wt)	PCL (50% Wt)	/
PLGA base	PLGA (50%	PLGA (50%	PLGA (100%

	Wt)	Wt)	Wt)

Table 7 Components of each group of samples used in mass loss study

Following the Table 7, create 54 sample scaffolds, 18 (6 sets of 3) from each of the groups/materials, so each tube weighs 60.00±3.00 mg. For each of the 54 sample scaffolds: weigh a microtube used as m_t, then place a sample scaffold into the microtube and weigh the microtube again to figure out the weight of the sample scaffold in the microtube. Record this value and use is as m_{st_0} to be used in Eq 7 for this sample scaffold. Then add 1000.0 µl PBS solution to each of the microtubes. Incubate all the samples at 37 °C. After (1, 2, 4, 6, 8, 10, 12, 14, 18, 20, 24, 30, 36, 42 days) extract 500.0 µl of each solution from each microtube, and throw it away and then top up each microtube with 500.0 µl fresh PBS. In addition, each week remove 1 set of 3 microtubes from each of the groups/materials and wash the sample scaffolds with dd-water, and freeze dry the sample scaffolds in their microtubes for 2 days. Then weigh the microtube containing the sample scaffold and compare this result with the weight of this microtube recorded at the beginning of the test to determine the mass of sample scaffold lost over time. Use this value as m_{st_n} in Eq 7 for this sample scaffold.

3.4.3 Mechanical Testing

Mechanical testing is one of the required design parameters for this study to enhance scaffolds' performance and to meet demands of native tissue with sufficient mechanical integrity. For material in compressive test, there is a linear region following Hooke's Law and presents by Young's modulus shown in Eq 8.

$$E = \frac{compressive\ stress}{compressive\ strain} = \frac{\sigma}{\varepsilon} = \frac{\frac{F}{A_0}}{\frac{\Delta L}{L_0}} = \frac{FL_0}{A_0 \Delta L} = \frac{FL_0}{\left[\pi(\frac{D}{2})^2 - \pi(\frac{D}{2} - d)^2\right]\Delta L}$$

Eq 8

Where

E stands for Young's modulus (modulus of elasticity)

F stands for the force exerted on an object under tension;

A_0 stands for the original cross-sectional area through which the force is applied;

ΔL stands for the amount by which the length of the object changes;

L_0 stands for the original length of the object;

D stands for the outer diameter of the object;

d stands for the wall thickness of the object.

Following the Table 6 create 54 sample scaffolds, 18 (6 sets of 3) from each of the groups/materials so each tube is 5.00±0.02 mm (length± standard deviation) long, and smooth both ends of the sample scaffold with sandpaper so the ends are square. Measure the length of all the scaffolds 5 times, and make sure the length of all the sample scaffolds are within 0.01mm. Then put each of the 54 scaffolds into separate microtube and add 1000.0 µl PBS solution (with 0.1% W/V sodium azide) to each of the microtube. All the samples are then incubated at 37 °C. After (1, 2, 4, 6, 8, 10, 12, 14, 18, 20, 24, 30, 35 days) extract 500.0 µl of each solution from each microtube, and throw it away and then top up each microtube with 500.0 µl fresh PBS (with 0.1% W/V sodium azide). In addition, each week remove 1 set of 3 microtubes from each of the groups/materials and wash the sample scaffolds with dd-water. For each of the 3 tube: measure the outer diameter, the inner diameter and the length of the scaffold with vernier calipers 5 times, and make sure the value of all the same measurements are within 0.01mm difference. These values are entered into the compression tester (purchased from Instron, Canton, MA) and are used as parameters in Eq 8. Place each tube in-between compression platen of the compression tester and adjust the platen so they are just touching both ends of the scaffold. The compression tester is then set with 250N load cell and 0.2 in extensional strain. The compression tester measures the extensional stress and the compressive strain and reports Young's modulus. Results are exported with automatic modulus and raw data in tensile stress and strain. Plots in modulus regarding to time graph shows changing of mechanical property.

Chapter 4 Results and Discussions

4.1 Release Study

Results of release studies of EGF growth factors, FGF-b growth factor, and BSA are shown in Figures 13 to 16.

In the BSA release study, BSA is the only molecule encapsulated in the microspheres, PLGA base, or both. The same polymer components and procedures were used to synthesize PLLA microsphere (MS)-PLGA scaffolds or PCL (MS) microsphere-PLGA scaffolds with BSA encapsulated at different locations. In each type of scaffold, the BSA released from microspheres, PLGA base and microspheres with PLGA base are presented in the same graph.

In the growth factor release studies, both EGF and FGF-b are released from the same scaffold for example PLLA microsphere in PLGA scaffold or PCL microsphere in PLGA scaffold. The released growth factors for the scaffold are presented on one graph.

4.1.1 BSA Release Studies

BSA released from PCL (MS)-PLGA scaffolds and PLLA (MS)-PLGA scaffolds are shown in Figure 13 and Figure 14. BSA encapsulated in both PLLA and PCL microspheres gradually released in 42 days, but in PLGA base, BSA has an initial

release in 6 days, followed by steady stage with no release in the rest of the test. The PCL (BSA)-PLGA (BSA) scaffold plot is for BSA encapsulated in both microspheres and the PLGA base of the scaffold. As the BSA is gradually released from the microspheres, the release profile soon catch up with that of BSA released from the PCL-PLGA (BSA) scaffold, which only has BSA just encapsulated in PLGA base. The quantity of BSA released versus time is presented in units **(µg BSA/ mg sample)** versus days.

Results of BSA released from PCL (BSA)-PLGA scaffolds are shown in 13. The BSA in the microspheres has 1.36 µg /mg (42.57%) of BSA released in the first 4 days; an additional 1.84 µg /mg is released from day 4 to day 42. For the PCL-PLGA (BSA) scaffold with BSA localized in PLGA base, 12.83 µg /mg of BSA (85.82%) is released in the initial 6 days and a small quantity of 2.13 µg /mg of BSA is released in a long period of 33 days from day 7 to day 42. Compared with the quantity of BSA released at the initial time, it has almost no BSA releases in the following stage. The BSA released from the PCL (BSA)-PLGA (BSA) scaffold confirms the release behavior has both the initial release rate of the PCL-PLGA (BSA) scaffold and the long-term release rate of the PCL (BSA)-PLGA scaffold.

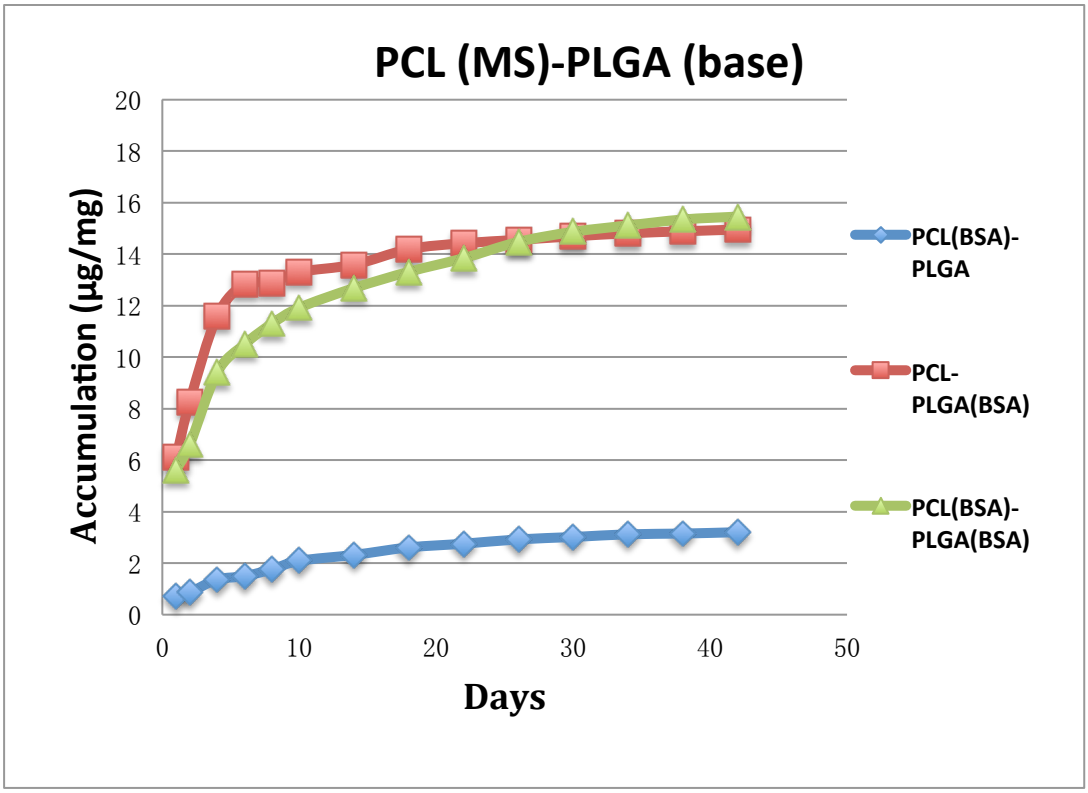

Figure 13 In vitro release studies of BSA release from PCL (MS)-PLGA (base) scaffold in 42 days.

Results of BSA released from PLLA (MS)-PLGA scaffolds are shown in Figure 14. The BSA in the microspheres has 2.05 µg /mg (44.28%) of BSA released in first 4 days; an additional 2.58 µg/mg released from day 4 to day 42. For the scaffold with BSA localized in the PLGA base, 16.03µg/mg of BSA (95.02%) is released in the initial 6 days and a small quantity (0.84µg) of BSA released in a long period of 33 days from day 7 to day 42. Compared with the quantity of BSA released at the initial time, it has almost no BSA releases in the following stage. The BSA released from the PLLA (BSA)-PLGA (BSA) scaffold confirms the release behavior has both the initial release

rate of the PLLA-PLGA (BSA) scaffold and the long-term release rate of the PLLA (BSA)-PLGA scaffold.

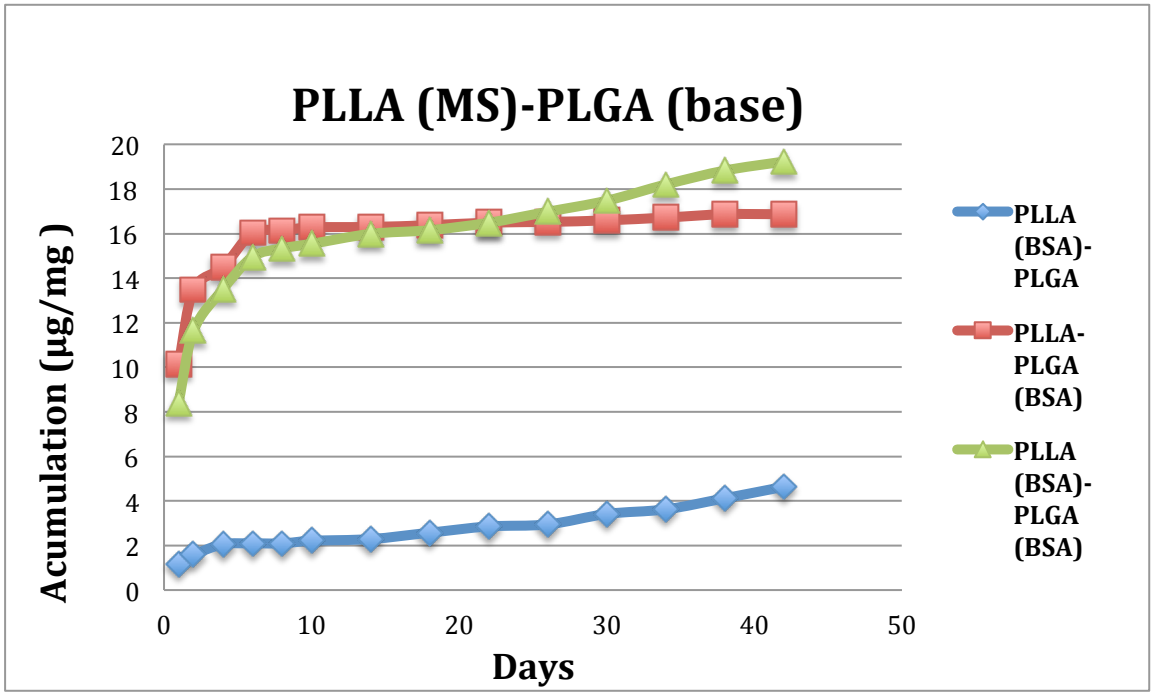

Figure 14 In vitro release studies of BSA release from PLLA (MS)-PLGA (base) scaffold in 42 days.

Theoretically speaking, when BSA is loaded on both microsphere (PLLA/PCL) and PLGA base of one scaffold, the release profiles should go over that of the scaffold with BSA loaded on PLGA base only. Unfortunately, the scaffolds are not synthesized at the same time. The uncontrollable conditions, for example, the differences in batch reaction and the BSA lost during supercritical CO_2 foaming process together affect the total amount of BSA loaded in each scaffold. A test that can preform release profiles form different parts of one scaffold could minimize the differences caused by the uncontrollable situation stated above. Therefore to

confirm the BSA release results, growth factor test was performed.

4.1.2 Growth Factors Release Studies

Released growth factors from PCL (MS EGF)-PLGA (FGF-b) scaffolds and PLLA (MS EGF)-PLGA (FGF-b) scaffolds are shown in Figure 15 and Figure 16. EGF encapsulated in both PLLA and PCL microspheres has a small initial release and is followed by a continual release up to 36 days. In PLGA base, FGF-b has an initial release in 8 days, followed by steady stage with no release in the rest of the test. The quantity of growth factor released versus time is presented by **(pg growth factor/ mg sample)** versus days.

In the PCL (MS EGF)-PLGA (FGF-b) scaffold release study shown in Figure 15, EGF encapsulated in PCL microspheres, 396.22 pg/mg of EGF is released in first four days followed by 162.05 pg/mg EGF a sustained release from day 4 to day 36 due to degradation and erosion of PCL microsphere. For FGF-b localized in PLGA base, 963.46 pg/mg (95.43%) is released in the initial 8 days. From day 8 to day 36, FGF-b release finished with a total amount of 1009.50 pg/mg.

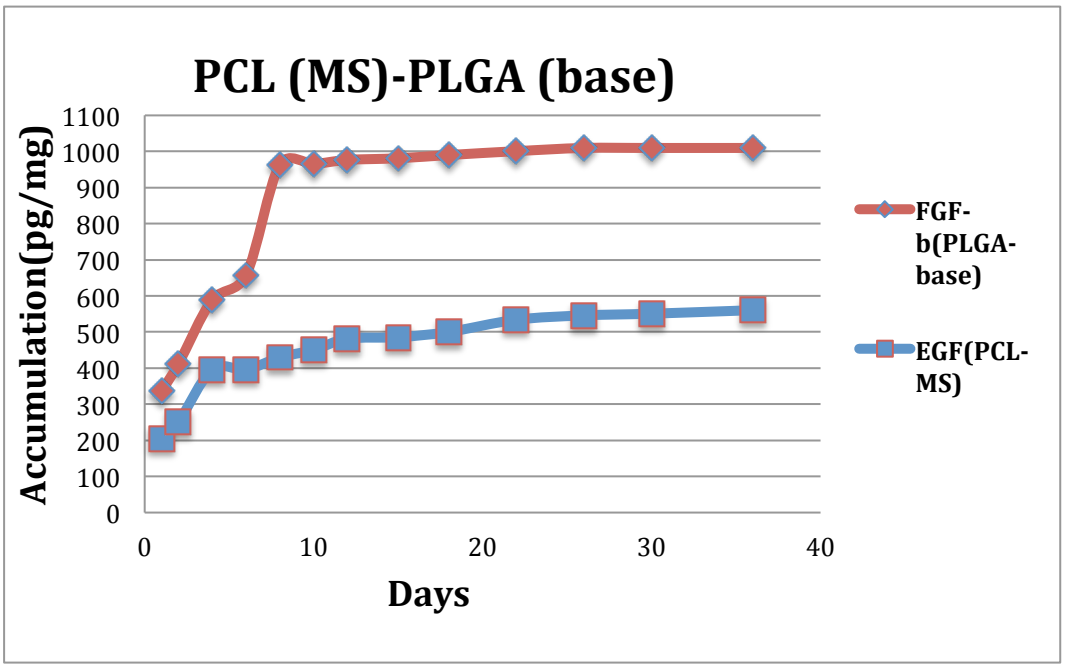

Figure 15 In vitro release studies of EGF and FGF-b from PCL (MS)-PLGA scaffold in36 days.

In the PLLA (MS EGF)-PLGA (FGF-b) scaffold release study shown in Figure 16, In EGF encapsulated PCL microspheres, 321.27 pg/mg of EGF is released in the first 4 days. From day 4 to 36 and additional 165.45 pg/mg EGF is released due to degradation and erosion of PLLA microsphere. For FGF-b localized in PLGA base, 720.09 pg/mg (91.65 %) is released in the initial 8 days. From day 8 to day 36, FGF-b release finished with a total amount of 785.74 pg/mg.

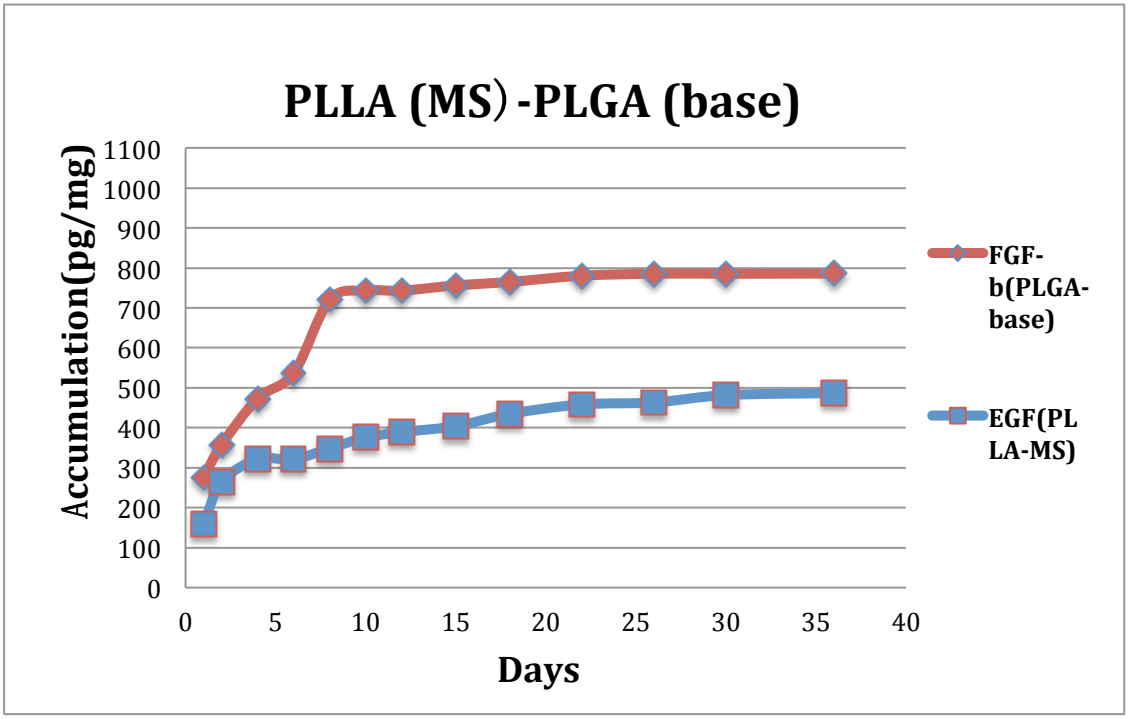

Figure 16 In vitro release studies of EGF and FGF-b from PLLA (MS)-PLGA scaffold in 36 days.

Similar release behaviors of release from PLGA base and PLLA/PCL microspheres have been shown in both BSA and Growth factors EGF and FGF-b release studies.

4.1.3 Sequential Release Approach

Releasing more than one growth factor sequentially requires controlling when the growth factors are released and the sequence that the growth factors released in. Sequential release can be achieved by accelerating the release of the first molecule and by delaying the release of the second one. The sequence of the growth factors released from the system is generally determined by the reverse sequence of growth factors built

into the release system.

4.1.3.1 First Release Approach

The initial burst is assigned to the leaching of molecules through the porous surface of polymer microspheres [215]. Therefore initial release is greatly affected by porosity and pore size. Increasing either parameter of the delivery vehicle may lead to a quick molecule release rate [216]. Based on this idea highly porous hydrogels, for example hyaluronanmethylcellulose, and alginate [154-156] are commonly used as the first release material. Similar to the hydrogels, PLGA scaffolds foamed by supercritical CO_2 have high porosity as well as large pore sizes. The release starts immediately and then finishes in a relatively short time. In a similar study, FGF-b was released from a PLGA scaffold foamed by supercritical CO_2 process. The FGF-b exhibited a great initial burst release, and the release was completed in seven days [217], which is similar to the results obtained in this research. Both BSA release profiles (in Figure 13 and 14) and growth factor FGF-b release profiles (in Figure 15 and 16) show the release from PLGA based scaffold was completed in 7 days. These results demonstrate the ability of PLGA based scaffolds to achieve a fast first release of FGF-b. Scaffolds synthesized from PLGA have higher release control and mechanical strength than scaffolds made of gels, but it is hard to incorporate another molecule to be released at different time.

4.1.3.2 Second Release Control

Molecule release kinetics from polymetric microspheres is affected by polymer erosion, dissolution, and diffusion [218-220] and can be used to create a second drug release phase [200]. As shown in Figure 13 and Figure 14, the release of BSA from microspheres has a steady second release period starting after day 4 and a similar result has been found for EGF released from scaffolds with the same structure (release profiles shown in Figure 15 and 16). This second release phase from microspheres proves the designed scaffolds have the possibility to release a different growth factor in a controlled and delayed manner. By taking advantage of this characteristic of delaying and extending the second release stage, the designed scaffolds have the ability to release two growth factors in different periods. In the initial design, there are several critical parameters involved to achieve this goal.

The crystalline of different polymers is used in the designed scaffold to manipulate the release profile. PLLA and PCL have higher crystalline than that of PLGA, which provides the materials with a slower degradation rate and lower solubility in supercritical CO_2 [19, 221]. Therefor, material wise, the degradation related release from both PLLA and PCL microspheres is slower than that from a PLGA base. The lower solubility of PLLA and PCL in CO_2 makes it possible to create microspheres with a smoother surface than the sponge structured PLGA base shown in SEM pictures in Figure 17. This results in reduced porosity and pore size, which also contributes to

slowing down the release rate. Both of the effects make PLLA and PCL microspheres promising candidates for the second sustainable growth factor delivery vehicle.

4.1.4 BSA Release Versus Growth Factors Release

Both the BSA release study and the growth factor release studies establish the same trends for release kinetics from microspheres or PLGA based tube. Compared with the BSA release study, initial EGF released from both PLLA (MS)-PLGA (66.00%) and PCL (MS)-PLGA (70.97%) scaffolds at day 4 are higher than that found in BSA released from PLLA (MS)-PLGA (44.28%) and PCL (MS)-PLGA (42.57%). These differences may be caused by the bioactivity of growth factors used in long-term in vitro release studies [130]. Research using different encapsulated molecules obtains different release profiles, but the release trends were similar [138]. BSA can maintain its bioactivity in harsh environments, which makes it very popular for use as a release model in most studies [222]. After the initial burst, BSA and growth factors gradually release of the remaining 35 to 60% of the protein encapsulated in the microspheres integrated into these scaffolds.

4.1.5 Encapsulation Efficiency in Growth Factor Release

The encapsulation efficiency of biomolecules in microspheres is less than that in PLGA base. In growth factors release study, EGF is released more slowly from microspheres than that of FGF-b from PLGA base. In BSA release study, BSA is

released more slowly from microspheres than from the PLGA base. Encapsulation efficiency of biomolecules in microspheres is 20.4 ± 4.8 % through single emulsion synthesize process and 83.1 ± 3.5% for dip coating process. Data has been collected by pre-research studies and been calculated among five samples. BSA and FGF-b have higher efficiency to be encapsulated in PLGA than BSA and EGF in PCL or PLLA microspheres. Consequently, higher quantity of accumulation is obtained for studies of release from PLGA than microspheres.

Similar performance was observed in PLLA (MS)-PLGA and PCL (MS)-PLGA scaffolds. Due to their dissolubility in ethyl acetate, PLLA microspheres encapsulate biomolecules better than PCL microspheres, however, PCL degrades more slowly than PLLA and creates a more uniform structure for PCL (MS)-PLGA scaffolds. For these reasons, both exhibit a good sustained slow second release, which may provide a promising guidance to related cell behaviors.

4.2 Scanning Electron Microscopy

In this study, SEM is used to characterize the morphologies of sections from scaffolds in different compositions. The results present a general view of scaffolds as well as detailed images of pore size and microsphere distributions.

In Figure 17, an overview of scan images of scaffolds is shown in A, C, E with a 200μm scale bar with structure details shown in B, D, F with an 80μm in the scale bar. The overview images show one fifth of each ring shaped scaffold, and indicate the location of the corresponding detailed picture. The detail images are chosen from marked areas for general geometry observation.

The PLGA scaffold in Figure 17 A and B has macro pore sizes in the range of 50-200μm, uniformly distributed inside tubes. These pores easily uptake water and leach away hydrophilic biomolecule loading from the material with diffusion effect. This sponge structured tube also creates space to provide the scaffold with loading capability.

The PLLA (MS)-PLGA scaffold shown in C and D are more uniform with smaller pore size distribution. The detailed picture D also shows the microspheres evenly distributed embedded in the PLGA based tube. Sizes of microspheres are in a limited range of size distribution of 15-20μm. The microspheres of certain size can easily fit in the high porosity PLGA base. With 50 wt% of PLLA microspheres in PLGA scaffolds (C and D) and 50 wt% of PCL microspheres in PLGA scaffolds (E and F), PLGA is not be able to keep its original shape, the PLGA is pushed to go around non-foamed PLLA microsphere and stuffs the space in-between microspheres, working like glue to connect particles together. In the dip-coating fabrication process, microspheres are evenly distributed in scaffolds. In Figure 17-D some of the microspheres are cut in half by chance. Inside the microsphere, a solid encapsulated structured core can be seen

confirming the biomolecule loaded microsphere syntheses process. Polymer shell for microspheres is made of PLLA, which is not foamed in supercritical CO_2, resulting in a more solid and high density surface with a less porous structure. Compared with sponged structure PLGA, PLLA microspheres then provide better structure to delay the biomolecule diffusion. The longer it takes for the biomolecule to travel from the microsphere makes it possible to provide a time difference for biomolecule released from PLGA base and PLLA microspheres.

Images E and F show sections of PCL (MS)-PLGA scaffolds. Different from the first two scaffolds, they have a smoother surface with fewer pores with a maximum pore diameter of 50μm. Due to being partially dissolved PCL in ethyl acetate, the dissolved PCL together with the PLGA is well mixed and covers all the integrated microspheres. As a result, microspheres are not shown well on sections in PCL (MS)-PLGA scaffolds. The dissolved PCL in ethyl acetate also changes the PLGA porous structure after supercritical carbon dioxide foam. The more solid structure with fewer pores provides it with different characteristics than in other studies.

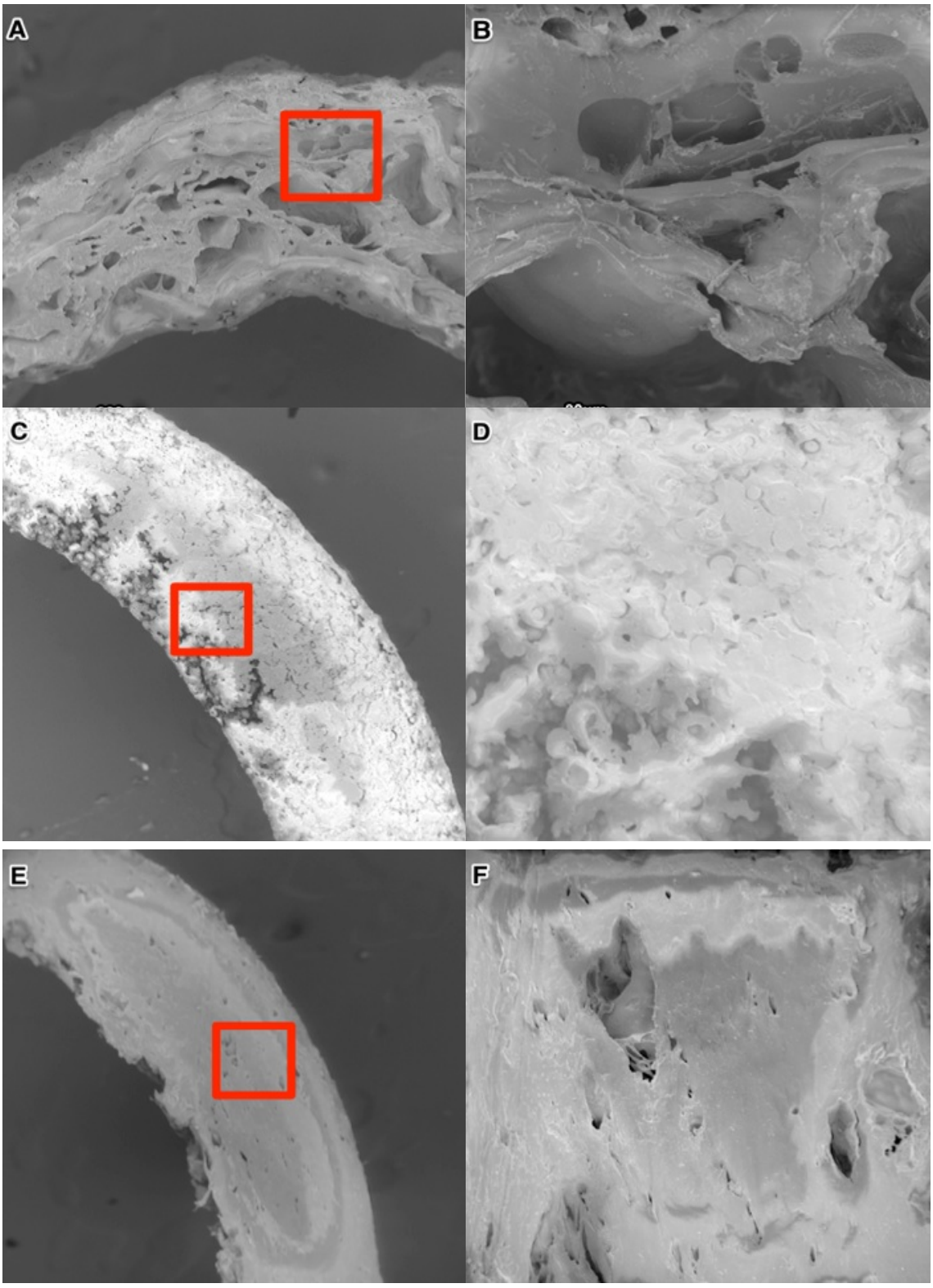

Figure 17 SEM images of PLGA in A, B; PLLA (MS)-PLGA in C, D ; PCL (MS)-PLGA in E, F ; different

magnifications A, C, E with a scale bar of 300 μm and B, D, E with a scale bar of 80 μm

4.3 In Vitro Degradation Study

The degradation of PLGA, PLLA (MS)-PLGA, and PCL (MS) -PLGA scaffolds is shown in both the mass loss profile in Figure 18 and in the morphology structure changes over time as shown in the SEM images in Figure 19. To highlight the degradation of just the polymers no biomolecule has been encapsulated in either microspheres or PLGA base.

4.3.1 Mass Loss

Figure 18 shows, mass loss for all scaffolds is low for the first three weeks. Mass loss of PLGA scaffolds starts to accelerate right after the third week, PLLA (MS)-PLGA scaffolds start to loss their weight after the fourth week, and PCL (MS)-PLGA scaffolds start after the fifth week. PCL starts more slowly than PLLA, and PLLA degrades more slowly than PLGA.

Shown in Figure 18, up to week 3, 5.93 ± 0.01 % of PLGA scaffolds degraded, 4.5 ± 0.01 % of PLLA (MS)-PLGA degraded, and 2.63 ± 0.003 % of PCL (MS)-PLGA degraded. Accelerated degradation of PLGA starts after week 3, 23.97 ± 0.05% degraded up to week 4, 42.9 ± 0.05% up to week 5, and 58.26 ± 0.06% up to week 6. Compared with PLGA scaffolds degradation accelerates on PLLA (MS)-PLGA

scaffolds from week 4 and 11.5 ±0.01% degraded up to week 5, followed by 23.27 ± 0.02 % up to week 6. PCL (MS)-PLGA scaffolds' degradation accelerates one week after PLLA (MS)-PLGA scaffolds. Up to week 69.57 ± 0.01 % of scaffold degraded.

In each testing point, newly designed scaffolds degrade slower than PLGA scaffold. Compared between PCL (MS)-PLGA scaffold and PLLA (MS)-PLGA scaffold, PCL (MS)-PLGA scaffold degrade slower than PLLA (MS)-PLGA scaffold.

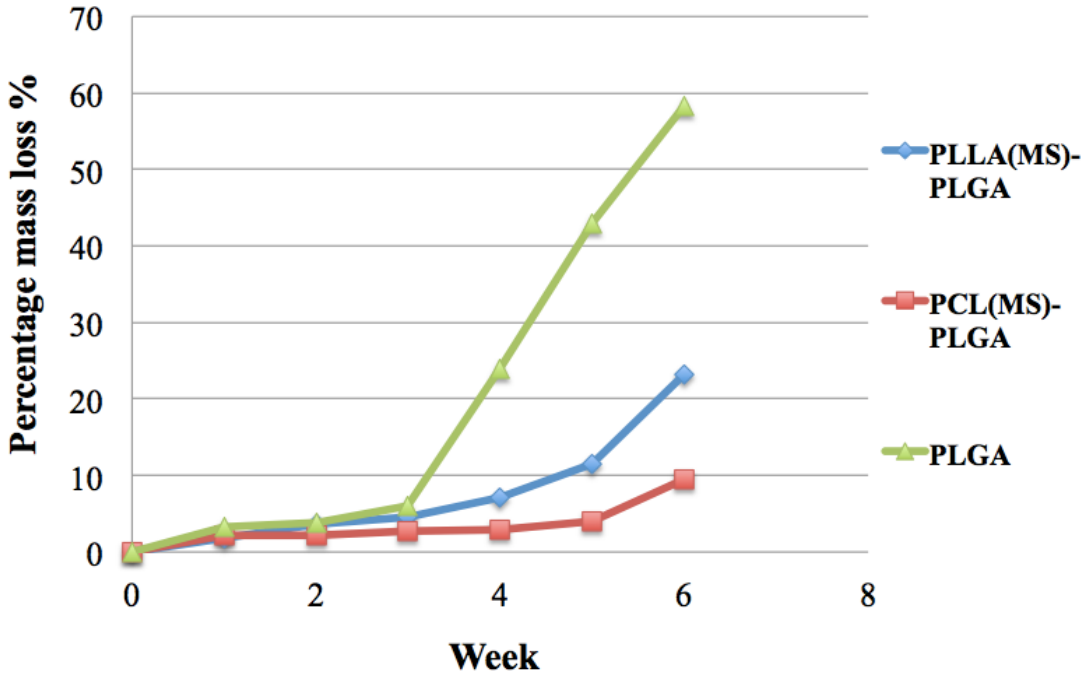

Figure 18 Percentage of mass loss for in vitro degradation study of PLGA, PLLA (MS)-PLGA, and PCL (MS)-PLGA scaffolds in 6 weeks.

Based on mass loss, bulk polymer degradation consists of two stages. In the first stage, the degradation of bulk-degrade polymer backbones hydrolyzed over time into

smaller chains [200], then over time these chains break down into smaller chains. This is reflected in the mass loss result in Figure 18 during week 1 to week 3, in that no sharp mass loss occurs during this period. In the second stage, small fragments can be further hydrolyzed [200] and when the molar mass of fragments goes down to 100 g/mol [223], hydrolysis products can dissolve in water creating an accelerated mass loss. For PLGA and PLLA a second sharp mass loss stage can be observed in their degradation profiles. Due to the slow degradation characteristic of PCL, its degradation profile is not visible in the 5 week test conducted in this research project, but other research has shown that PCL mass loss starts after approximately 10 weeks [224]. This result is shown by the rate of scaffold degradation over time in Figure 18. PLGA scaffolds exhibit significant mass loss one week earlier than PLLA (MS)-PLGA scaffolds, and two weeks earlier than PCL (MS)-PLGA scaffolds.

4.3.2 SEM Image Analysis

In Figure 19, PLGA scaffolds, PLLA (MS) -PLGA (50/50wt%) scaffolds, and PCL (MS)-PLGA (50/50 wt%) scaffolds morphologies have been scanned by SEM on week 1, 3 and 5. The surfaces for all the scaffolds are getting rough as well as the structures are getting loose and weak over time

The morphology changes in PLGA scaffolds are shown in images a, b, and c indicating the changed structures of scaffolds in week 1, 3 and 5. The section cut

samples from scaffolds get rough on the surface over time. The small pores, with diameter around 60-100μm in week 1, can be found in week 3. In week 5, the whole structure of the PLGA scaffold is broken into small pieces. After five weeks, taking mass loss data into consideration; 58.27% of material degraded, the rest of the PLGA is no longer able to hold the structure. Due to the weak structure of degraded scaffold, they collapse during the freeze-drying process and cannot be made into SEM samples after five weeks.

The morphology changes on PLLA (MS)-PLGA scaffolds are shown in images d, e, and f indicating the changed structures of scaffolds in week 1, 3 and 5. After the first week of degradation, microspheres are slightly shown better compared with Figure 17 D. On week t 3, as shown in the Figure 19 e, surface is rougher, but the porosity didn't change a lot. On week five, most of the PLGA base is degraded, the pore size has increased greatly, and similar result in an increased mass loss shown in Figure 18. The porosity in week compared with first week has increased, but the pore size didn't change a lot. In week 5, the pore size greatly increased due to degradation of scaffold and the number of microspheres is reduced.

The morphology changes on PCL (MS)-PLGA scaffolds are shown in images g, h, and i, indicating the changed structures of the scaffolds in week 1, 3 and 5. Compare among the pictures, the fist week has fewer pores than week 3, but the pore size stays the same. In week five, the morphology of the scaffold greatly changed. Due to partially dissolved PCL in ethyl acetate, however, at week three, microspheres could be found in

the pores, together with increased surface roughness. In week five, more not perfect sphere particles are seen, and more roughed surfaces can be found compared with images in week 1 and 3.

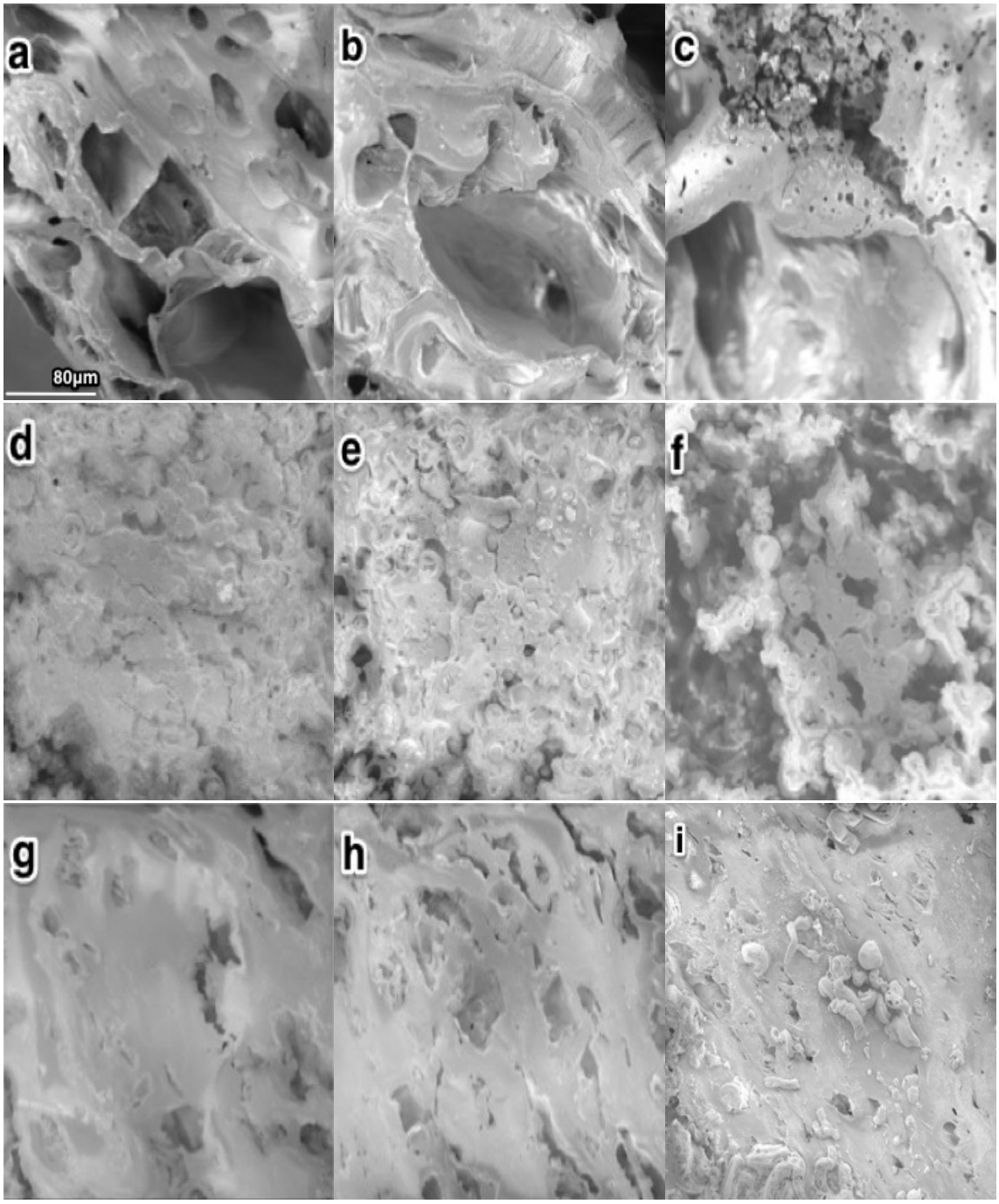

Figure 19 SEM images of PLGA scaffolds in week 1 a, 3 b, 5 c; PLLA (MS)-PLGA scaffolds in week 1 d, 3 e, 5 f ; PCL (MS)-PLGA scaffolds in week 1 g, 3 h, 5 i. All images are under the same magnification with a scale bar of 80 μm

Recent practical research studies indicate there is no significant correlation between the hydrolysis products catalytic reaction and scaffold degradation [225]. Therefor, scaffolds having high porosity and large pore size lead to high degradation rates [226]. The mass loss related degradation is strongly influenced by initial scaffold structure design in this project. This is demonstrated in the SEM images in Figures 17 D, and F, where the pore size is decreased and a uniform structure is created. Due to the different solubility of PLLA and PCL microspheres in ethyl acetate, the cross-sectional area remains more intact than for the PLGA scaffold showed in Figure 17 B. The designed PLLA (MS)-PLGA and PCL (MS)-PLGA scaffolds contain equal masses of microspheres and PLGA. Theoretically speaking, these newly designed scaffolds should degrade at half the rate of pure PLGA scaffolds. This is borne out by the results shown in Figure 18 showing that most of the scaffolds lose less than half as much mass as the pure PLGA scaffolds. The microspheres in PLGA tubes reduce the porosity and the pore size consequently reduced the degradation rate of the scaffolds. Compared with PLLA (MS)-PLGA scaffolds, PCL (MS)-PLGA scaffolds have lower porosity and pore size and degrade more slowly than PLLA (MS)-PLGA scaffolds. The delayed onset of mass loss is due to their structure and the characteristics of PLLA and PCL. Thus the

newly designed scaffolds should sustain longer in vivo, meeting the need of long-term reparation.

In Figure 19, the pore size and porosity change in a and b, d and e, g and h are not significant in the first three weeks, and the same trend can be found in mass loss plot in Figure 18. In the first three weeks, mass loss stays within less than 5%. In the fifth week, both pore size and porosity in Figure 19 c, f, and i, are increased, and in f and i the microspheres are easily visible. In Figure 18, consequently mass loss decreases sharply over time.

4.3.3 Structure Change in Mass Loss Studies

Comparing the two newly designed scaffolds, the PLLA (MS)-PLGA scaffold exhibits faster mass loss than the PCL (MS)-PLGA scaffold. This may be caused by microsphere loss during degradation. A follow up study has been done on the designed scaffolds by incubating them for up to 6 months. In this time the PLGA scaffolds are totally degraded. In the same time the PLLA (MS)-PLGA scaffolds is still visible and particles are visible in the bottom of micro-tubes, but the scaffolds collapse when shaken. Meanwhile, the PCL (MS)-PLGA scaffolds hardly have any particles in the bottom of the microtubes, but the wall thickness has decreased. According to these observations, the mass loss of the scaffolds may be caused by microsphere leaching. In the case of the PLGA base containing the PCL MS, the PCL partly dissolves into the base. As a result, the PLGA/PCL base degrades more slowly, thus the MS are lost more

slowly. In comparison the PLGA base containing the PLLA MS degrades more quickly resulting in the more loss of its MS, which equates to higher mass loss.

4.4 Compressive Test

The compressive strength was tested on PLGA scaffolds, PCL (MS)-PLGA scaffolds and PLLA (MS)-PLGA scaffolds. **Young's Modulus ± standard deviation** regarding the degradation over time in each type of scaffolds is shown in Figure 20

According to the physical properties provided by manufacturer, the modulus of PLGA (50:50) is 1.38-2.76×10^6 MPa [227]. Scaffolds synthesized by different techniques， with different synthesized conditions and different materials make scaffolds with different mechanical strength. Specifically produced by supercritical carbon dioxide, the mechanical properties of scaffolds are affected by molecule weight, chemical composition, temperature, pressure, and foaming time [199, 228]. PLGA hollow fiber membrane has an modulus of 109 MPa [229].

In this research PLGA scaffolds have an initial modulus of 151.15 ± 0.30 MPa, while PLLA (MS)-PLGA scaffolds have an initial modulus of 205.31 ± 10.43 MPa, and PCL (MS)-PLGA scaffolds have a modulus of 260.42 ± 12.35 MPa. The mechanical property of both the PLLA (MS)-PLGA and the PCL (MS)-PLGA scaffolds have been improved compared to pure PLGA scaffolds.

After the first week of degradation, PLGA scaffolds lost half of their mechanical properties and go down to 73.26 ± 18.90 MPa, however, both PLLA (MS)-PLGA and PCL (MS)-PLGA scaffolds keep their modulus at 202.47 ± 41.68 MPa and 237.03 ± 20.77 MPa. During the second week, mechanical properties for both PLGA and PLLA (MS)-PLGA scaffolds start to go down to 59.45 ± 4.62 MPa and 179.85 ± 9.25 MPa. PCL (MS)-PLGA scaffolds keep their mechanical properties until week three. A slightly decreased modulus of 11.95 MPa happened at this period.

In week four, the modulus of PLGA scaffolds goes down to 1.48 ± 0.81 MPa and basically loose their mechanical properties. For PLLA (MS)-PLGA and PCL (MS)-PLGA still keep 95.68 ± 3.82 MPa and 136.04 ± 17.94 MPa of their original mechanical properties. In week five, the modulus of PLLA (MS)-PLGA scaffolds is 60.03 ± 24.36 MPa, compared to the modulus of PCL (MS)-PLGA scaffolds, which is 68.95 ± 12.20 MPa. Both newly designed scaffolds, PLLA (MS)-PLGA and PCL (MS)-PLGA, preform better at the fifth week than PLGA scaffolds at the second week with modulus of 59.45 ± 4.62 MPa through compressive test.

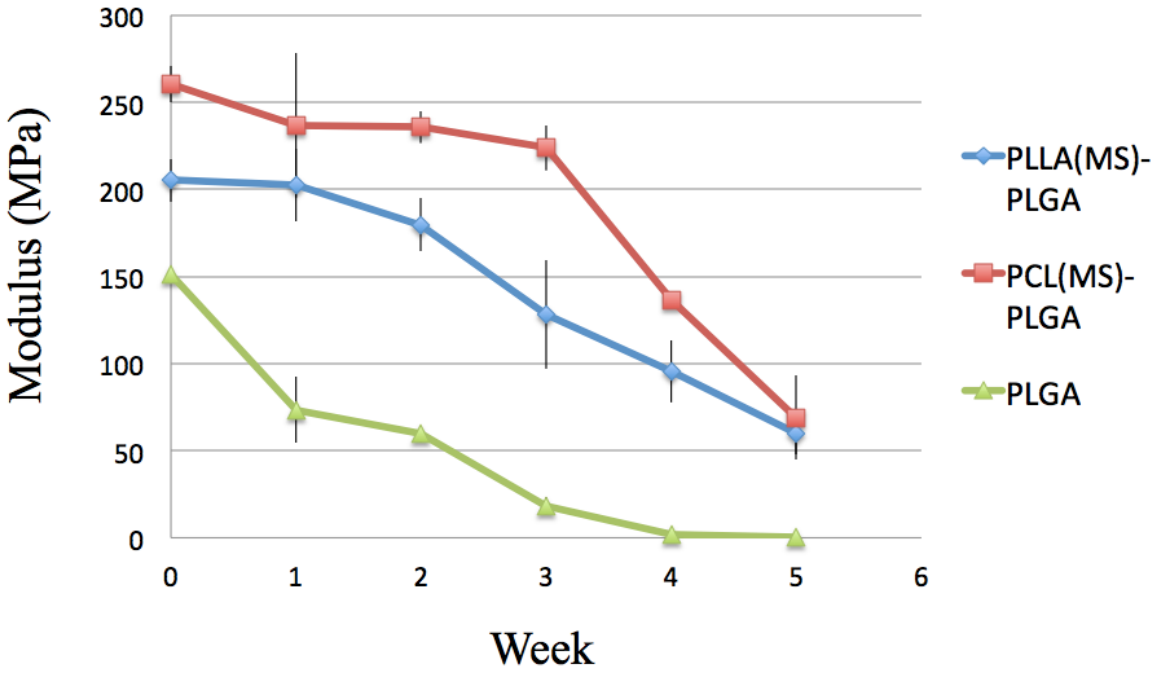

Figure 20 Young's Modulus for PLGA, PLLA (MS)-PLGA, PCL (MS)-PLGA scaffolds over time.

4.4.1Mechanical Properties of Scaffolds

From a typical compressive stress-strain curve, there are three regions exhibited during the test: the linear elasticity at low stresses region, where compressive stress rises with the strain; the long collapse plateau region, where scaffold cells collapse; and the densification region, where continued application of force on the already collapsed sample increases the stress [230]. As shown in Figure 21, for example, the test of PLGA scaffold fits the three regions in stress-strain graph. To be usable for SCI studies, the mechanical strength of the scaffold needs to be strong enough to prevent collapsing. The mechanical strength of each scaffold is determined by calculating the slope of the

initial linear region in each of its stress versus strain graph. A similar technique to test mechanical strength has been performed in other studies, for example, in PCL-PLGA blended scaffold [231] and poly(2-hydroxyethyl methacrylate-co-methyl methacrylate) hydrogel tubes [232].

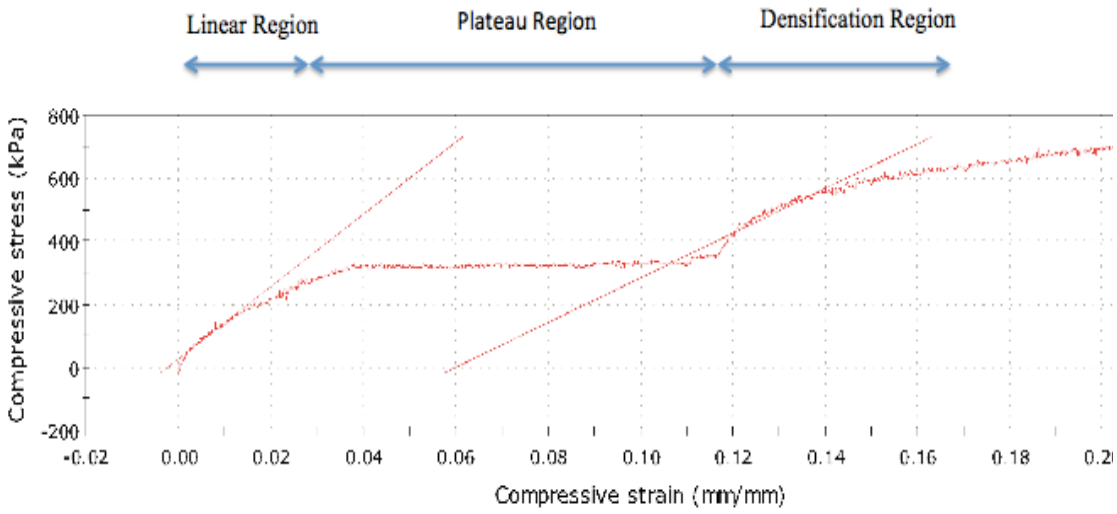

Figure 21 Compression stress-strain curve of PLGA scaffold.

Scaffolds utilized for tissue engineering are required to reach appropriate mechanical properties. The optimum value is dependent on the target tissue, and a minimum value of 0.1 MPa is required for ultimate tissue or organ formation [233]. Scaffolds used for in vitro studies may degrade faster than those used for in vivo studies [224]. Thus, scaffolds having high initial mechanical strength and long lasting mechanical strength are required for in vivo studies.

Blending PLGA with various materials has been studied in other research and has been shown to improve the modulus of single PLGA. For instance PLGA scaffolds blended with poly (ethyleneoxide)- poly (propyleneoxide)- poly (ethyleneoxide) has an initial modulus of 160 MPa [234], and PLGA (50:50) mixed with different percentage of NaCl and TCP have a range of modulus from 54±17 to 450±79 MPa [235].

In other research PLLA has been made into various structured scaffolds with initial modulus from 85.80 ± 37.70 to 642.26 ± 161.54 [225] respectively on various structures, which are higher than PLGA. The mechanical strength of PLLA also decreases more slowly than PLGA [236]. PCL scaffolds remain 20% of the original mechanical strength after 70 weeks [237], which also decrease more slowly than PLGA scaffolds. Scaffolds created by integrating PLLA or PCL can elevate the mechanical strength of PLGA scaffolds. Therefor in the comprehensive test, designed scaffolds have high mechanical strength than PLGA scaffold in any testing point.

For the scaffolds synthesized in this project, the PLLA (MS)-PLGA scaffolds have an initial modulus of 205.31 ± 10.43 MPa, and the PCL (MS)-PLGA scaffolds have a modulus of 260.42 ± 12.35 MP. Both of the moduli are in a regular range for PLGA based blended scaffolds.

4.4.2 Structure Change in Mechanical Testing

The modulus and tensile strength also affected by the cross-sectional area. Increased porosity and pore size decrease the estimated of cross-sectional area under

stress [238]. As a result, less porous scaffolds have a higher modulus [225]. The detailed structures of the tubes synthesized from different materials in this research are showed in the SEM images in Figure 17 B, D, and F. The PLGA tubes have the highest porosity, largest pore size distribution and the lowest mechanical strength. With microspheres added into PLGA tubes, the pores are reduced in size and the strength of the scaffold is aided by the presence of the PLLA microspheres. Similar reduced porosity and pore size result in the increased mechanical strength occurs when PCL microspheres are added to PLGA scaffolds. Due to the solubility of PCL is higher than PLLA in ethyl acetate, fewer microspheres but smoother surface can be found compared between D and F in Figure 17. The result in the compressive test also indicates the PCL (MS)-PLGA has better mechanical strength than PLLA (MS)-PLGA. The change of the mechanical properties of the PLGA scaffolds over time, due to degradation, is shown in Figure 19. As the pore sizes increase and the structures get loose over time, the mechanical properties decrease. Comparing the week-to-week images (b, e, h,) and (c, f, i) the designed scaffolds increase their porosity and pore size more slowly than PLGA scaffolds. Similarly, as shown in Figure 20, the mechanical strength of the designed scaffolds decreases more slowly and the scaffold maintains its structure longer than that of PLGA scaffolds.

4.4.3 Degradation in Mechanical Testing

During degradation, the decrease of strength stage comes earlier than loss of

weight stage [239]. Similar tendencies have been found in degradation tests and compressive tests. Decrease of strength and mass loss for PLGA scaffolds occur one week earlier than for PLLA (MS)-PLGA scaffolds, and two weeks earlier than PCL (MS)-PLGA scaffolds. Though they have similar trends, in degradation tests, the significant mass loss begins in week 4 (when the small chains are to degrade into monomers), while in the compressive tests the large modulus changes begin in week 1.

4.5 Compare Between Scaffolds

In this project, two types of scaffold PLLA (MS)-PLGA and PCL (MS)-PLGA are synthesized with same process. Due to the different parameters, for example, dissolvability and degradation speed of PLLA and PCL, two designed scaffolds show some different characteristics in tests.

In the growth factor study, FGF-b is released from PLGA base to obtain the first burst release. The PCL (MS)- PLGA scaffold achieves better first release approach with 95.43% compared with 91.65% from PLLA (MS)- PLGA scaffold. In the second release control, when EGF encapsulated in PCL microspheres initial burst release 396.22 pg/mg, which is higher than 321.27 pg/mg released from PLLA microspheres. This results is due to the partially dissolved PCL makes the microspheres partially loss their function of a physical barrier. PCL degrades slower than PLLA that makes it lowly release the encapsulated EGF from day 4 to

day 36. Therefore, two newly designed scaffolds eventually achieve similar sequential release profiles.

PCL has stronger initial mechanical strength and slower degradation speed compared with PLLA. In degradation test, PCL (MS)-PLGA scaffold shows less mass loss than PLLA (MS)-PLGA scaffold at any testing point. In mechanical test, similar result has been found that PCL (MS)- PLGA scaffold has stronger mechanical strength and slower mechanical strength loss than PLLA (MS)-PLGA scaffold over time. A followed up study shows, PLLA (MS)-PLGA scaffold will collapse when applied shaking after three months, however PCL (MS)- PLGA scaffold still maintains its shape even after six months.

Both of the designed scaffolds have the similar function to sequential release of two growth factors, however, PCL (MS)-PLGA scaffold has longer duration and stronger mechanical strength compared with PLLA (MS)-PLGA scaffold. Therefore PCL (MS)-PLGA scaffold is more capable for long-term regeneration study.

4.6 Conclusions

As shown above, the newly designed PLLA (MS)-PLGA scaffolds and the PCL (MS)-PLGA scaffolds can function well as growth factors co-delivery systems. One delivery process can be finished within a week and the other has a sustainable delivery up to 5 to 6 weeks, which meets the demands of delivery of two different types of

biomolecules at different periods of spinal cord regeneration. During the synthesize process biocompatible materials are used and no harmful solvents are used, thereby preventing immune responses that would inhibit regeneration. By combining microspheres made of PLLA or PCL that degrade more slowly with PLGA base scaffolds, both the structure and the degradation rate of the scaffolds have been changed. The resulting decrease in the pore size and the improved structure of the new scaffolds' mechanical properties compare positively with pure PLGA scaffolds. Finally, the extended degradation periods make the newly designed scaffolds suitable for long SCI reparation.

Chapter 5 Suggestions for Future Work

In this research, co-delivery scaffolds were synthesized for spinal cord injury repairs. These improved scaffolds have a significant feature of sequential release two molecules as well as better mechanical properties and longer duration compared with other scaffolds. Although the new scaffolds provide better performance than the original scaffolds, there are still some further modifications that could provide further functional improvements.

5.1 Materials

For the co-delivery study PLLA (MS)-PLGA and PCL (MS)-PLGA scaffolds were used to deliver two different growth factors with different release behaviors at different periods of time, but they still have interaction during the first week. Stem cells can be either proliferated or differentiated into determined therapeutic tissues by molecules. Hypothetically speaking, if the system could co-deliver the two different biomolecules at completely different times, the stem cells will get distinct signal to first proliferate, and then later to differentiate. In this study, all the polymer materials (PLGA, PCL, PLLA) used in the delivery systems are bulk-degradable. The diffusion rate of the molecule is determined by character of the materials, resulting in some of the growth factor used in second phase of regeneration being released from the microspheres in the

first week. If different materials are used it might be possible to prevent the release of the second stage growth factor during the first week of reparation.

An option might be to use a different material to modify the surface of the PCL or the PLLA microspheres. Cellulose acetate phthalate, which studied in two-dimensional release model, has been proved with a sign to inhibit the initial release and in return to archive sequential release of growth factors [150]. Using cellulose acetate phthalate by coating it on the chitosan microspheres indicates the inhibit of the initial release [240]. Both of the results provide a possible clue of using it in future design to enhance the sequential release profiles.

5.2 Microsphere Fabrication Process

Microspheres synthesized by the emulsion fabrication process as molecule-loading system forms non-uniform molecule particles in sphere structures. In general, one microsphere has many molecule particles distributed inside rather than one molecule stays in the center shown in Figure 22. When doing release studies, the molecules localized near the surface of microsphere released first [241]. If the technique could be improved in making uniformed center molecule-loaded microspheres without damaging the bioactivity of the molecule in shell structure, a lower initial burst of release may be achieved. Precision particle fabrication (PPF) technology for example, by controlling

either speed of ejects solutions or concentration could adjust the size of the microsphere [242] and achieve more uniform microspheres.

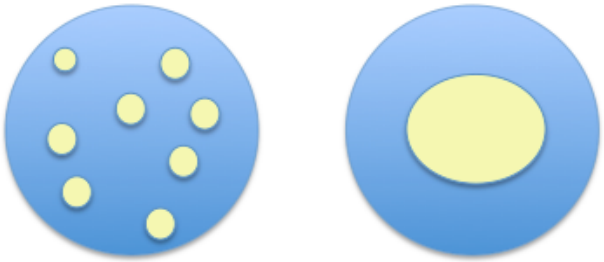

Figure 22 Non-ideal and ideal molecule distributions in microsphere

5.3 Micro-architecture

The micro-architecture of the newly designed scaffold can still be improved to match spinal cord injury repair. To achieve high yield fabricated scaffolds, it is easy to approach by modifying the scaffolds after they are synthesized. The desired scaffold could be stuffed with another material as a core column, which can be easily shaped into a “butterfly” to mimic the real spinal cord structure. Highly cross-linked hydrogels have been used to bind cells with specific attachment and non-specific attachment to cells. These cell loaded gels could be used together with the co-delivery scaffolds developed in this thesis to achieve better functional recover after SCI.

5.4 Inner Structure of the Scaffold

The uniform three-dimensional release of biomolecules from scaffolds is required in various treatments. In this research, microspheres-in-tubes scaffolds were researched to grantee a uniform release in three-dimensions. This sequential release function can be optimized by controlling initial release of the second released molecule, for example, by add more barrier layers to control the diffusion speed by separating microspheres from the molecule loaded PLGA. For this idea, non-foamed and less porous material PCL can be used as the barrier.

In Figure 23 FGF-b loaded in highly porous PLGA theoretically has the same release kinetics as shown in this thesis. However adding the scaffold a coating material mixed with FGF-b loaded on both the inner and outer surfaces, the FGF-b can quickly release from both surfaces first. PCL is more resistant to CO_2 diffusion in the foaming process, creating a high density, smooth surface and slower degrading layer that works like a barrier.

Such a design could have a more promising release profile by both accelerating the first molecule release and delaying the second molecule release from microspheres. This potential design has a disadvantage that, due to the non-molecule loaded PCL barrier layers, it might be limited in the number of molecules it can deliver, when compared to the scaffolds designed in this thesis. Since the biomolecules have an

advantage of working in low concentration, this new possible design of scaffold could still work for spinal cord injury repairs

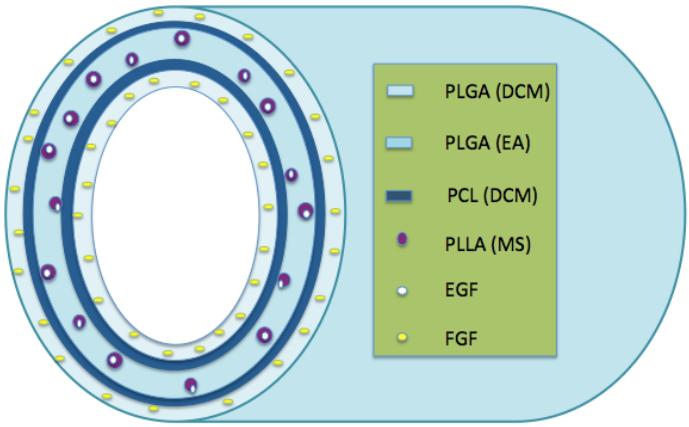

Figure 23 Section view structure of improved scaffold

Attachment

ELISA protocol

1. Coating with capture antibody

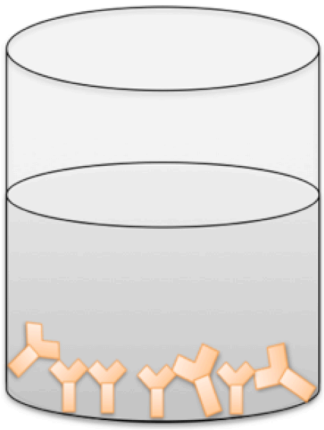

Add 100 μl prepared capture antibody in each well of the 96 well plate. Seal the plate and incubate at room temperature over night. After incubation is done aspirate the solution and wash the plate four times with wash buffer (300 μl in each well every time).

2. Non-specific binding of BSA

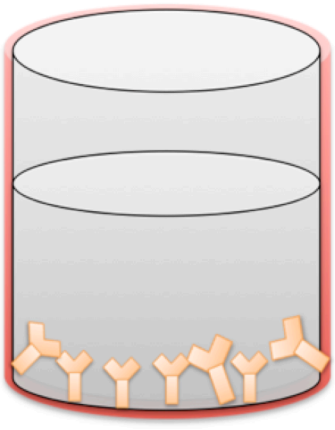

Add 300 μl prepared BSA blocking agent in each well of the 96 well plate. Seal the plate and incubate at room temperature for one hour and thirty minutes. After incubation is done, aspirate the solution and wash the plate four times with wash buffer (300 μl in each well every

3. Specific binding of antigen

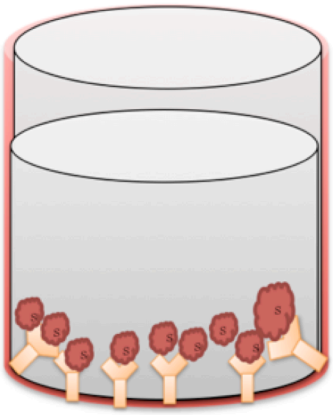

Add 100 μl prepared standard solutions or samples in each well of the 96 well plate. Seal the plate and incubate at room temperature for two hours. After incubation is done, aspirate the solution and wash the plate four times with wash buffer (300 μl in each well every time).

ELISA protocol

4. Sandwich formation

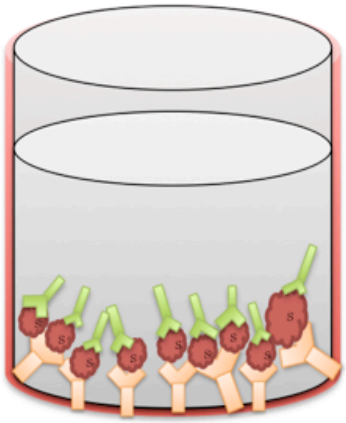

Add 100 μl detection antibody in each well of the 96 well plate. Seal the plate and incubate at room temperature for two hours. After incubation is done, aspirate the solution and wash the plate four times with wash buffer（300 μl in each well every time）.

5. Addition of enzyme-linked acidin to sandwich

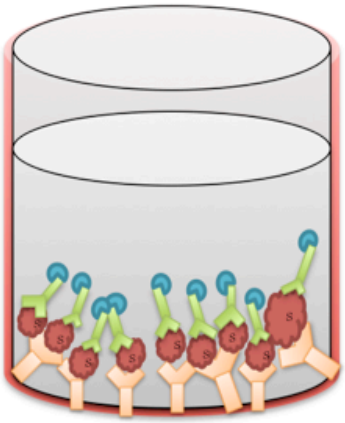

Add 100 μl acidin-HRP conjugate in each well of the 96 well plate. Seal the plate and incubate at room temperature for thirty minutes. After incubation is done, aspirate the solution and wash the plate four times with wash buffer（300 μl in each well every time）.

6. Color conversion

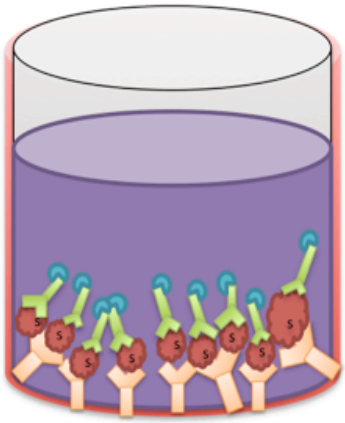

Add 100 μl ABTS substrate solution in each well of the 96 well plate. Seal the plate and incubate at room temperature for 5 minutes. Color conversions can be detected by plate reader set at 405 nm with a 650nm wavelength correction.

Solution

	Wash Buffer	0.05% Tween-20 in PBS
	Block Buffer	1% BSA in PBS
	Diluent	0.05% Tween-20 with 0.1% BSA in PBS
	Capture Antibody	100 μg with 1 ml dd-water balance with PBS to get 100 ml of solution
	Detection Antibody	100 μg with 1 ml dd-water balance with PBS to get 100 ml of solution
	Avidin-HRP	60 μl with balance with diluent to get 120 ml of solution
	Standard	1 μg growth factor with 1ml dd-water and then dilute to get 500 μl of standard sample with concentrations listed with diluent

Concentration of standard solutions for both EGF and FGF-b

	A	B	C	D	E	F	G	H
EGF	1000	250	125	62.5	31.25	15.625	7.8125	0
FGF-b	4000	2000	1000	500	250	125	62.5	0

Bibliography

1. Wyndaele, M. and J.J. Wyndaele, *Incidence, prevalence and epidemiology of spinal cord injury: what learns a worldwide literature survey?* Spinal Cord, 2006. **44**(9): p. 523-529.

2. *Apparelyzed* 2013; Available from: http://www.apparelyzed.com/.

3. *Spinal Cord Injury Awareness Ribbon Gifts - T-Shirts, Posters, & other Gift Ideas*. 2000-2014; Available from: http://www.zazzle.ca/spinal+cord+injury+awareness+ribbon+gifts.

4. Becker, D. and J.W. McDonald, *Approaches to repairing the damaged spinal cord: overview.* 2012. **109**: p. 445-461.

5. McDonald, J.W. and C. Sadowsky, *Spinal-cord injury.* The Lancet, 2002. **359**(9304): p. 417-425.

6. Michael, S.B., F. Akhlaq, and C.B. Jacqueline, *Review of current evidence for apoptosis after spinal cord injury.* Neurotrauma, 2000. **17**(10): p. 915-934.

7. John, W.M. and J.H. Michael, *Repairing the damaged spinal cord- a summary of our early success with embryonic stem cell transplantation and remyelination* Elsevier Science, 2002. **137**: p. 299-309.

8. Thuret, S., L.D. Moon, and F.H. Gage, *Therapeutic interventions after spinal cord injury.* Nat Rev Neurosci, 2006. **7**(8): p. 628-43.

9. Philip, J.H. and H.G. Fred, *Regenerating the damaged central nervous system.* Macmillian Magazines Ltd, 2000. **407**: p. 963-970.

10. An, Y., K.K. Tsang, and H. Zhang, *Potential of stem cell based therapy and tissue engineering in the regeneration of the central nervous system.* Biomed Mater, 2006. **1**(2): p. R38-44.

11. Hulsebosch, C.E., *Recent advances in pathophysiology and treatment of spinal cord injury.* Advances is physiology education, 2002. **26**(4): p. 238-255.

12. Casha, S., W.R. Yu, and M.G. Fehlings, *Oligodendroglial apoptpsis occurs along degeneration axons and is associated with fas and p75 wxpression following spinal cord injury in the rat.* Neuroscience, 2001. **103**(1): p. 203-218.

13. Hagg, T. and M. Oudega, *Degenerative and spontaneous regenerative processes after spinal cord injury.* Journal of neurotrauma, 2006. **23**: p. 264-280.

14. Beattie, M.S., A.A. Farooqui, and J.C. Bresnahan, *Current evidence for apoptosis after spinal cord injury.* Journal of neurotrauma, 2000. **17**(10): p. 915-925.

15. Bareyre, F.M. and M.E. Schwab, *Inflammation, degeneration and regeneration in the injured spinal cord: insights from DNA microarrays.* Trends Neurosci, 2003. **26**(10): p. 555-63.

16. Ning, Z., et al., *Inflammation & apoptosis in spinal cord injury.* Indian Journal, 2012. **17**(10): p. 915-925.

17. Bordes, C., et al., *Determination of poly(epsilon-caprolactone) solubility parameters: application to solvent substitution in a microencapsulation process.* Int J Pharm, 2010. **383**(1-2): p. 236-43.

18. Tan, H. and J. Ye, *Surface morphology and in vitro release performance of double-walled PLLA/PLGA microspheres entrapping a highly water-soluble drug.* Applied Surface Science, 2008. **255**(2): p. 353-356.

19. Oliveira, N.S., et al., *Gas solubility of carbon dioxide in poly(lactic acid) at high pressures: Thermal treatment effect.* Journal of Polymer Science Part B: Polymer Physics, 2007. **45**(5): p. 616-625.

20. Davies, O.R., et al., *Applications of supercritical CO2 in the fabrication of polymer systems for drug delivery and tissue engineering.* Adv Drug Deliv Rev, 2008. **60**(3): p. 373-87.

21. Louro, J. and D.D. Pearse, *Stem and progenitor cell therapies- recent progress for spinal cord injury repair.* Neurological Research, 2008. **30**(2): p. 5-16.

22. Theodore, T., et al., *Expression of endoderm stem cell markers- Evidence for the presence of adult stem cells in human thyroid glands.* Thyroid, 2006. **16**: p. 537-544.

23. Chowa, S.Y., et al., *Characterization and intraspinal grafting of EGF/bFGF-dependent neurospheres derived from embryonic rat spinal cord.* Brain Research, 2000. **874**(2): p. 87-106.

24. McKay, R., *Stem Cells in the Central Nervous System.* Science, 1997. **276**(5309): p. 66-71.

25. Johansson, C.B., et al., *Identification of a neural stem cell in the adult mammalian*

central nervous system. Cell Press, 1999. **96**: p. 25-43.

26. Haas, C., et al., *Phenotypic analysis of astrocytes derived from glial restricted precursors and their impact on axon regeneration.* Exp Neurol, 2012. **233**(2): p. 717-32.

27. Lepore, A.C. and I. Fischer, *Lineage-restricted neural precursors survive, migrate, and differentiate following transplantation into the injured adult spinal cord.* Exp Neurol, 2005. **194**(1): p. 230-42.

28. Willerth, S.M. and S.E. Sakiyama-Elbert, *Cell therapy for spinal cord regeneration.* Adv Drug Deliv Rev, 2008. **60**(2): p. 263-76.

29. Iwanami, A., et al., *Transplantation of human neural stem cells for spinal cord injury in primates.* J Neurosci Res, 2005. **80**(2): p. 182-90.

30. Cao, Q., *Differentiation of engrafted neuronal-restricted precursor cells Is inhibited in the traumatically injured spinal cord.* Experimental Neurology, 2002. **177**(2): p. 349-359.

31. White, R.E., *Manipulation of astrocytes after spinal cord injury using transforming growth factor alpha*, 2009, The Ohio State University.

32. Enzmann, G.U., et al., *Consequences of noggin expression by neural stem, glial, and neuronal precursor cells engrafted into the injured spinal cord.* Exp Neurol, 2005. **195**(2): p. 293-304.

33. Ishii, K., et al., *Neutralization of ciliary neurotrophic factor reduces astrocyte production from transplanted neural stem cells and promotes regeneration of corticospinal tract fibers in spinal cord injury.* J Neurosci Res, 2006. **84**(8): p. 1669-81.

34. Bareyre, F.M., *Neuronal repair and replacement in spinal cord injury.* J Neurol Sci, 2008. **265**(1-2): p. 63-72.

35. Hatami, M., et al., *Human embryonic stem cell-derived neural precursor transplants in collagen scaffolds promote recovery in injured rat spinal cord.* Cytotherapy, 2009. **11**(5): p. 618-30.

36. Brustle, O., et al., *Embryonic stem cell-derived glial precursors: A source of myelinating transplants.* Science, 1999. **285**(5428): p. 754-756.

37. Jendelova, P., et al., *Magnetic resonance tracking of transplanted bone marrow and embryonic stem cells labeled by iron oxide nanoparticles in rat brain and*

spinal cord. J Neurosci Res, 2004. **76**(2): p. 232-43.

38. Wyatt, L.A. and H.S. Keirstead, *Stem cell-based treatments for spinal cord injury.* Prog Brain Res, 2012. **201**: p. 233-52.

39. Ronaghi, M., et al., *Challenges of stem cell therapy for spinal cord injury: human embryonic stem cells, endogenous neural stem cells, or induced pluripotent stem cells?* Stem Cells, 2010. **28**(1): p. 93-9.

40. Faulkner, J. and H.S. Keirstead, *Human embryonic stem cell-derived oligodendrocyte progenitors for the treatment of spinal cord injury.* Transpl Immunol, 2005. **15**(2): p. 131-42.

41. Ruff, C.A., J.T. Wilcox, and M.G. Fehlings, *Cell-based transplantation strategies to promote plasticity following spinal cord injury.* Exp Neurol, 2012. **235**(1): p. 78-90.

42. Rismanchi, N., et al., *Cell death and long-term maintenance of neuron-like state after differentiation of rat bone marrow stromal cells: a comparison of protocols.* Brain Research, 2003. **991**(1-2): p. 46-55.

43. Lu, P., L.L. Jones, and M.H. Tuszynski, *BDNF-expressing marrow stromal cells support extensive axonal growth at sites of spinal cord injury.* Exp Neurol, 2005. **191**(2): p. 344-60.

44. Lu, P., L.L. Jones, and M.H. Tuszynski, *Axon regeneration through scars and into sites of chronic spinal cord injury.* Exp Neurol, 2007. **203**(1): p. 8-21.

45. Oudega, M., et al., *Axonal regeneration into Schwann cell grafts within resorbable poly(-hydroxyacid) guidance channels in the adult rat spinal cord.* Biomaterials, 2001. **22**: p. 1125-1136.

46. Blakemore, W.F. and R.J.M. Franklin, *Remyelination in Experimental Models of Toxin-Induced Demyelination*, in *Advances in multiple Sclerosis and Experimental Demyelinating Diseases*, M. Rodriguez, Editor. 2008, Springer Berlin Heidelberg. p. 193-212.

47. Silva, N.A., et al., *From basics to clinical: A comprehensive review on spinal cord injury.* Prog Neurobiol, 2014. **114C**: p. 25-57.

48. Su, Z. and C. He, *Olfactory ensheathing cells: biology in neural development and regeneration.* Prog Neurobiol, 2010. **92**(4): p. 517-32.

49. Radtke, C. and K. Wewetzer, *Translating basic research into clinical practice or*

what else do we have to learn about olfactory ensheathing cells? Neurosci Lett, 2009. **456**(3): p. 133-6.

50. Li, Y., *Repair of adult rat corticospinal tract by transplants of olfactory ensheathing cells.* Science, 1997. **277**(5334): p. 2000-2002.

51. Gage, F.H., J. Ray, and I. Fisher, *Isolation, characterization, and use of stem cells from the CNS.* Neuroscience Letters, 1995. **18**: p. 159-192.

52. Svendsen, C.N., M.A. Caldwell, and T. Ostenfeld, *Human neural stem cells-isolation, expansion and transplantation.* Brain Pathology, 1999. **9**: p. 419-513.

53. Wu, S., Y. Suzuki, and M. Kitada, *Migration, integration, and differentiation of hippocampus-derived neurosphere cells after transplantation into injured rat spinal cord.* Neuroscience Letters, 2001. **312**(3): p. 173-176.

54. Thomas, K.E. and L.D. Moon, *Will stem cell therapies be safe and effective for treating spinal cord injuries?* Br Med Bull, 2011. **98**: p. 127-42.

55. Blum, B. and N. Benvenisty, *The Tumorigenicity of Human Embryonic Stem Cells.* 2008. **100**: p. 133-158.

56. Schulz, T.C., et al., *Differentiation of human embryonic stem cells to dopaminergic neurons in serum-free suspension culture.* Stem Cells, 2004. **22**(7): p. 1218-38.

57. Curtis, M.A., R.L. Faull, and M. Glass, *A novel population of progenitor cells expressing cannabinoid receptors in the subependymal layer of the adult normal and Huntington's disease human brain.* J Chem Neuroanat, 2006. **31**(3): p. 210-5.

58. Ma, N., et al., *Umbilical cord blood cell transplantation for myocardial regeneration.* Transplant Proc, 2006. **38**(3): p. 771-773.

59. Horky, L.L., et al., *Fate of endogenous stem/progenitor cells following spinal cord injury.* The Journal of Comparative Neurology, 2006. **498**(4): p. 525-538.

60. Lipson, A.C. and P.J. Horner, *Potent possibilities- endogenous stem cells in the adult spinal cord.* Progress in Brain Research, 2002. **137**: p. 283-297.

61. Beattie, M.S., et al., *Endogenous repair after spinal cord contusion injuries in the rat.* Experimental Neurology, 1997. **148**: p. 453-463.

62. Masaaki, K., et al., *Differentiation of choroid plexus ependymal cells into astrocytes after grafting into the pre-lesioned spinal cord in mice.* Peer Reviewed Journal, 2001. **36**(3): p. 364-374.

63. Schanzer, A., et al., *Direct stimulation of adult neural stem cells in vitro and neurogenesis in vivo by vascular endothelial growth factor.* Brain Pathology, 2004. **14**(3): p. 237-248.

64. Butovsky, O., et al., *Microglia activated by IL-4 or IFN-gamma differentially induce neurogenesis and oligodendrogenesis from adult stem/progenitor cells.* Mol Cell Neurosci, 2006. **31**(1): p. 149-60.

65. Tropepe, V., et al., *Distinct neural stem cells proliferate in response to EGF and FGF in the developing mouse telencephalon.* Developmental Biology, 1999. **208**: p. 166-188.

66. Cummings, B.J., et al., *Human neural stem cells differentiate and promote locomotor recovery in spinal cord-injured mice.* Proc Natl Acad Sci U S A, 2005. **102**(39): p. 14069-74.

67. Pearse, D.D. and D.J. Barakat, *Cellular repair strategies for spinal cord injury.* Expert Opinion, 2006. **6**: p. 639-652.

68. Dertinger, S.K., et al., *Gradients of substrate-bound laminin orient axonal specification of neurons.* Proc Natl Acad Sci U S A, 2002. **99**(20): p. 12542-7.

69. Logan, A., et al., *Neurotrophic factor synergy is required for neuronal survival and disinhibited axon regeneration after CNS injury.* Brain, 2006. **129**(Pt 2): p. 490-502.

70. Sirén, A., et al., *Erythropoietin prevents neuronal apoptosis after cerebral ischemia and metabolic stress.* Proceedings of the National Academy of Sciences, 2001. **98**(7): p. 4044-4049.

71. Erbayraktar, S., et al., *Asialoerythropoietin is a nonerythropoietic cytokine with broad neuroprotective activity in vivo.* Proceedings of the National Academy of Sciences, 2003. **100**(11): p. 6741-6746.

72. Leist, M., et al., *Derivatives of erythropoietin that are tissue protective but not erythropoietic.* Science, 2004. **305**(5681): p. 239-42.

73. Heo, K., et al., *Minocycline inhibits caspase-dependent and -independent cell death pathways and is neuroprotective against hippocampal damage after treatment with kainic acid in mice.* Neurosci Lett, 2006. **398**(3): p. 195-200.

74. Guimaraes, J.S., et al., *Minocycline treatment reduces white matter damage after excitotoxic striatal injury.* Brain Res, 2010. **1329**: p. 182-93.

75. Yune, T.Y., et al., *Minocycline alleviates death of oligodendrocytes by inhibiting pro-nerve growth factor production in microglia after spinal cord injury.* J Neurosci, 2007. **27**(29): p. 7751-61.

76. Eskdale, J., et al., *Mapping of the human IL10 gene and further characterization of the 5'flanking sequence.* Immunogenetics, 1997. **46**(2): p. 120-128.

77. Bethea, J., et al., *Systemically administered interleukin-10 reduces tumor necrosis factor-alpha production and significantly improves functional recovery following traumatic spinal cord injury in rats.* Journal of neurotrauma, 1999. **16**(10): p. 851-863.

78. Zhou, Z., et al., *Interleukin-10 provides direct trophic support to neurons.* Journal of neurochemistry, 2009. **110**(5): p. 1617-1627.

79. Busch, S.A. and J. Silver, *The role of extracellular matrix in CNS regeneration.* Current opinion in neurobiology, 2007. **17**(1): p. 120-127.

80. Jones, L.L., R.U. Margolis, and M.H. Tuszynski, *The chondroitin sulfate proteoglycans neurocan, brevican, phosphacan, and versican are differentially regulated following spinal cord injury.* Experimental neurology, 2003. **182**(2): p. 399-411.

81. Jefferson, S.C., N.J. Tester, and D.R. Howland, *Chondroitinase ABC promotes recovery of adaptive limb movements and enhances axonal growth caudal to a spinal hemisection.* J Neurosci, 2011. **31**(15): p. 5710-20.

82. Quarles, R.H., *Myelin-associated glycoprotein (MAG): past, present and beyond.* J Neurochem, 2007. **100**(6): p. 1431-48.

83. Babensee, J.E., L.V. McIntire, and A.G. Mikos, *Growth factor delivery for tissue engineering.* Pharmaceutical research, 2000. **17**(5).

84. Fiore, M., G.N. Chaldakov, and L. Aloe, *Nerve growth factor as a signaling molecule for nerve cells and also for the neuroendocrine-immune systems.* Reviews in the Neurosciences, 2009. **20**(2): p. 133-145.

85. Oudega, M., E.J. Bradbury, and M.S. Ramer, *Combination therapies.* Handb Clin Neurol, 2012. **109**: p. 617-36.

86. Sofroniew, M.V., *Nerve growth factor signaling, neuroprotection, and neural repair.* Neuroscience, 2001. **24**: p. 1217-1281.

87. Marsh, D.R., et al., *Neutralizing intraspinal nerve growth factor with a trkA-IgG*

fusion protein blocks the development of autonomic dysreflexia in a clip-compression model of spinal cord injury. Journal of neurotrauma, 2002. **19**(12): p. 1531-1541.

88. Snider, W.D., *Functions of the neurotrophins during nervous system development- What the knockouts are teaching us* Cell Press, 1994. **77**(5): p. 627-638.

89. Zhou, L., et al., *Neurotrophin-3 expressed in situ induces axonal plasticity in the adult injured spinal cord.* The Journal of Neuroscience, 2003. **23**(4): p. 1424-1431.

90. Wilson-Gerwing, T.D., et al., *Neurotrophin-3 significantly reduces sodium channel expression linked to neuropathic pain states.* Exp Neurol, 2008. **213**(2): p. 303-14.

91. Huang, E. and L.F. Reichardt, *Neurotrophins- Roles in neuronal development and function.* Annual Review of Neuroscience 2001. **24**(1): p. 677-736.

92. Lu, P., A. Blesch, and M.H. Tuszynski, *Neurotrophism without neurotropism-BDNF promotes survival but not growth of lesioned corticospinal neurons.* The Journal of Comparative Neurology, 2001. **436**: p. 456-470.

93. Awad, B.I., M.A. Carmody, and M.P. Steinmetz, *Potential Role of Growth Factors in the Management of Spinal Cord Injury.* World Neurosurg, 2013.

94. Balaratnasingam, S. and A. Janca, *Brain Derived Neurotrophic Factor: a novel neurotrophin involved in psychiatric and neurological disorders.* Pharmacol Ther, 2012. **134**(1): p. 116-24.

95. Xiao, M.X., et al., *A Combination of BDNF and NT-3 Promotes Supraspinal Axonal Regeneration into Schwann Cell Grafts in Adult Rat Thoracic* Experimental Neurology, 1995. **134**(2): p. 261-272.

96. De Nicolo, S., et al., *Effects of olive polyphenols administration on nerve growth factor and brain-derived neurotrophic factor in the mouse brain.* Nutrition, 2013. **29**(4): p. 681-7.

97. Kirkpatrick, P.J., *Head Trauma: Basic, Preclinical, and Clinical Directions.* Journal of Neurology, Neurosurgery and Psychiatry, 2002. **72**: p. 279.

98. Sapieha, P.S., et al., *Fibroblast growth factor-2 gene delivery stimulates axon growth by adult retinal ganglion cells after acute optic nerve injury.* Molecular and Cellular Neuroscience, 2003. **24**(3): p. 656-672.

99. Pataky, D.M., et al., *Fibroblast growth factor treatment produces differential effects on survival and neurite outgrowth from identified bulbospinal neurons in vitro.* Exp Neurol, 2000. **163**(2): p. 357-72.

100. Erlandsson, A., et al., *Immunosuppression promotes endogenous neural stem and progenitor cell migration and tissue regeneration after ischemic injury.* Exp Neurol, 2011. **230**(1): p. 48-57.

101. Jimenez Hamann, M.C., C.H. Tator, and M.S. Shoichet, *Injectable intrathecal delivery system for localized administration of EGF and FGF-2 to the injured rat spinal cord.* Exp Neurol, 2005. **194**(1): p. 106-19.

102. Zurn, A.D., et al., *Glial cell line-derived neurotrophic factor (GDNF), a new neurotrophic factor for motoneurones.* Neuroreport, 1994. **6**(1): p. 113-118.

103. Gomes, C.A., et al., *Glial cell line-derived neurotrophic factor (GDNF) enhances dopamine release from striatal nerve endings in an adenosine A2A receptor-dependent manner.* Brain Res, 2006. **1113**(1): p. 129-36.

104. Consales, C., et al., *GDNF signaling in embryonic midbrain neurons in vitro.* Brain Res, 2007. **1159**: p. 28-39.

105. Allen, S.J., et al., *GDNF, NGF and BDNF as therapeutic options for neurodegeneration.* Pharmacol Ther, 2013. **138**(2): p. 155-75.

106. Belair, D.G. and W.L. Murphy, *Specific VEGF sequestering to biomaterials: influence of serum stability.* Acta Biomater, 2013. **9**(11): p. 8823-31.

107. Ferrara, N., H. Gerber, and J. LeCouter, *The biology of VEGF and its receptors.* Nature medicine, 2003. **9**(6): p. 669-676.

108. Peters, K.G., D.V. C., and L.T. Williams, *Vascular endothelial growth factor receptor expression during embryogenesis and tissue repair suggests a role in endothelial differentiation and blood vessel growth.* Proceedings of the National Academy of Sciences, 1993. **90**(19): p. 8915-8919.

109. Heidaran, M.A., et al., *Role of alpha beta receptor heterodimer formation in beta platelet-derived growth factor (PDGF) receptor activation by PDGF-AB.* Journal of Biological Chemistry, 1991. **266**(30): p. 20232-20237.

110. Khademhosseini, A., et al., *Embryonic Stem Cells as a Cell Source for Tissue Engineering.* 2014: p. 609-638.

111. Hoch, R.V. and P. Soriano, *Roles of PDGF in animal development.* Development,

2003. **130**(20): p. 4769-84.

112. Johe, K.K., et al., *Single factors direct the differentiation of stem cells from the fetal and adult central nervous system.* Genes & Development, 1996. **10**(24): p. 3129-3140.

113. Krieglstein, K., et al., *TGF-β and the regulation of neuron survival and death.* Journal of Physiology-Paris, 2002. **96**(1): p. 25-30.

114. Adam, P.J., et al., *Positive-and negative-acting Krüppel-like transcription factors bind a transforming growth factor β control element required for expression of the smooth muscle cell differentiation marker SM22α in vivo.* Journal of Biological Chemistry, 2000. **275**(48): p. 37798-37806.

115. Unsicker, K., C. Suter-Crazzolara, and K. Krieglstein, *Neurotrophic roles of GDNF and related factors*, in *Neurotrophic Factors*. 1999, Springer. p. 189-224.

116. Gomes, F.C., O. Sousa Vde, and L. Romao, *Emerging roles for TGF-beta1 in nervous system development.* Int J Dev Neurosci, 2005. **23**(5): p. 413-24.

117. Roussa, E. and K. Krieglstein, *Induction and specification of midbrain dopaminergic cells: focus on SHH, FGF8, and TGF-β.* Cell and tissue research, 2004. **318**(1): p. 23-33.

118. Li, W., C.A. Cogswell, and J.J. LoTurco, *The response of early neural genes to FGF signaling or inhibition of BMP indicate the absence of a conserved neural induction module.* The Journal of Neuroscience, 1998. **18**(21): p. 8853-8862.

119. Muroyama, Y., H. Kondoh, and S. Takada, *Wnt proteins promote neuronal differentiation in neural stem cell culture.* Biochemical and Biophysical Research Communications, 2004. **313**(4): p. 915-921.

120. Kim, D.J., et al., *Differential expression of the Wnt and Frizzled genes in Flk1+ cells derived from mouse ES cells.* Cell Biochem Funct, 2008. **26**(1): p. 24-32.

121. Kleber, M. and L. Sommer, *Wnt signaling and the regulation of stem cell function.* Curr Opin Cell Biol, 2004. **16**(6): p. 681-7.

122. Lie, D.C., et al., *Wnt signalling regulates adult hippocampal neurogenesis.* Nature, 2005. **437**(7063): p. 1370-5.

123. Zhu, G., et al., *Sonic hedgehog and BMP2 exert opposing actions on proliferation and differentiation of embryonic neural progenitor cells.* Development Biology, 1999. **215**: p. 118-129.

124. Lowry, N., et al., *The effect of long-term release of Shh from implanted biodegradable microspheres on recovery from spinal cord injury in mice.* Biomaterials, 2012. **33**(10): p. 2892-901.

125. Charron, F., et al., *The morphogen sonic hedgehog is an axonal chemoattractant that collaborates with netrin-1 in midline axon guidance.* Cell, 2003. **113**: p. 11-23.

126. Bain, G., et al., *Retinoic acid promotes neural and represses mesodermal gene expression in mouse embryonic stem cells in culture.* Biochemical and biophysical research communications, 1996. **223**(3): p. 691-694.

127. Lakard, S., et al., *In vitro induction of differentiation by retinoic acid in an immortalized olfactory neuronal cell line.* Acta Histochem, 2007. **109**(2): p. 111-21.

128. Glaser, T. and O. Brustle, *Retinoic acid induction of ES-cell-derived neurons: the radial glia connection.* Trends Neurosci, 2005. **28**(8): p. 397-400.

129. Tuinstra, H.M., et al., *Multifunctional, multichannel bridges that deliver neurotrophin encoding lentivirus for regeneration following spinal cord injury.* Biomaterials, 2012. **33**(5): p. 1618-26.

130. Lee, K., E.A. Silva, and D.J. Mooney, *Growth factor delivery-based tissue engineering: general approaches and a review of recent developments.* J R Soc Interface, 2011. **8**(55): p. 153-70.

131. Vo, T.N., F.K. Kasper, and A.G. Mikos, *Strategies for controlled delivery of growth factors and cells for bone regeneration.* Adv Drug Deliv Rev, 2012. **64**(12): p. 1292-309.

132. Zhang, L., et al., *Co-delivery of hydrophobic and hydrophilic drugs from nanoparticle-aptamer bioconjugates.* ChemMedChem, 2007. **2**(9): p. 1268-71.

133. Chen, F.M., M. Zhang, and Z.F. Wu, *Toward delivery of multiple growth factors in tissue engineering.* Biomaterials, 2010. **31**(24): p. 6279-308.

134. S., M.S., et al., *Neural Progenitor Cells Grown on Hydrogel Surfaces Respond to the Product of the Transgene of Encapsulated Genetically Engineered Fibroblasts.* Biomacromolecules, 2010. **11**: p. 2936-2943.

135. Novikova, L.N., L.N. Novicov, and J.O. Kellerth, *Survival effects of BDNF and NT-3 on axotomized rubrospinal neurons depend on the temporal pattern of neurotrophin administration.* European Journal of Neuroscience, 2000. **12**: p.

776-780.

136. Freeman, I. and S. Cohen, *The influence of the sequential delivery of angiogenic factors from affinity-binding alginate scaffolds on vascularization.* Biomaterials, 2009. **30**(11): p. 2122-31.

137. Yilgor, P., N. Hasirci, and V. Hasirci, *Sequential BMP-2/BMP-7 delivery from polyester nanocapsules.* J Biomed Mater Res A, 2010. **93**(2): p. 528-36.

138. Jaklenec, A., et al., *Sequential release of bioactive IGF-I and TGF-beta 1 from PLGA microsphere-based scaffolds.* Biomaterials, 2008. **29**(10): p. 1518-25.

139. Richardson, T.P., et al., *Polymeric system for dual growth factor delivery.* Nature, 2001. **10**: p. 1029-1034.

140. Carmeliet, P., *Angiogenesis in life, disease and medicine.* Nature, 2005. **438**(7070): p. 932-6.

141. Chapanian, R. and B.G. Amsden, *Combined and sequential delivery of bioactive VEGF165 and HGF from poly(trimethylene carbonate) based photo-cross-linked elastomers.* J Control Release, 2010. **143**(1): p. 53-63.

142. Shin, S.H., et al., *Sequential delivery of TAT-HSP27 and VEGF using microsphere/hydrogel hybrid systems for therapeutic angiogenesis.* J Control Release, 2013. **166**(1): p. 38-45.

143. Eldar, B.A., et al., *Nano-sized polymers and liposomes designed to deliver combination therapy for cancer.* Curr Opin Biotechnol, 2013. **24**(4): p. 682-9.

144. Wang, H., et al., *Enhanced anti-tumor efficacy by co-delivery of doxorubicin and paclitaxel with amphiphilic methoxy PEG-PLGA copolymer nanoparticles.* Biomaterials, 2011. **32**(32): p. 8281-90.

145. Gill, K.K., A. Kaddoumi, and S. Nazzal, *Mixed micelles of PEG(2000)-DSPE and vitamin-E TPGS for concurrent delivery of paclitaxel and parthenolide: enhanced chemosenstization and antitumor efficacy against non-small cell lung cancer (NSCLC) cell lines.* Eur J Pharm Sci, 2012. **46**(1-2): p. 64-71.

146. Kim, J.Y., et al., *Tumor vasculature targeting following co-delivery of heparin-taurocholate conjugate and suberoylanilide hydroxamic acid using cationic nanolipoplex.* Biomaterials, 2012. **33**(17): p. 4424-30.

147. Olivier, J., et al., *Indirect evidence that drug brain targeting using polysorbate 80-coated polybutylcyanoacrylate nanoparticles is related to toxicity.*

Pharmaceutical Research, 1999. **16**(12): p. 1836-1842.

148. King, W.J. and P.H. Krebsbach, *Growth factor delivery: how surface interactions modulate release in vitro and in vivo.* Adv Drug Deliv Rev, 2012. **64**(12): p. 1239-56.

149. Aw, M.S., J. Addai-Mensah, and D. Losic, *A multi-drug delivery system with sequential release using titania nanotube arrays.* Chem Commun (Camb), 2012. **48**(27): p. 3348-50.

150. Sundararaj, S.C., et al., *Bioerodible system for sequential release of multiple drugs.* Acta Biomater, 2014. **10**(1): p. 115-25.

151. Raiche, A.T. and D.A. Puleo, *In vitro effects of combined and sequential delivery of two bone growth factors.* Biomaterials, 2004. **25**(4): p. 677-685.

152. Strobel, C., et al., *Sequential release kinetics of two (gentamicin and BMP-2) or three (gentamicin, IGF-I and BMP-2) substances from a one-component polymeric coating on implants.* J Control Release, 2011. **156**(1): p. 37-45.

153. Kim, S., et al., *Sequential delivery of BMP-2 and IGF-1 using a chitosan gel with gelatin microspheres enhances early osteoblastic differentiation.* Acta Biomater, 2012. **8**(5): p. 1768-77.

154. Hori, Y., A.M. Winans, and D.J. Irvine, *Modular injectable matrices based on alginate solution/microsphere mixtures that gel in situ and co-deliver immunomodulatory factors.* Acta Biomater, 2009. **5**(4): p. 969-82.

155. Wang, Y., et al., *Bioengineered sequential growth factor delivery stimulates brain tissue regeneration after stroke.* J Control Release, 2013. **172**(1): p. 1-11.

156. Hao, X., et al., *Angiogenic effects of sequential release of VEGF-A165 and PDGF-BB with alginate hydrogels after myocardial infarction.* Cardiovasc Res, 2007. **75**(1): p. 178-85.

157. Lin, C.C. and A.T. Metters, *Hydrogels in controlled release formulations: network design and mathematical modeling.* Adv Drug Deliv Rev, 2006. **58**(12-13): p. 1379-408.

158. Fournier, E., et al., *Biocompatibility of implantable synthetic polymeric drug carriers: focus on brain biocompatibility.* Biomaterials, 2003. **24**(19): p. 3311-3331.

159. Straley, K.S., C.W.P. Foo, and S.C. Heilshorn, *Biomaterial design strategies for the*

treatment of spinal cord injuries. Journal of Neurotrauma, 2010. **27**: p. 1-19.

160. Wang, M., et al., *A spheres-in-sphere structure for improving protein-loading poly (lactide-co-glycolide) microspheres.* Polymer Degradation and Stability, 2010. **95**(1): p. 6-13.

161. Wischke, C. and S.P. Schwendeman, *Principles of encapsulating hydrophobic drugs in PLA/PLGA microparticles.* Int J Pharm, 2008. **364**(2): p. 298-327.

162. Kokai, L.E., A.M. Ghaznavi, and K.G. Marra, *Incorporation of double-walled microspheres into polymer nerve guides for the sustained delivery of glial cell line-derived neurotrophic factor.* Biomaterials, 2010. **31**(8): p. 2313-22.

163. Berkland, C., et al., *Three-month, zero-order piroxicam release from monodispersed double-walled microspheres of controlled shell thickness.* J Biomed Mater Res A, 2004. **70**(4): p. 576-84.

164. Shi, M., et al., *Double walled POE/PLGA microspheres: encapsulation of water-soluble and water-insoluble proteins and their release properties.* Journal of Controlled Release, 2003. **89**(2): p. 167-177.

165. McMillan, M.R., T. Doud, and W. Nugent, *Catheter-associated masses in patients receiving intrathecal analgesic therapy.* Anesth analg, 2003. **96**: p. 186-190.

166. Thorne, R.G. and W.H. Frey, *Delivery of neurotrophic factors to the central nervous system.* Drug disposition 2001. **40**(12): p. 907-946.

167. Blesch, A. and M.H. Tuszynski, *Transient growth factor delivery sustains regenerated axons after spinal cord injury.* J Neurosci, 2007. **27**(39): p. 10535-10545.

168. Edlund, U.A. and C. Albertsson, *Degradable polymer microspheres for controlled drug delivery.* Advances in polymer science, 2002. **157**: p. 68-114.

169. Gupta, D., C.H. Tator, and M.S. Shoichet, *Fast-gelling injectable blend of hyaluronan and methylcellulose for intrathecal, localized delivery to the injured spinal cord.* Biomaterials, 2006. **27**(11): p. 2370-9.

170. Ijkema, P.J., et al., *Transection of peripheral nerves, bridging strategies and effect evaluation.* Biomaterials, 2004. **25**(9): p. 1583-1592.

171. Henrich, C., et al., *Gait Analysis of Adult Paraplegic Rats after Spinal Cord Repair.* Experimental Neurology, 1997. **148**(2): p. 544-557.

172. Quirk, R.A., et al., *Supercritical fluid technologies and tissue engineering scaffolds.* Current Opinion in Solid State and Materials Science, 2004. **8**(3-4): p. 313-321.

173. Orive, G., et al., *Encapsulated cell technology- from research to market.* Trends in Biotechnology, 2002. **20**(9): p. 382-387.

174. Hou, S., et al., *The repair of brain lesion by implantation of hyaluronic acid hydrogels modified with laminin.* J Neurosci Methods, 2005. **148**(1): p. 60-70.

175. Woerly, S., V.D. Doan, and N. Sosa, *Prevention of Gliotic Scar Formation by NeuroGel™ Allows Partial Endogenous Repair of Transected Cat Spinal Cord.* Neuroscience Research, 2004(75): p. 262-272.

176. Orive, G., et al., *Bioactive cell-hydrogel microcapsules for cell-based drug delivery.* J Control Release, 2009. **135**(3): p. 203-10.

177. Li, X., et al., *Engineering neural stem cell fates with hydrogel design for central nervous system regeneration.* Progress in Polymer Science, 2012. **37**(8): p. 1105-1129.

178. Karin, S.S., P.F. Cheryl-Wong, and C.H. Sarah, *Biomaterial Design Strategies for the Treatment of Spinal Cord Injuries.* Journal of Neurotrauma, 2010. **27**(2): p. 1-19.

179. Llias, K., et al., *The neural stem cell microenvironment.* StemBook, 2008: p. 1-25.

180. Luginbuehl, V., et al., *Localized delivery of growth factors for bone repair.* Eur J Pharm Biopharm, 2004. **58**(2): p. 197-208.

181. Miele, V.J., M.M. Panjabi, and E.C. Benzel, *Anatomy and biomechanics of the spinal column and cord.* Handb Clin Neurol, 2012. **109**: p. 31-43.

182. Tsai, E.C., et al., *Matrix inclusion within synthetic hydrogel guidance channels improves specific supraspinal and local axonal regeneration after complete spinal cord transection*. Vol. 27. 2006.

183. Hiroshi, N., H.T. Charles, and S.S. Molly, *Bioengineered strategies for spinal cord repair*. Vol. 23. 2006, Journal of neurotrauma.

184. Haipeng, G., et al., *Studies on nerve cell affinity of chitosan-derived materials.* Journal of biomedical materials research, 2000. **52**(2).

185. Belkas, J.S., et al., *Long-term in vivo biomechanical properties and biocompatibility of poly(2-hydroxyethyl methacrylate-co-methyl methacrylate)*

nerve conduits. Biomaterials, 2005. **26**(14): p. 1741-9.

186. Wahl, D.A. and J.T. Czernuszka, *Collagen-hydroxyapatite composites for hard tissue repair.* Eur Cell Master, 2006. **11**.

187. Rajiv, M., et al., *Growth factor enhancement of peripheral nerve regeneration through a novel synthetic hydrogel tube.* Neurosurg, 2003. **99**: p. 555-565.

188. Nomura, H., et al., *Extramedullary chitosan channels promote survival of transplanted neural stem and progenitor cells and create a tissue bridge after complete spinal cord transection.* Tissue Eng Part A, 2008. **14**(5): p. 649-65.

189. Freier, T., et al., *Chitin-based tubes for tissue engineering in the nervous system.* Biomaterials, 2005. **26**(22): p. 4624-32.

190. Tobias, C.A., et al., *Alginate encapsulated BDNF-producing fibroblast grafts permit recovery offunction after spinal cord injury in the absence of immune suppression.* Journal of neurotrauma, 2005. **22**: p. 138-156.

191. Kataoka, K., et al., *Alginate enhances elongation of early regenerating axons in spinal cord of young rats.* Tissue engineering, 2004. **10**: p. 493-506.

192. Avitabile, T., et al., *Biocompatibility and biodegradation of intravitreal hyaluronan implants in rabbits.* Biomaterials, 2001. **22**: p. 195-200.

193. Tian, W.M., et al., *Hyaluronic acid–poly-D-lysine-based three-imensional hydrogel for traumatic brain injury.* Tissue Engineering, 2005. **11**: p. 513-525.

194. Barbuccia, R., et al., *Hyaluronic acid hydrogel in the treatment of osteoarthritis.* Biomaterials, 2002. **23**: p. 4503-4513.

195. Zhong, S.P., et al., *Biodegradation of hyaluronic acid derivatives by hyaluronidase.* Biomaterials, 1993. **15**: p. 359-365.

196. Peter, H.L., et al., *A preliminary study of intravenous surfactants in paraplegic dogs: polymer therapy in canine clinical SCI*. Vol. 21. 2004, Journal of neurotrauma.

197. Makadia, H.K. and S.J. Siegel, *Poly Lactic-co-Glycolic Acid (PLGA) as Biodegradable Controlled Drug Delivery Carrier.* Polymers (Basel), 2011. **3**(3): p. 1377-1397.

198. Teng, Y.D., et al., *Functional recovery following traumatic spinal cord injury mediated by a unique polymer scaffold seeded with neural stem cells*. Vol. 99. 2002, CrossMak.

199. Hongyun, T., et al., *Control of pore size and structure of tissue engineering scaffolds produced by superctitical fluid processing.* European cell and materials, 2007. **14**: p. 64-77.

200. Lao, L.L., et al., *Modeling of drug release from bulk-degrading polymers.* Int J Pharm, 2011. **418**(1): p. 28-41.

201. Jia-Huei, Z., et al., *In Vitro Degradation of Polylactide and Poly (lactide-co-glycolide) Microspheres* Journal of Applied Polymer Science 1991. **43**(11): p. 2099-2106.

202. Darensbourg, D.J., *Poly(lactic acid): synthesis, structures, properties, processing, and applications.* Journal of the American Chemical Society, 2011. **18**: p. 7237-7237.

203. Chen, C., et al., *Preparation and characterization of biodegradable PLA polymeric blends*. Vol. 24. 2003, Biomaterials.

204. Choi, W., H. Kim, and Y. Koh, *Production, mechanical properties and in vitro biocompatibility of highly aligned porous poly(ε-caprolactone) (PCL)/hydroxyapatite (HA) scaffolds.* Journal of Porous Materials, 2012. **20**(4): p. 701-708.

205. Tsuji, H. and Y. Ikada, *Blends of aliphatic polyesters. I. Physical properties and morphologies of solution-cast blends from poly(DL-lactide) and poly(ε-caprolactone).* Journal of applied polymer science, 1996. **60**.

206. Nakafuku, C. and S.-y. Takehisa, *Glass transition and mechanical properties of PLLA and PDLLA-PGA copolymer blends.* Journal of Applied Polymer Science, 2004. **93**(5): p. 2164-2173.

207. Copper, A.I., *Porous materials and supercritical fluids.* Advanced material, 2003. **15**(13): p. 1049-1059.

208. Howdle, S.M., et al., *Supercritical fluid mixing: preparation of thermally sensitive polymer composites containing bioactive materials.* Chemical Communications, 2001(1): p. 109-110.

209. Yoshimoto, H., et al., *A biodegradable nanofiber scaffold by electrospinning and its potential for bone tissue engineering.* Biomaterials, 2003. **24**(12): p. 2077-2082.

210. Whang, H., et al., *Ectopic bone formation via rhBMP-2 delivery from porous bioabsorbable polymer scaffolds.* Jone Wiley & Sons, Inc, 1998. **25**: p. 491-499.

211. Hua, F.J., et al., *Macroporous poly(L-lactide) scaffold 1. Preparation of a macroporous scaffold by liquid–liquid phase separation of a PLLA–dioxane–water system.* Journal of Biomedical Materials Research, 2002. **63**(2): p. 161-167.

212. Li, Q., et al., *Fabrication of PGA/PLA Scaffold with the Shape of Human Nose.* 2013.

213. Evans, G.R.D., et al., *In vivo evaluation of poly(L-lactic acid) porous conduits for peripheral nerve regeneration.* Biomaterials, 1999. **20**: p. 1109-1115.

214. Lee, L.Y., C.H. Wang, and K.A. Smith, *Micro-porous paclitaxel-loaded PLGA foams - a new implant material for controlled release of chemotherapeutic agents.* Singapore-MIT Alliance, 2007: p. 1-6.

215. Ghaderi, R., C. Sturesson, and J. Carlfors, *Effect of preparative parameters on the characteristics of poly(d,l-lactide-co-glocolide) microspheres made by the double emulsion method.* International Joural of Pharmaceurics, 1996. **141**: p. 205-216.

216. Yang, Y., H. Chia, and T. Chung, *Effect of preparation conditions on morphology and release profiles of biodegradable polymeric microspheres containing protein fabricated by double-emulsion method.* Journal of Controlled Release, 2000. **69**: p. 81-96.

217. Hile, D.D., et al., *Active growth factor delivery from poly(D,L-lactide-co-glycolide) foams prepared in supercritical CO2.* Journal of Controlled Release, 2000. **66**(2-3): p. 177-185.

218. Batycky, R.P., et al., *A theoretical model of erosion and macromolecular drug relwase from biodegrading microspheres* Journal of Pharmaceurical Sciences, 1997. **86**(12): p. 1464-1477.

219. Zhang, M., et al., *Simulation of drug release from biodegradable polymeric microspheres with bulk and surface erosions.* Journal of Fharmaceutical Science, 2003. **92**(10): p. 2040-2056.

220. Raman, C., et al., *Modeling small-molecule release from PLG microspheres: effects of polymer degradation and nonuniform drug distribution.* Journal of Controlled Release, 2005. **103**(1): p. 149-158.

221. Edlund, U.A. and A.C. Albertsson, *Morphology engineering of a novel poly(L-lactide)/poly(1,5-dioxepan-2-one) microsphere system for controlled drug delivery.* Journal of Polymer Science Part A: Polymer Chemistry, 2000. **38**(5): p. 786-796.

222. Sun, H., et al., *Development and characterization of a novel nanoemulsion*

drug-delivery system for potential application in oral delivery of protein drugs. Int J Nanomedicine, 2012. **7**: p. 5529-43.

223. Odelius, K., et al., *Porosity and pore size regulate the degradation product profile of polylactide.* Biomacromolecules, 2011. **12**(4): p. 1250-8.

224. Lim, Y., et al., *Preparation of porous poly(ε-caprolactone) scaffolds by gas foaming process and in vitro/in vivo degradation behavior using γ-ray irradiation.* Journal of Industrial and Engineering Chemistry, 2008. **14**(4): p. 436-441.

225. Saito, E., et al., *Strut size and surface area effects on long-term in vivo degradation in computer designed poly(L-lactic acid) three-dimensional porous scaffolds.* Acta Biomater, 2012. **8**(7): p. 2568-77.

226. Wu, L. and J. Ding, *Effects of porosity and pore size on in vitro degradation of three-dimensional porous poly(D,L-lactide-co-glycolide) scaffolds for tissue engineering.* J Biomed Mater Res A, 2005. **75**(4): p. 767-77.

227. *Chemical & physical properties of select polymer*. 2014; Available from: http://www.absorbables.com/technical/properties.html.

228. Mou, Z., et al., *Preparation of porous PLGA/HA/collagen scaffolds with supercritical CO2 and application in osteoblast cell culture.* The Journal of Supercritical Fluids, 2011. **58**(3): p. 398-406.

229. Meneghello, G., et al., *Fabrication and characterization of poly(lactic-co-glycolic acid)/polyvinyl alcohol blended hollow fibre membranes for tissue engineering applications.* Journal of Membrane Science, 2009. **344**(1-2): p. 55-61.

230. Sultana, N. and M. Wang, *PHBV/PLLA-based composite scaffolds fabricated using an emulsion freezing/freeze-drying technique for bone tissue engineering: surface modification and in vitro biological evaluation.* Biofabrication, 2012. **4**(1): p. 015003.

231. Kim, J.Y. and D.-W. Cho, *Blended PCL/PLGA scaffold fabrication using multi-head deposition system.* Microelectronic Engineering, 2009. **86**(4-6): p. 1447-1450.

232. Dalton, P.D., L. Flynn, and M.S. Shoichet, *Manufacture of poly (2-hydroxyethyl methacrylate-co-methyl methacrylate) hydrogel tubes for use as nerve guidance channels.* Biomaterials, 2002. **23**(18): p. 3843-3851.

233. Zhang, J., et al., *Fabrication of three dimensional polymeric scaffolds with spherical pores.* Journal of Materials Science, 2006. **41**(6): p. 1725-1731.

234. Kehoe, S., et al., *Characterization of PLGA based composite nerve guidance conduits: effect of F127 content on modulus over time in simulated physiological conditions.* J Mech Behav Biomed Mater, 2012. **14**: p. 180-5.

235. Sherwood, J.K., et al., *A three-dimensional osteochondral composite scaffold for articular cartilage repair.* Biomaterials, 2002. **23**(24): p. 4739-4751.

236. Phong, L., et al., *Properties and hydrolysis of PLGA and PLLA cross-linked with electron beam radiation.* Polymer Degradation and Stability, 2010. **95**(5): p. 771-777.

237. Zhang, Q., et al., *Effect of porosity on long-term degradation of poly (ε-caprolactone) scaffolds and their cellular response.* Polymer Degradation and Stability, 2013. **98**(1): p. 209-218.

238. Sharifpoor, S., et al., *A study of vascular smooth muscle cell function under cyclic mechanical loading in a polyurethane scaffold with optimized porosity.* Acta Biomater, 2010. **6**(11): p. 4218-28.

239. Wu, L. and J. Ding, *In vitro degradation of three-dimensional porous poly(D,L-lactide-co-glycolide) scaffolds for tissue engineering.* Biomaterials, 2004. **25**(27): p. 5821-30.

240. Ganguly, K., T.M. Aminabhavi, and A.R. Kulkarni, *Colon Targeting of 5-Fluorouracil Using Polyethylene Glycol Cross-linked Chitosan Microspheres Enteric Coated with Cellulose Acetate Phthalate.* Industrial & Engineering Chemistry Research, 2011. **50**(21): p. 11797-11807.

241. Arifin, D.Y., L.Y. Lee, and C.H. Wang, *Mathematical modeling and simulation of drug release from microspheres: Implications to drug delivery systems.* Adv Drug Deliv Rev, 2006. **58**(12-13): p. 1274-325.

242. Kyekyoon, K.K. and W.P. Daniel, *Microspheres for Drug Delivery*. BioMEMS and Biomedical Nanotechnology. 2006. 19-50.